

# ACTA PHARMACEUTICA SCIENCIA

International Journal in Pharmaceutical Sciences, Published Quarterly

ISSN: 2636-8552

e-ISSN: 1307-2080,

Volume: 61, No: 3, 2023

Formerly: Eczacılık Bülteni / Acta Pharmaceutica Turcica

Founded in 1953 by Kasım Cemal GÜVEN

# ACTA PHARMACEUTICA SCIENCIA

International Journal in Pharmaceutical Sciences  
is Published Quarterly

ISSN: 2636-8552

e-ISSN: 1307-2080,

Volume: 61, No: 3, 2023

Formerly: Eczacılık Bülteni/Acta Pharmaceutica Turcica

Founded in 1953 by Kasim Cemal Güven

## **Editor in Chief**

Gülden Zehra OMURTAG

## **Associate Editors**

Ayşe Esra KARADAĞ

Sevde Nur BİLTEKİN KALELİ

## **Language Editors**

Neda TANER

Rashida Muhammad UMAR

## **Biostatistics Editors**

Mehmet KOÇAK

Pakize YİĞİT

## **Copy Editors**

Ayşegül ÇAŞKURLU

Büşra Nur ÇATTIK

Elif Sümeyye KAHYA

Fatma SARI

Huriye ERARSLAN

Melih Buğra AĞ

Melike Zeynep ÜNÜKÜR

Meryem Nur BAŞ

Nursu Aylin KASA

Mert SARSAG

## **Editorial Board**

Complete list of editors and reviewers can be found on <http://www.actapharmsci.com/static.php?id=2>

## **Graphic-Design**

Sertan VURAL

## **Art Director**

Levent KARABAĞLI

## **Address**

İstanbul Medipol Üniversitesi

Kavacık Güney Kampüsü

Göztepe Mah. Atatürk Cad.

No: 40 34810 Beykoz/İSTANBUL

Tel: 0216 681 51 00

## **E-mail**

[editor@actapharmsci.com](mailto:editor@actapharmsci.com)

[secretary@actapharmsci.com](mailto:secretary@actapharmsci.com)

## **Web site**

<http://www.actapharmsci.com>

## **Web site**

<http://www.actapharmsci.com>

# Contents

|  |              |
|--|--------------|
| Aims and Scope of Acta Pharmaceutica Scientia<br>Gülden Zehra OMURTAG .....  | V            |
| <b>Instructions for Authors</b> .....  | <b>VI</b>    |
| <b>EDITORIAL</b> .....   | <b>XXIV</b>  |
| <b>Role of clinical pharmacists in post-COVID management</b><br>Neda TANER .....   | XXV          |
| <b>ORIGINAL ARTICLES</b> .....   | <b>XXVII</b> |
| <b>Chemical constituents of <i>Ailanthus altissima</i> (Mill.) swingle leaves growing in Egypt and their antioxidant activity</b><br>Heba R. MOHAMED, Eman A. EL-WAKIL, Maher M. EL-HASHASH<br>El-Sayed S. ABDEL-HAMEED .....  | 213          |
| <b>Development of a liquid chromatographic method to monitorization of medazepam and lorazepam in plasma and its validation</b><br>Melike ALPERTENGE, Emrah DURAL .....  | 235          |
| <b>Biological activity and chemical composition of the essential oil from the fruits of <i>Ferula rigidula</i> Fisch. ex DC.</b><br>Gökalp İŞCAN, Mine KÜRKÇÜOĞLU, Fatma TOSUN, Mahmut MİSKİ .....   | 257          |
| <b>Chemical composition, antimicrobial and antioxidant activity of a “lipid phase” from <i>Zanthoxylum pistaciifolium</i> Griseb leaves</b><br>Yamilé HEREDIA DÍAZ, Julio C. ESCALONA ARRANZ, Ania OCHOA PACHECO,<br>Rosalia GONZÁLEZ FERNÁNDEZ, Pedro L. BATISTA CORBAL, Paul COS, Alexandra<br>ESCALONA CAPARROS ..... | 269          |
| <b>Formulation and evaluation of atorvastatin tablets by solid dispersion technique</b><br>Reza GOUDARZI, Mohammad Mehdi MAHBOOBAN .....   | 285          |
| <b>Determination of riboflavin bioaccessibility in legumes by In Vitro digestion using different cooking methods</b><br>Sultan KESİK, Jale ÇATAK, Kübra ADA, Kübra DEMİR, Halime UĞUR<br>Mustafa YAMAN .....   | 303          |
| <b>Assessment of compressional, mechanical and release properties of <i>Terminalia randii</i> gum in paracetamol tablet formulation</b><br>Oluyemisi A. BAMIRO, Lateef G. BAKRE, Olutayo A. ADELEYE .....  | 317          |



## **Aims and Scope of Acta Pharmaceutica Scientia**

Acta Pharmaceutica Scientia is a continuation of the former “Eczacılık Bülteni” which was first published in 1953 by Prof. Dr. Kasım Cemal GÜVEN’s editorship. At that time, “Eczacılık Bülteni” hosted scientific papers from the School of Medicine-Pharmacy at İstanbul University, Türkiye.

In 1984, the name of the journal was changed to “Acta Pharmaceutica Turcica” and it became a journal for national and international manuscripts, in all fields of pharmaceutical sciences in both English and Turkish. (1984-1995, edited by Prof. Dr. Kasım Cemal GÜVEN, 1995-2001, edited by Prof. Dr. Erden GÜLER, 2002-2011, edited by Prof. Dr. Kasım Cemal GÜVEN)

Since 2006, the journal has been published only in English with the name, “Acta Pharmaceutica Scientia” which represents internationally accepted high-level scientific standards. The journal has been published quarterly except for an interval from 2002 to 2009 in which its issues were released at intervals of four months. The publication was also temporarily discontinued at the end of 2011 but since 2016, Acta Pharmaceutica Scientia has continued publication with the reestablished Editorial Board and also with the support of you as precious scientists.

Yours Faithfully

**Prof. Dr. Güliden Zehra OMURTAG**  
**Editor**

## **INSTRUCTIONS FOR AUTHORS**

Manuscripts must be prepared using the manuscript template

Manuscripts should contain the following elements in the following order :

Title Page

Abstract

Keywords

Introduction (Without author names and affiliations)

Methodology

Results and Discussion

Statement of Ethics

Conflict of interest Statement

Author Contributions

Funding Sources (optional)

Acknowledgments (optional)

References

It is best to use the Times New Roman' font, 11 font size, and all kinds of articles must be 1.5 spaced including text, references, tables, and legends.

The title should be concise and informative. Avoid abbreviations and formulae, where possible. The title page should include full title, author names and affiliations, present addresses, corresponding author, and ORCID numbers for every author Also, the full manuscript should include a full title page

Abstracts should not be separated into categories, it should be written in a paragraph format. Keywords: Max. 5

Graphics may be included with both in the text and uploaded as separate files

Sections: (Capital letters should be used in) Introduction, Methodology, Results and Discussion, Statement of Ethics, Conflict of Interest Statement, Author Contributions, Funding Sources (optional), Acknowledgement (optional).

Table and figure titles should not be abbreviated exp. fig. is not acceptable. It should be written as; Table 1. .... Figure 1. ....

Figure captions: A caption should comprise a brief title (not on the figure itself) and a description of the illustration. Keep text in the illustrations themselves

to a minimum but explain all symbols and abbreviations used. Figure captions should be written on the bottom.

**Titles:** Number tables consecutively by their appearance in the text and place any table notes below the table body. Table captions should be written on the top.

References in the text should be identified using Arabic numerals. Years of the references should not be written boldly. More than one reference from the same author(s) in the same year must be identified by the letters “a”, “b”, “c”, etc., placed after the year of publication. References should conform to Vancouver style and be numbered consecutively in the order in which they are cited in the text.

\*Obligatory files are manuscript main document, title page and copyright form for submission. If exist, supplementary files should also be added.

## **1. Scope and Editorial Policy**

### **1.1. Scope of the Journal**

Acta Pharmaceutica Scientia (Acta Pharm. Sci.), formerly known as Bulletin of Pharmacy and Acta Pharmaceutica Turcica is a peer-reviewed scientific journal publishing current research and reviews covering all fields of pharmaceutical sciences since 1953.

The original studies accepted for publication must be unpublished work and should contain data that have not been published elsewhere as a whole or a part. The reviews must provide critical evaluation of the state of knowledge related with the subject.

All manuscripts has to be written in clear and concise English.

Starting from 2016, the journal will be issued quarterly both in paper and online formates also publish special issues for national or international scientific meetings and activities in the coverage field.

### **1.2. Manuscript Categories**

Manuscripts can be submitted as Research Articles. Review articles will not be accepted.

Research Articles are definitive accounts of significant, original studies. They are expected to present important new data or provide a fresh approach to an established subject.

### **1.3. Prior Publication**

Authors should submit only original work that has not been previously published and is not under consideration for publication elsewhere. Academic theses, including those on the Web or at a college Web site, are not considered to be prior publication.

### **1.4. Patents and Intellectual Property**

Authors need to resolve all patent and intellectual property issues. Acceptance and publication will not be delayed for pending or unresolved issues of this type. Note that Accepted manuscripts and online manuscripts are considered as published documents.

### **1.5. Professional Ethics**

Editors, reviewers, and authors are expected to adhere to internationally accepted criteria's for scientific publishing. Helsinki declaration is applied and accepted for the ethical standards of the journal.

World Medical Association. (2001). World Medical Association Declaration of Helsinki. Ethical principles for medical research involving human subjects.. Bulletin of the World Health Organization, 79 (4), 373- 374.

#### **1.5.1 Author Consent**

Submitting authors are reminded that consent of all coauthors must be obtained prior to submission of manuscripts. If an author is removed after submission, the submitting author must have the removed author consent to the change by e-mail or faxed letter to the assigned Editor.

#### **1.5.2. Plagiarism**

Manuscripts must be original with respect to concept, content, and writing. It is not appropriate for an author to reuse wording from other publications, including one's own previous publications, whether or not that publication is cited. Suspected plagiarism should be reported immediately to the editorial office. Report should specifically indicate the plagiarized material within the manuscripts. Acta Pharmaceutica Scientia uses iThenticate or Turnitin software to screen submitted manuscripts for similarity to published material. Note that your manuscript may be screened during the submission process.

#### **1.5.3. Use of Human or Animal Subjects**

For research involving biological samples obtained from animals or human subjects, editors reserve the right to request additional information from au-

thors. Studies submitted for publication approval must present evidence that the described experimental activities have undergone local institutional review assessing safety and humane usage of study subject animals. In the case of human subjects authors must also provide a statement that study samples were obtained through the informed consent of the donors, or in lieu of that evidence, by the authority of the institutional board that licensed the use of such material. Authors are requested to declare the identification or case number of institution approval as well as the name of the licensing committee in a statement placed in the section describing the studies' Material and Methods.

World Medical Association. (2001). World Medical Association Declaration of Helsinki. Ethical principles for medical research involving human subjects.. Bulletin of the World Health Organization, 79 (4), 373- 374.

## **1.6 Issue Frequency**

The Journal publishes 4 issues per year.

## **2. Preparing the Manuscript**

### **2.1. General Considerations**

Manuscripts should be kept to a minimum length. Authors should write in clear, concise English, employing an editing service if necessary. For professional assistance with improving the English, figures, or formatting in the manuscript before submission please contact to editorial office by e-mail for suggestions. Authors are required to subject their manuscript for

The responsibility for all aspects of manuscript preparation rests with the authors. Extensive changes or rewriting of the manuscript will not be undertaken by the Editors. A standard list of Abbreviations, Acronyms and Symbols is in section 5.

It is best to use the font "Times New Roman". Other fonts, particularly those that do not come bundled with the system software, may not translate properly. Ensure that all special characters (e.g., Greek characters, math symbols) are present in the body of the text as characters and not as graphic representations. Be sure that all characters are correctly represented throughout the manuscript—e.g., 1 (one) and l (letter l), o (zero) and O (letter o).

All text (including the title page, abstract, all sections of the body of the paper, figure captions, scheme or chart titles, and footnotes and references) and tables should be in one file. Graphics may be included with the text or uploaded as separate files. Manuscripts that do not adhere to the guidelines may be returned to authors for correction.

### **2.1.1 Articles of all kind**

Use page size A4. Vertically orient all pages. Articles of all kind must be double-spaced including text, references, tables, and legends. This applies to figures, schemes, and tables as well as text. They do not have page limitations but should be kept to a minimum length. The experimental procedures for all of experimental steps must be clearly and fully included in the experimental section of the manuscripts.

### **2.1.2 Nomenclature**

It is the responsibility of the authors to provide correct nomenclature. It is acceptable to use semisynthetic or generic names for certain specialized classes of compounds, such as steroids, peptides, carbohydrates, etc. In such a case, the name should conform to the generally accepted nomenclature conventions for the compound class. Chemical names for drugs are preferred. If these are not practical, generic names, or names approved by the World Health Organization, may be used.

Authors may find the following sources useful for recommended nomenclature:

- The ACS Style Guide; Coghill, A. M., Garson, L. R., Eds.; American Chemical Society: Washington DC, 2006.
- Enzyme Nomenclature; Webb, E. C., Ed.; Academic Press: Orlando, 1992.
- IUPHAR database of receptors and ion channels (<http://www.guidetopharmacology.org/>).

### **2.1.3 Compound Code Numbers**

Code numbers (including peptides) assigned to a compound may be used as follows:

- Once in the manuscript title, when placed in parentheses AFTER the chemical or descriptive name.
- Once in the abstract.
- Once in the text (includes legends) and once to label a structure. Code numbers in the text must correspond to structures or, if used only once, the chemical name must be provided before the parenthesized code number, e.g., “chemical name (JEM-398).” If appearing a second time in the text, a bold Arabic number must be assigned on first usage, followed by the parenthesized code number, e.g., “1 (JEM-398).” Subsequently, only the bold Arabic number may be used. All code numbers in the text must have a citation to a publication or a

patent on first appearance.

Compounds widely employed as research tools and recognized primarily by code numbers may be designated in the manuscript by code numbers without the above restrictions. Their chemical name or structure should be provided as above. Editors have the discretion of determining which code numbers are considered widely employed.

#### **2.1.4 Trademark Names**

Trademark names for reagents or drugs must be used only in the experimental section. Do not use trademark or service mark symbols.

#### **2.1.5 Interference Compounds**

Active compounds from any source must be examined for known classes of assay interference compounds and this analysis must be provided in the General Experimental section. Many of these compounds have been classified as Pan Assay Interference Compounds (PAINS; see Baell & Holloway, *J. Med. Chem.* 2010, 53, 2719-2740). These compounds shown to display misleading assay readouts by a variety of mechanisms by forming reactive compounds. Provide firm experimental evidence in at least two different assays that reported compounds with potential PAINS liability are specifically active and their apparent activity is not an artifact.

### **2.2 Manuscript Organization**

#### **2.2.1 Title Page. Title**

The title of the manuscript should reflect the purposes and findings of the work in order to provide maximum information in a computerized title search. Minimal use of nonfunctional words is encouraged. Only commonly employed abbreviations (e.g., DNA, RNA, ATP) are acceptable. Code numbers for compounds may be used in a manuscript title when placed in parentheses AFTER the chemical or descriptive name.

**Authors' Names and Affiliations:** The authors' full first names, middle initials, last names, and affiliations with addresses at time of work completion should be listed below the title. The name of the corresponding author should be marked with an asterisk (\*).

#### **2.2.2 Abstract and keywords**

Articles of all types must have an abstract following the title page. The maximum length of the Abstract should be 200 words, organized in a findings-oriented format in which the most important results and conclusions are sum-

marized. Code numbers may be used once in the abstract. After the abstract, a section of Keywords not more than five has to be given. Be aware that the keywords, chosen according to the general concept, are very significant during searching and indexing of the manuscripts.

**Keywords:** instructions for authors, template, journal

### **2.2.3 Introduction**

The Introduction should argue the case for the study, outlining only essential background, and should not include the findings or the conclusions. It should not be a review of the subject area, but should finish with a clear statement of the question being addressed. Authors should use this template when preparing a manuscript for submission to the ACTA Pharmaceutica Scientia.

### **2.2.4. Methodology**

Materials, synthetic, biological, demographic, statistical or experimental methods of the research should be given detailed in this section. The authors are free to subdivide this section in the logical flow of the study. For the experimental sections, authors should be as concise as possible in experimental descriptions. General reaction, isolation, preparation conditions should be given only once. The title of an experiment should include the chemical name and a bold Arabic identifier number; subsequently, only the bold Arabic number should be used. Experiments should be listed in numerical order. Molar equivalents of all reactants and percentage yields of products should be included. A general introductory section should include general procedures, standard techniques, and instruments employed (e.g., determination of purity, chromatography, NMR spectra, mass spectra, names of equipment) in the synthesis and characterization of compounds, isolates and preparations described subsequently in this section. Special attention should be called to hazardous reactions or toxic compounds. Provide analysis for known classes of assay interference compounds.

The preferred forms for some of the more commonly used abbreviations are mp, bp, °C, K, min, h, mL, µL, g, mg, µg, cm, mm, nm, mol, mmol, µmol, ppm, TLC, GC, NMR, UV, and IR. Units are abbreviated in table column heads and when used with numbers, not otherwise. (See section 4 for more abbreviations)

### **2.2.5 Results and Discussion**

This section could include preparation, isolation, synthetic schemes and tables of biological and statistical data. The discussions should be descriptive. Authors should discuss the analysis of the data together with the significance of results and conclusions. An optional conclusions section is not required.

### 2.2.6 Ancillary Information

Include pertinent information in the order listed immediately before the references.

**PDB ID Codes:** Include the PDB ID codes with assigned compound Arabic number. Include the statement “Authors will release the atomic coordinates and experimental data upon article publication.”

**Homology Models:** Include the PDB ID codes with assigned compound Arabic number. Include the statement “Authors will release the atomic coordinates upon article publication.”

**Corresponding Author Information:** Provide telephone numbers and email addresses for each of the designated corresponding authors.

**Present/Current Author Addresses:** Provide information for authors whose affiliations or addresses have changed.

**Author Contributions:** Include statement such as “These authors contributed equally.”

**Acknowledgment:** Authors may acknowledge people, organizations, and financial supporters in this section.

**Abbreviations Used:** Provide a list of nonstandard abbreviations and acronyms used in the paper, e.g., YFP, yellow fluorescent protein. Do not include compound code numbers in this list. It is not necessary to include abbreviations and acronyms from the Standard Abbreviations and Acronyms listed in section 4.

### 2.2.7 References and Notes

Vancouver style is used in the reference list and citations. List manuscripts as “in press” only accepted for publication. Manuscripts available on Web with a DOI number are considered published. For manuscripts not accepted, use “unpublished work” after the names of authors. Incorporate notes in the correct numerical sequence with the references. Footnotes are not used. List submitted manuscripts as “in press” only if formally accepted for publication. Manuscripts available on the Web with a DOI number are considered published. For manuscripts not accepted, use “unpublished results” after the names of authors. Incorporate notes in the correct numerical sequence with the references. Footnotes are not used. In-text citations should be given superscript numbers (see examples) according to order in the manuscript.

## References

Please check with your faculty for any specific referencing or formatting requirements

- References are listed in numerical order, and in the same order in which they are cited in text. The reference list appears at the end of the paper.
- Begin your reference list on a new page and title it 'References'.
- The reference list should include all and only those references you have cited in the text. (However, do not include unpublished items such as correspondence.)
- Use Arabic numerals (1, 2, 3, 4, 5, 6, 7, 8, 9) as a superscripts.
- Abbreviate journal titles in the style used in the NLM Catalog.
- Check the reference details against the actual source - you are indicating that you have read a source when you cite it.
- Use of doi URL at the end of reference is strongly advised.

## Examples

For printed articles

- Article with 1-6 authors:

Author AA, Author BB, Author CC, Author DD. Title of article. Abbreviated title of journal. Date of publication YYYY;volume number(issue number):page numbers.

Sahin Z, Ertas M, Berk B, Biltekin SN, Yurttas L, Demirayak S. Studies on non-steroidal inhibitors of aromatase enzyme; 4-(aryl/heteroaryl)-2-(pyrimidin-2-yl)thiazole derivatives. *Bioorg Med Chem*, 2018; 26(8): 1986–1995. <https://doi.org/10.1016/j.bmc.2018.02.048>.

- Article with more than 6 authors:

Author AA, Author BB, Author CC, Author DD, Author EE, Author FF, et al. Title of article. Abbreviated title of journal. Date of publication YYYY Mon DD;volume number(issue number):page numbers.

### Electronic journal article:

Author AA, Author BB. Title of article. Abbreviated title of Journal [Internet]. Date of publication YYYY MM [cited YYYY Mon DD];volume number(issue number):page numbers. Available from: URL

### **Electronic journal article with DOI:**

Author AA, Author BB, Author CC, Author DD, Author EE, Author FF. Title of article. Abbreviated title of Journal [Internet]. Year of publication [cited YYYY Mon DD]; volume number(issue number):page numbers. Available from: URL DOI

### **Books and book chapters**

Book :a.) Print book OR b.) Electronic book

a.) Author AA. Title of book. # edition [if not first]. Place of Publication: Publisher; Year of publication. Pagination.

b.) Author AA. Title of web page [Internet]. Place of Publication: Sponsor of Website/Publisher; Year published [cited YYYY Mon DD]. Number of pages. Available from: URL DOI: (if available)

### **2.2.8 Tables**

Tabulation of experimental results is encouraged when this leads to more effective presentation or to more economical use of space. Tables should be numbered consecutively in order of citation in the text with Arabic numerals. Footnotes in tables should be given italic lowercase letter designations and cited in the tables as superscripts. The sequence of letters should proceed by row rather than by column. If a reference is cited in both table and text, insert a lettered footnote in the table to refer to the numbered reference in the text. Each table must be provided with a descriptive title that, together with column headings, should make the table self-explanatory. Titles and footnotes should be on the same page as the table. Tables may be created using a word processor's text mode or table format feature. The table format feature is preferred. Ensure each data entry is in its own table cell. If the text mode is used, separate columns with a single tab and use a return at the end of each row. Tables may be inserted in the text where first mentioned or may be grouped after the references.

### **2.2.9 Figures, Schemes/Structures, and Charts**

The use of illustrations to convey or clarify information is encouraged. Structures should be produced with the use of a drawing program such as ChemDraw. Authors using other drawing packages should, in as far as possible, modify their program's parameters so that they conform to ChemDraw preferences. Remove all color from illustrations, except for those you would like published in color. Illustrations may be inserted into the text where mentioned or may be consolidated at the end of the manuscript. If consolidated, legends should be grouped on a separate page(s). Include as part of the manuscript file.

To facilitate the publication process, please submit manuscript graphics using the following guidelines:

1. The preferred submission procedure is to embed graphic files in a Word document. It may help to print the manuscript on a laser printer to ensure all artwork is clear and legible.

2. Additional acceptable file formats are: TIFF, PDF, EPS (vector artwork) or CDX (ChemDraw file). If submitting individual graphic files in addition to them being embedded in a Word document, ensure the files are named based on graphic function (i.e. Scheme 1, Figure 2, Chart 3), not the scientific name. Labeling of all figure parts should be present and the parts should be assembled into a single graphic.

EPS files: Ensure that all fonts are converted to outlines or embedded in the graphic file. The document settings should be in RGB mode. NOTE: While EPS files are accepted, the vector-based graphics will be rasterized for production. Please see below for TIFF file production resolutions.

3. TIFF files (either embedded in a Word doc or submitted as individual files) should have the following resolution requirements:

- Black & White line art: 1200 dpi

- Grayscale art (a monochromatic image containing shades of gray): 600 dpi

- Color art (RGB color mode): 300 dpi

· The RGB and resolution requirements are essential for producing high-quality graphics within the published manuscript. Graphics submitted in CMYK or at lower resolutions may be used; however, the colors may not be consistent and graphics of poor quality may not be able to be improved.

· Most graphic programs provide an option for changing the resolution when you are saving the image. Best practice is to save the graphic file at the final resolution and size using the program used to create the graphic.

4. Graphics should be sized at the final production size when possible. Single column graphics are preferred and can be sized up to 240 points wide (8.38 cm.). Double column graphics must be sized between 300 and 504 points (10.584 and 17.78 cm's). All graphics have a maximum depth of 660 points (23.28 cm.) including the caption (please allow 12 points for each line of caption text).

Consistently sizing letters and labels in graphics throughout your manuscript will help ensure consistent graphic presentation for publication.

### **2.2.10 Image Manipulation**

Images should be free from misleading manipulation. Images included in an account of research performed or in the data collection as part of the research require an accurate description of how the images were generated and produced. Apply digital processing uniformly to images, with both samples and controls. Cropping must be reported in the figure legend. For gels and blots, use of positive and negative controls is highly recommended. Avoid high contrast settings to avoid overexposure of gels and blots. For microscopy, apply color adjustment to entire image and note in the legend. When necessary, authors should include a section on equipment and settings to describe all image acquisition tools, techniques and settings, and software used. All final images must have resolutions of 300 dpi or higher. Authors should retain unprocessed data in the event that the Editors request them.

## **2.3 Specialized Data**

### **2.3.1 Biological Data**

Quantitative biological data are required for all tested compounds. Biological test methods must be referenced or described in sufficient detail to permit the experiments to be repeated by others. Detailed descriptions of biological methods should be placed in the experimental section. Standard compounds or established drugs should be tested in the same system for comparison. Data may be presented as numerical expressions or in graphical form; biological data for extensive series of compounds should be presented in tabular form.

Active compounds obtained from combinatorial syntheses should be resynthesized and retested to verify that the biology conforms to the initial observation. Statistical limits (statistical significance) for the biological data are usually required. If statistical limits cannot be provided, the number of determinations and some indication of the variability and reliability of the results should be given. References to statistical methods of calculation should be included.

Doses and concentrations should be expressed as molar quantities (e.g., mol/kg,  $\mu\text{mol/kg}$ , M, mM). The routes of administration of test compounds and vehicles used should be indicated, and any salt forms used (hydrochlorides, sulfates, etc.) should be noted. The physical state of the compound dosed (crystalline, amorphous; solution, suspension) and the formulation for dosing (micronized, jet-milled, nanoparticles) should be indicated. For those compounds found to be inactive, the highest concentration (*in vitro*) or dose level (*in vivo*) tested should be indicated.

If human cell lines are used, authors are strongly encouraged to include the following information in their manuscript:

- the cell line source, including when and from where it was obtained;
- whether the cell line has recently been authenticated and by what method;
- whether the cell line has recently been tested for mycoplasma contamination.

### **2.3.2 Purity of Tested Compounds**

**Methods:** All scientifically established methods of establishing purity are acceptable. If the target compounds are solvated, the quantity of solvent should be included in the compound formulas. No documentation is required unless asked by the editors.

**Purity Percentage:** All tested compounds, whether synthesized or purchased, should possess a purity of at least 95%. Target compounds must have a purity of at least 95%. In exceptional cases, authors can request a waiver when compounds are less than 95% pure. For solids, the melting point or melting point range should be reported as an indicator of purity.

**Elemental analysis:** Found values for carbon, hydrogen, and nitrogen (if present) should be within 0.4% of the calculated values for the proposed formula.

### **2.3.3 Confirmation of Structure**

Adequate evidence to establish structural identity must accompany all new compounds that appear in the experimental section. Sufficient spectral data should be presented in the experimental section to allow for the identification of the same compound by comparison. Generally, a listing of  $^1\text{H}$  or  $^{13}\text{C}$  NMR peaks is sufficient. However, when the NMR data are used as a basis of structural identification, the peaks must be assigned.

List only infrared absorptions that are diagnostic for key functional groups. If a series contains very closely related compounds, it may be appropriate merely to list the spectral data for a single representative member when they share a common major structural component that has identical or very similar spectral features.

## **3. Submitting the Manuscript**

### **3.1. Communication and log in to Author's Module**

All submissions to *Acta Pharmaceutica Scientia* should be made by using e-Collittera (Online Article Acceptance and Evaluation) system on the journal main page ([www.actapharmsci.com](http://www.actapharmsci.com))

### 3.2. Registration to System

It is required to register into the e-Collittera system for the first time while entering by clicking “Create Account” button on the registration screen and the fill the opening form with real information. Some of the information required in form is absolutely necessary and the registration will not work if these fields are not completely filled.

After the registration, a “Welcome” mail is sent to the user by the system automatically reminding user name and password. Authors are expected to return to the entry screen and log on with their user name and password for the submission. Please use only English characters while determining your username and password.

If you already registered into the e-Collittera system and forget your password, you should click on “Forgot My Password” button and your user name and password will be mailed to your e-mail in a short while.

### 3.3 Submitting A New Article

The main page of author module consists of various parts showing the situation of manuscripts in process. By clicking the New Manuscript button, authors create the beginning of new submission, a process with a total of 9 consecutive levels. In first 7 levels, information such as the article’s kind, institutions, authors, title, summary, keywords etc. are asked respectively as entered. Authors can move back and forth while the information is saved automatically. If the transaction is discontinued, the system move the new submission to “Partially Submitted Manuscripts” part and the transaction can be continued from here.

**3.1.1. Sort of Article** Authors should first select the type of article from the drop down menu.

Warning. If “Return to Main Page” button is clicked after this level, the article automatically assigned as “Partially Submitted Manuscripts”.

**3.2.2. Institutions** Authors should give their institutional information during submission.

**3.2.3. Authors** The authors’ surnames, names, institutional information appear as entered order in the previous page. Filling all e-mail addresses are required. Institutional information is available in Manuscript Details table at the top of the screen. After filling all required fields, you may click the Continue button.

**3.2.4 Title** should be English, explaining the significance of the study. If the title includes some special characters such as alpha, beta, pi or gamma, they

can easily be added by using the Title window. You may add the character by clicking the relevant button and the system will automatically add the required character to the text.

Warning. No additions to cornered parenthesis are allowed. Otherwise the system will not be able to show the special characters.

**3.2.5. Abstract** The summary of the article should be entered to Abstract window at this level. There must be an English summary for all articles and the quantity of words must be not more than 200. If special characters such as alpha, beta, pi or gamma are used in summary, they can be added by Abstract window. You may add the character by clicking the relevant button and the system will automatically add the required character to the text. The abstract of the articles are accessible for arbitrators; so you should not add any information related to the institutions and authors in this summary part. Otherwise the article will returned without evaluation. Authors will be required to comply with the rules.

Warning. No additions to cornered parenthesis are allowed. Otherwise the system will not be able to show the special characters.

**3.2.6. Keywords** There must be five words to define the article at the keywords window, which will diverged with commas. Authors should pay attention to use words, which are appropriate for “Medical Subjects Headings” list by National Library of Medicine (NLM).

**3.2.7. Cover Letter** If the submitting article was published as thesis and/or presented in a congress or elsewhere, all information of thesis, presented congress or elsewhere should be delivered to the editor and must be mentioned by the “Cover Letter” field.

**3.3.1. Adding Article** This process consists four different steps beginning with the loading of the article in to system. Browse button is used to reach the article file, under the Choose a file to upload tab. After finding the article you may click to Choose File and file will be attached.

Second step is to select the file category. Options are: Main Document, Black and White Figure, Color Figure and Video.

The explanation of the files (E.g., Figure 1, Full Text Word File, supplements etc.) should be added on third step and the last step is submitting the prepared article into the system. Therefore, Download button under the Send your file by clicking on download button tab is clicked.

Reminder If the prepared article includes more than one file (such as main document, black and white figure, video), the transaction will be continued by starting from the first step. The image files must be in previously defined format. After all required files were added, Continue button should be clicked. All details and features of the article might be reached from the Article Information page.

This page is the last step of the transaction which ensures that entered information is controlled.

**3.3.2. Your Files** After adding the article you may find all information related to article under Your Files window.

**File Information** This window includes file names, sizes, forming dates, categories, order numbers and explanations of files. The details about the files can be reached by clicking on Information button.

If you click on Name of File, the file download window will be opened to reach the copy of the file in system.

**File Download** This window submits two alternatives, one of them is to ensure the file to be opened in valid site and the second one is to ensure to download submitted file into the computer.

Opening the Category part on fourth column can change the category of the file.

Opening the Order column on fifth column can change the order of file.

The file can be deleted by clicking on Delete button on the last column. Before deleting, system will ask the user again if it's appropriate or not.

**3.3.3 Sending Article** Last level is submitting the article and the files into the system. Before continuing the transaction, Article Information window must be controlled where it is possible to return back; by using Previous button and required corrections can be made. If not, clicking the Send the Article button completes transaction.

**3.3.4. Page to Follow The Article** The Main Page of Author ensures possibility to follow the article. This page consists three different parts; some information and bridges related to the sent articles, revision required articles and the articles that are not completed to be sent.

**3.3.4.1. Articles Not Completed to be Sent** After the sending transaction was started, if article is not able to continue until the ninth step or could not be sent due to technical problems shown at this part. Here you can find the

information such as the article's number which is assigned by system, title and formation date. You may delete the articles by using Delete button on the right column, if the article is not considered to send into the system.

**3.3.4.2. Articles That Require Revision** Articles, which were evaluated by the referee and accepted by the editor with revision, continues to Waiting for Revision table.

The required revisions can be seen in "Notes" part by clicking the articles title.

In order to send any revision, Submit Revision button on the last column should be clicked. This connection will take the author to the first level of Adding Article and the author can complete the revision transaction by carrying out the steps one by one. All changes must be made in the registered file and this changed file must be resent. Author's most efficacious replies relating to the changes must be typed in "Cover Letter" part.

If the is transaction is discontinued, the system move the revised article to Submitted Manuscripts part and the transaction can be continued from here.

After the transaction was completed, the system moves the revised article to "Submitted Manuscripts" part.

**3.3.5. Submitted Manuscripts** Information related to articles can be followed through the Submitted Manuscripts line. Here you can find the information such as the article's number assigned by system, title, sending date and transaction situation. The Manuscript Details and summary files can be reached by clicking the title of the article and the Processing Status part makes it possible to follow the evaluation process of the article.

### **Article review process**

Articles uploaded to the Manuscript submission system are checked by the journal administration for format consistency and similarity rate which is required to be less than 20%. Then sent to the chief editor if found appropriate.

Articles that are not suitable are sent back to the author for correction and re-submit (sent back to the author). Studies that have not been prepared using the draft for submitting to Acta Pharmaceutica Scientia "acta\_msc\_tmp" and that have not been adapted in terms of format, will be directed to the editor-in-chief, after the 3rd time, by giving the information that "the consistency requirements have not been met".

The manuscripts sent to the chief editor will be evaluated and sent to the "language and statistics editor" if deemed appropriate.

Studies found appropriate after language-statistics editor will be sent to field editors. If the field editor does not deem it appropriate after evaluating the article scientifically, he/she will inform the editor-in-chief of its negative comments, otherwise, at least two independent referee comments will be asked.

Authors should consider that this time may take time because of the reviewer assignments and acceptance for review may take time for some cases.

Our review system is double-blind. The editor, who evaluates according to the comments of the referees, submits his/her comment and suggestion to the editor-in-chief. In this way, the article takes one of the acceptance, rejection, or revision decisions. In the case of revision, after the author revises, the editor submits his/her final opinion to the editor in chief. Editor-in-Chief conveys his final decision to the author. After the accepted articles are subjected to the final control by the journal and the corresponding author, the article starts to be included in the “accepted papers” section by giving the inactive DOI number. When the article is placed in one of the following issues, the DOI number will be activated and displayed in the “current issue” section on the journal homepage.

# EDITORIAL

# Role of clinical pharmacists in post-COVID management

Neda TANER<sup>1\*</sup>

<sup>1</sup> Department of Clinical Pharmacy, School of Pharmacy, İstanbul Medipol University, İstanbul, Türkiye

---

As the world begins to emerge from the COVID-19 pandemic, there is a critical need for healthcare providers to focus on post-COVID management. Clinical pharmacists can play a vital role in this effort, as they possess unique skills and expertise in medication management, patient education, and collaborative care.

One of the key challenges in post-COVID management is addressing the long-term effects of the disease, commonly known as long COVID. Clinical pharmacists can help by assessing and managing the pharmacological treatment of these chronic conditions, as well as monitoring for potential drug interactions and adverse effects.

In addition, clinical pharmacists can provide education to patients and other healthcare providers about the proper use of medications and the importance of medication adherence. This is especially important in the post-COVID era, as many patients may have experienced disruptions in their healthcare during the pandemic and may need support to resume their medication regimens.

Finally, clinical pharmacists can work collaboratively with other healthcare providers, such as physicians and nurses, to optimize medication therapy and ensure that patients receive the best possible care. This includes reviewing medication orders, monitoring drug therapy, and providing recommendations for dose adjustments or alternative treatments.

In conclusion, clinical pharmacists are well-positioned to play a critical role in post-COVID management. By leveraging their unique skills and expertise, they can help to address the long-term effects of the disease, provide education to patients and healthcare providers, and work collaboratively to optimize medication therapy.

**Key words:** COVID-19, clinical pharmacist

---

\*Corresponding Author: E-mail: [ntaner@medipol.edu.tr](mailto:ntaner@medipol.edu.tr)

## REFERENCES

1. Forni V, Forni G, Torrabadella P. The role of pharmacists during the COVID-19 pandemic: A scoping review of the international literature. *Res Social Adm Pharm.* 2021 Jan 1;17(1):1799-806. <https://doi.org/10.1016/j.sapharm.2020.07.003>
2. Aiyegbusi OL, Hughes SE, Turner G, et al. Symptoms, complications and management of long COVID: a review. *J R Soc Med.* 2021;114(9):428-442. doi:10.1177/01410768211032850
3. Basu D, Chavda VP, Mehta AA. Therapeutics for COVID-19 and post COVID-19 complications: An update. *Curr Res Pharmacol Drug Discov.* 2022;3:100086. doi:10.1016/j.cr-phar.2022.100086
4. Altmann DM, Boyton RJ. Decoding the unknowns in long covid. *BMJ.* 2021;372:n132. Published 2021 Feb 4. doi:10.1136/bmj.n132

# ORIGINAL ARTICLES



# Chemical constituents of *Ailanthus altissima* (Mill.) Swingle leaves growing in Egypt and their antioxidant activity

Heba R. MOHAMED<sup>1\*</sup>, Eman A. EL-WAKIL<sup>1</sup>, Maher M. EL-HASHASH<sup>2</sup>,  
El-Sayed S. ABDEL-HAMEED<sup>1</sup>

<sup>1</sup> Department of Medicinal Chemistry, Theodor Bilharz Research Institute, Kornias El-Nile, 12411 Warrak El-Hadar, Giza, Egypt

<sup>2</sup> Department of Chemistry, Faculty of Science, Ain-Shams University, El-Khalifa El-Mamoun, 11566 Abasia, Cairo, Egypt

---

## ABSTRACT

*Ailanthus altissima* Swingle (Simaroubaceae), the tree of heaven, is characterized by its vast pharmacological potential beside its rich and diverse phytochemical profile. The plant leaves dry powder was extracted with 85% aqueous methanol and the crude extract was then fractionated in sequence with petroleum ether, methylene chloride, ethyl acetate and *n*-butanol. The bioactive phytochemicals were separated from the ethyl acetate and the *n*-butanol fractions through column chromatography (CC) and quantified through HPLC-DAD. The chemical structure of the isolated pure compounds was identified through UV-Vis, <sup>1</sup>H-NMR, <sup>13</sup>C-NMR and TLC-MS spectroscopic analyses. The antioxidant activity of the pure compounds was estimated through their scavenging potential of DPPH<sup>•</sup>. Nine compounds were isolated and structurally elucidated as corilagin, astragalgin, ellagic acid, gallic acid, isoquercetin, cynaroside, tellimoside, quercetin and luteolin. Ellagic acid, gallic acid and corilagin exhibited potent antioxidant activity. Corilagin derived from *A. altissima* can serve as potent natural antioxidant alternative.

**Keywords:** *Ailanthus altissima*, antioxidant, phenolics, HPLC-DAD, corilagin

---

## INTRODUCTION

*Ailanthus altissima* Swingle had been used in the Chinese folk medicine as a remedy of many ailments such as cough, anemia, hemorrhage, diarrhea, dys-

---

\*Corresponding Author: E-mail: hebaraafatp@sci.asu.edu.eg

ORCID:

Heba R. MOHAMED: 0000-0003-2114-775X

Eman A. EL-WAKIL: 0000-0003-1173-6024

Maher M. EL-HASHASH: 0000-0003-2550-8479

El-Sayed S. ABDEL-HAMEED: 0000-0002-0482-2170

(Received 24 Jan 2023, Accepted 8 Mar 2023)

entery, hemorrhoids as well as other gastric and intestinal disorders. Furthermore, many recent reports evaluated the medicinal value of *A. altissima* which was found to possess significant antimalarial, antiplasmodial, antiviral, anti-leukemic, antimicrobial, anti-inflammatory, cytotoxic and analgesic activities<sup>1-4</sup>. Many research concerned with studying the phytochemical constituents of the various parts of *A. altissima* and evaluating their medical properties. Different phytochemicals were isolated, purified and identified from *A. altissima* including quassinoids, alkaloids, sterols, terpenoids, flavonoids, phenolics, volatile components and lignans<sup>5-10</sup>.

Presently, there is a growing concern toward finding out new and effective therapeutic compounds from natural resources, since they were found to possess equipotent pharmacological activities to the conventional synthetic drugs producing minimal side effects and less toxicity<sup>11</sup>. Plant derived natural products especially polyphenols are the best choice as they were reported to possess multiple potent biological activities against pathogenesis of many degenerative and chronic disorders<sup>12</sup>.

Recently, the oxidative stress has been implicated in the induction of many maladies such as cardiovascular disorders, cancer, rheumatoid arthritis and neurological diseases. It occurs as a result of the disturbance of the oxidant-antioxidant homeostasis within the body when the oxidants mainly reactive oxygen species (ROS) exceeds the antioxidant defense ability of the body and hence they attack the various cell components; lipid, protein and DNA causing severe and irreversible oxidative destruction to them<sup>13, 14</sup>. So that both the natural and synthetic antioxidants play a vital role in the prevention of oxidative stress mediated diseases through their scavenging ability of ROS. As many recent researches discussed the toxicity and the side effects resulted from the use of synthetic antioxidant beside their high manufacturing costs, it becomes crucial to find out novel and potent antioxidants from natural sources<sup>15</sup>.

The aim of the current study was to separate, purify and quantify the major chemical constituents in the two bioactive fractions derived from the methanol extract of *A. altissima* leaves through combination of various chromatographic techniques. Also, elucidation of the chemical structure of the isolated pure compounds via different spectroscopic tools. Moreover, investigation of the antioxidant potential of the isolated pure compounds via DPPH<sup>•</sup> scavenging activity.

## METHODOLOGY

### Chemicals and reagents

DPPH (1, 1diphenyl-2-picryl hydrazyl radical) was purchased from Sigma–Aldrich (Steinheim, Germany); Organic solvents: methanol, petroleum ether (60–80°C), ethyl acetate, *n*-butanol, methylene chloride, sulphuric acid, acetic acid all were of analytical chemical grade obtained from El- Nasr pharmaceutical chemicals Co., Egypt; Adsorbents: Polyamide 6S (high purity grade) for column chromatography was purchased from Riedel-De Haën AG, Seelze-Hannover, Germany, Lipophilic sephadex LH-20, Silica gel 90 C<sub>18</sub> - reversed phase for column chromatography and Readymade silica gel TLC cards (with fluorescent indicator 254 nm, layer thickness 0.2 mm, 20 x 20 cm aluminum cards were purchased from Sigma –Aldrich, Germany and Whatmann filter papers No. 1 and 3 mm for paper chromatography were purchased from England.

### Plant material

The leaves of *Ailanthus altissima* were collected, in September 2017, from Orman Garden, Giza, Egypt. A plant specimen was identified by Mrs. Treaze Labib (a consultant of plant taxonomy at Agriculture Ministry and the ex-director of Orman Garden) and Mrs. Rehab Mohamed Eid (a botanist at Orman Garden Herbarium). A voucher specimen (No. 198 AC) was deposited in Orman Garden Herbarium. The collected fresh leaves were dried at ambient temperature away from the sunlight and were then ground to fine powder using electric mixer.

### Extraction and fractionation processes

The plant leaves dry powder (2 Kg) was extracted with 85% aqueous methanol (7 L) at room temperature. The filtrate was further concentrated at reduced temperature and pressure via rotary evaporator (BUCHI, Germany) and the extraction process was repeated five times affording crude extract of uniform weight with yield 23.50 %. The crude methanol extract (470 g) was successively fractionated by partition using different organic solvents; petroleum ether, dichloromethane, ethyl acetate and *n*-butanol which were also evaporated under vacuum till complete dryness yielding 2.41, 38.16, 63.62, 162.00 and 143.00 g corresponding to petroleum ether, dichloromethane, ethyl acetate, *n*-butanol and aqueous fractions, respectively. The ethyl acetate and the *n*-butanol fractions derived from the methanol extract of *A. altissima* leaves possessed significant antioxidant and cytotoxic potential which could be attributed to their high content of phenolics and flavonoids <sup>4</sup> so that they were selected for subsequent chromatographic isolation procedures in order to separate and purify their active chemical constituents.

## Chromatographic isolation of phenolic compounds from bioactive fractions

The ethyl acetate fraction (30 g) and the *n*-butanol fraction (50 g) were separately loaded into column chromatography (4×91cm) filled with polyamide. Elution was started with distilled water followed by gradient mixtures of water and methanol till pure methanol. Similar fractions on PC and TLC were collected. Promising groups were re-chromatographed on sephadex LH-20, RP-C18 silica gel and preparative paper chromatography and their products were monitored on PC and TLC. Four compounds were separated from the EtOAc fraction; Compound **1** was eluted with 100% water while compound **4** was eluted with 100% methanol. Compound **2** and **3** were eluted with 5-10% and 20-40% methanol, respectively. All four compounds were purified through applying over sephadex LH-20 except for compound **3** which was purified through preparative PC, after first purification with sephadex, using 15% AcOH as eluent system for PPC. Four other compounds were separated and purified from the *n*-BuOH fraction. Also, these compounds were purified on sephadex LH-20 using gradient elution of aqueous methanol. Compound **9** was further purified on RP-C18 after sephadex LH-20. The physical properties of each compound including color and retention factor ( $R_f$ ) in three different eluting systems were detected. The used eluting systems were; 15% AcOH ( $S_1$ , PC), BAW ( $S_1$ , PC) and EtOAc: MeOH: H<sub>2</sub>O (8: 1: 1) ( $S_3$ , TLC). Moreover, each compound was subjected to UV, NMR and TLC-MS spectral analyses as well as HPLC-DAD analyses to confirm its purity and detect its concentration in both the crude extract and the fraction. The scheme of extraction, fractionation and chromatographic separation is summarized in **Figure 1**.

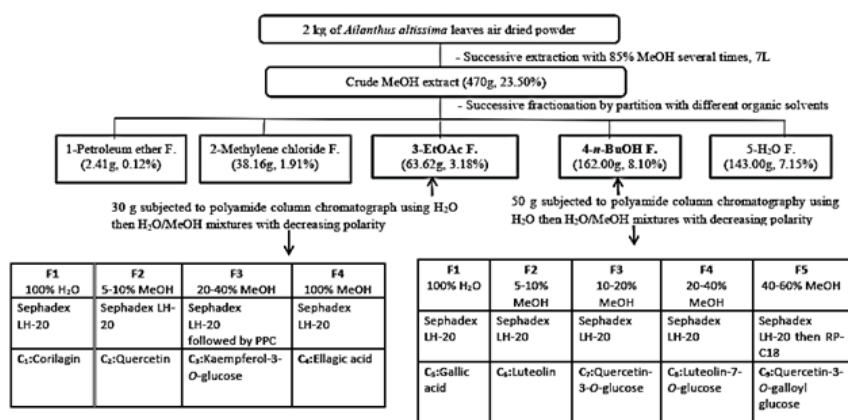


**Figure 1.** Schematic representation of extraction, fractionation and isolation of active constituents from *A. altissima* leaves

## Equipment and conditions of spectroscopic analyses

### NMR spectrometer

NMR spectrometer (Bruker Avance (III) NMR spectrometer, USA) 400MHz for  $^1\text{H}$  NMR and 100 MHz for  $^{13}\text{C}$  NMR. All analyzed compounds were dissolved in  $\text{DMSO-}d_6$ . The chemical shifts of the compounds' peaks were expressed in  $\delta_{\text{ppm}}$  and their coupling constants ( $J$ ) were expressed in Hz. The spectra were processed via MestReNova 6.0.2 software.

### Thin layer chromatography hyphenated with mass spectrometer TLC-ESI-MS

A readymade silica gel TLC card was prepared by loading the purified compounds, previously dissolved in highly purified methanol, using clean capillary tubes. The prepared card was then subjected to the TLC-MS apparatus (Advion compact mass spectrometer (CMS) NY, USA), at Nawah Scientific, which eluted each spot, separately with methanol by the assistance of the pump that is attached to the device at a flow rate of  $10\ \mu\text{L}/\text{min}$  to  $1\ \text{mL}/\text{min}$ , into the ESI mass spectrometer. The mass spectra were detected in the ESI (negative mode) between  $m/z$  100–1200. The peaks and the spectra were processed using the CheMass and Advion Data Express software.

### High performance liquid chromatography hyphenated with photodiode array detector (HPLC-DAD)

The methanol extract, the ethyl acetate, the *n*-butanol derived fractions as well as the compounds isolated and purified from *A. altissima* fractions were dissolved in HPLC grade MeOH at known concentrations, filtered using a filter membrane (pore size  $0.45\ \mu\text{m}$ , Phenex, USA) and centrifuged for 5 min at 6000 rpm then injected to the HPLC apparatus; HPLC-DAD (LC-8A liquid chromatography system hyphenated with SPD-M20A photodiode array detector Shimadzu, Kyoto, Japan) with LC solution software. The chromatographic separation was performed through RESTEK ( $5\ \mu\text{m}$ ) RP-C18 analytical column ( $4.6 \times 150\ \text{mm}$ ) and the elution occurred at a flow rate of  $1\ \text{mL}/\text{min}$ . The solvent system consisted of gradient mixtures of methanol (B) and acidified water with 0.1 % formic acid (A) starting with 5% B at 0–5 min, 5–35% B at 5–25 min, 35–40 % B at 25–49 min, 40–46 % B at 49–55 min, 46–80 % B at 55–56 min and 80–100 % B at 65–65 min. The eluate was monitored at 210 and 280 nm for the detection of the major chemical constituents in the plant extract and both fractions. The injection volume was  $40\ \mu\text{L}$  and the total run time was 65 min. The  $R_f$  and the area under the peaks corresponding to the purified compounds were recorded and hence their concentrations were calculated in both the

crude extract and the fraction from which they were separated. The column was reconditioned for 10 min before each analysis. All chromatographic operations were carried out at room temperature.

## Estimation of *in vitro* antioxidant potential

### DPPH radical scavenging activity

The antioxidant potential of the purified compounds was evaluated through their ability to neutralize DPPH<sup>•</sup> (1, 1-diphenyl-2-picrylhydrazyl radical) which is a stable dark purple radical that converts into yellow upon reduction. Different concentrations of the pure isolated compounds (60–1.25 μg/mL) in methanol were mixed with freshly prepared DPPH solution in methanol (0.09 mM) in a ratio of 1:1 according to the method described by <sup>16</sup>. The reaction mixtures were allowed to stand for 30 minutes in the dark at room temperature then the decrease in the optical density was measured at 517 nm against a blank. Ascorbic acid (AA) was used as a positive control. The scavenging ability of the isolated compounds toward DPPH<sup>•</sup> was calculated according to the following equation: DPPH<sup>•</sup> scavenging activity % =  $(A_{\text{control}} - A_{\text{sample}} / A_{\text{control}}) \times 100$  where  $A_{\text{control}}$  is the absorbance of the control solution containing methanol instead of the test sample while  $A_{\text{sample}}$  is the absorbance of the isolated compound. The determinations were carried out in triplicates and the results were expressed as SC<sub>50</sub> which is the concentration of the isolated compound required to reduce half of DPPH<sup>•</sup>.

### Statistical analysis

The statistical analyses were carried out using IBM SPSS Statistics (25) software. The results were expressed as means ± standard deviation (SD) and all experimental analyses were performed in triplicate.

### Spectroscopic data of the isolated pure compounds

**Corilagin (1''-O-galloyl-3'', 6''-hexahydroxydiphenoyl-β-D-glucopyranoside) (1):** White powder (300 mg). R<sub>f</sub> values: 0.56 (S<sub>1</sub>), 0.51 (S<sub>2</sub>) and 0.57 (S<sub>3</sub>). Color UV dark purple. UV (MeOH): λ<sub>max</sub> 209, 268 nm. C<sub>27</sub>H<sub>23</sub>O<sub>18</sub>, negative ESI-MS *m/z* 633 [M-H]<sup>-</sup>; MS<sup>2</sup> *m/z* 482 [M-H- galloyl moiety (152 amu)]<sup>-</sup>, *m/z* 301 [M-H- galloylglucose (332 amu)]<sup>-</sup>. <sup>1</sup>H NMR (400 MHz, d<sub>6</sub>-DMSO): δ<sub>H</sub> 9.05 (9H, brs, OH), 7.02 (2H, s, H-2'', 6''), 6.57 (1H, s, H-3'), 6.50 (1H, s, H-3), 6.21 (1H, d, *J* = 7.2 Hz, H-1'''), 5.82 (1H, br s, H-3'''), 4.60 (1H, s, H-4'''), 4.36 (1H, t, *J* = 8.1 Hz, H-5'''), 4.24 (1H, dd, *J* = 11.0, 7.8 Hz, H-6'''a), 3.95 (1H, dd, *J* = 10.7, 8.8 Hz, H-6'''b), 3.88 (1H, d, *J* = 7.3 Hz, H-2'''). <sup>13</sup>C NMR (100 MHz, d<sub>6</sub>-DMSO): HHDP δ<sub>c</sub> 167.62 (C-7), 167.24 (C-7'), 165.35 (C-7''), 146.00 (C-3'', 5''), 145.22 (C-4), 145.13 (C-6), 144.78 (C-4'), 144.44 (C-6'), 139.49 (C-4'').

136.00(C-5), 135.83 (C-5'), 124.33 (C-2'), 123.62 (C-2), 119.16 (C-1''), 116.24 (C-1), 115.91 (C-1'), 109.51 (C-2'',6''), 107.49 (C-3), 106.50 (C-3'), 92.73 (C-1'''), 77.68 (C-5'''), 76.71 (C-3'''), 71.86 (C-2'''), 64.37 (C-6'''), 62.57 (C-4''').

**Astragalín (kaempferol-3-O-β-D-glucopyranoside) (3):** Green powder (78 mg).  $R_f$  values: 0.57 ( $S_1$ ), 0.78 ( $S_2$ ) and 0.58 ( $S_3$ ). Color UV dark purple. UV (MeOH):  $\lambda_{\max}$  (nm): 265, 348; NaOMe: 272, 325<sup>Sh</sup>, 401;  $\text{AlCl}_3$ : 273, 303<sup>Sh</sup>, 349, 398;  $\text{AlCl}_3/\text{HCl}$ : 271, 304<sup>Sh</sup>, 348, 397; NaOAc: 274, 305<sup>Sh</sup>, 368; NaOAc/ $\text{H}_3\text{BO}_3$ : 265, 349.  $\text{C}_{21}\text{H}_{19}\text{O}_{11}$ , negative ESI-MS  $m/z$  447  $[\text{M-H}]^-$ ;  $\text{MS}^2$   $m/z$  285  $[\text{M-H-hexose unit (162 amu)}]^-$ .  $^1\text{H NMR}$  (400 MHz,  $d_6$ -DMSO):  $\delta_{\text{H}}$  12.63 (1H, s, OH-5), 8.04 (2H, d,  $J = 8.5$  Hz, H-2', 6'), 6.89 (2H, d,  $J = 8.4$  Hz, H-3', 5'), 6.41 (1H, d, 1H, H-8), 6.20 (1H, d, H-6), 5.46 (1H, d,  $J = 6.1$  Hz, H-1''), 3.60-3.10 (6H, m, H-2'',3'',4'',5'',6'').  $^{13}\text{C NMR}$  (100 MHz,  $d_6$ -DMSO):  $\delta_{\text{C}}$  177.88 (C-4), 164.72 (C-7), 161.66 (C-5), 160.41 (C-4'), 156.80 (C-2, 9), 133.76 (C-3), 131.35 (C-6'), 122.06 (C-1'), 115.60 (C-5'), 104.38 (C-10), 101.33 (C-1''), 99.18 (C-6), 94.04 (C-8), 77.94 (C-3''), 76.92 (C-5''), 74.55 (C-2''), 70.33 (C-4'), 61.38 (C-4'').

**Ellagic acid (4):** Green powder (200 mg).  $R_f$  values: 0.068 ( $S_1$ ), 0.57 ( $S_2$ ) and 0.10( $S_3$ ). Color UV violet. UV (MeOH):  $\lambda_{\max}$  253, 368 nm.  $\text{C}_{14}\text{H}_5\text{O}_8$ , negative ESI-MS  $m/z$  301  $[\text{M-H}]^-$ .  $^1\text{H NMR}$  (400 MHz,  $d_6$ -DMSO):  $\delta_{\text{H}}$  7.44(2H, s, H-5, 5').  $^{13}\text{C NMR}$  (100 MHz,  $d_6$ -DMSO):  $\delta_{\text{C}}$  159.32 (C-7, 7'), 148.26 (C-4, 4'), 139.90 (C-3, 3'), 112.46 (C-1, 1'), 110.30 (C-5, 5'), 107.62 (C-6, 6').

**Gallic acid (5):** Yellow powder (38 mg).  $R_f$  values: 0.61 ( $S_1$ ), 0.89 ( $S_2$ ) and 0.80( $S_3$ ). Color UV violet. UV (MeOH):  $\lambda_{\max}$  207, 271 nm.  $\text{C}_7\text{H}_5\text{O}_5$ , negative ESI-MS  $m/z$  168.90  $[\text{M-H}]^-$ .  $^1\text{H NMR}$  (400 MHz,  $d_6$ -DMSO):  $\delta_{\text{H}}$  6.92 (2H, s, H-2, 6);  $^{13}\text{C NMR}$  (100 MHz,  $d_6$ -DMSO):  $\delta_{\text{C}}$  168.20 (C-7), 146.01 (C-3, C-5), 138.61 (C-4), 121.14 (C-1), 109.36 (C-2, C-6).

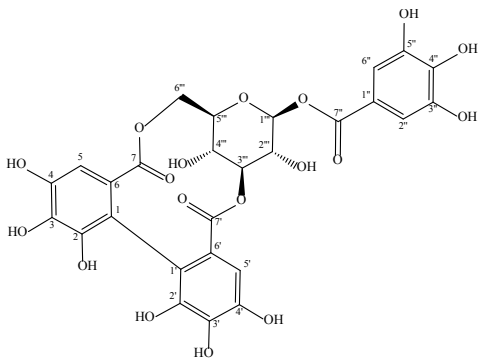
**Isoquercetin (Quercetin-3-O-β-D-glucopyranoside) (7):** Yellow amorphous powder (13 mg).  $R_f$  values: 0.54 ( $S_1$ ), 0.76 ( $S_2$ ) and 0.55 ( $S_3$ ). Color UV dark purple. UV (MeOH):  $\lambda_{\max}$  (nm) 256, 295<sup>Sh</sup>, 354; NaOMe: 271, 325<sup>Sh</sup>, 403;  $\text{AlCl}_3$ : 273, 303<sup>Sh</sup>, 332, 433;  $\text{AlCl}_3/\text{HCl}$ : 271, 301<sup>Sh</sup>, 355, 401; NaOAc: 270, 320<sup>Sh</sup>, 375; NaOAc/ $\text{H}_3\text{BO}_3$ : 265, 298<sup>Sh</sup>, 375.  $\text{C}_{21}\text{H}_{19}\text{O}_{12}$ ; negative ESI-MS  $m/z$  463  $[\text{M-H}]^-$ ;  $\text{MS}^2$   $m/z$  301  $[\text{M-H-glucosyl moiety (162 amu)}]^-$  and  $m/z$  255  $[\text{M-H-glucosyl-CO}_2\text{-H}]^-$ .  $^1\text{H NMR}$  (400 MHz,  $d_6$ -DMSO):  $\delta_{\text{H}}$  12.63 (1H, s, OH-5), 7.59 (1H, dd, H-6'), 7.57 (1H, d,  $J = 2.0$  Hz, H-2'), 6.85 (1H, d,  $J = 8.2$  Hz, H-5'), 6.40 (1H, d,  $J = 1.5$  Hz, H-8), 6.18 (1H, d,  $J = 1.6$  Hz, H-6), 5.45 (1H, d,  $J = 7.2$  Hz, H-1''), 3.58 (2H, d,  $J = 11.3$  Hz, H-6''), 3.35 (1H, d,  $J = 4.3$  Hz, H-2''), 3.32 (1H, d,  $J = 4.7$  Hz, H-3''), 3.24 (1H, d,  $J = 5.2$  Hz, H-4''), 3.09 (1H, s, H-5'').  $^{13}\text{C}$

NMR (100 MHz,  $d_6$ -DMSO):  $\delta_c$  177.81 (C-4), 165.07 (C-7), 161.61 (C-5), 156.83 (C-2), 156.66 (C-9), 148.97 (C-4'), 145.27 (C-3'), 133.71 (C-3), 122.06 (C-6'), 121.55 (C-1'), 116.60 (C-5'), 115.71 (C-2'), 104.25 (C-10), 101.35 (C-1''), 99.30 (C-6), 94.12 (C-8), 77.85 (C-3''), 76.87 (C-5''), 74.52 (C-2''), 70.28 (C-4''), 61.32 (C-6'').

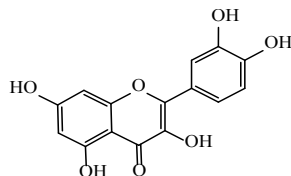
**Cynaroside (luteolin-7-O- $\beta$ -D-glucopyranoside)** (8): Yellow powder (26 mg).  $R_f$  values: 0.23 ( $S_1$ ), 0.76 ( $S_2$ ) and 0.54 ( $S_3$ ). Color UV dark purple. UV (MeOH):  $\lambda_{max}$  (nm) 255, 265<sup>Sh</sup>, 295<sup>Sh</sup>, 349; NaOMe: 265, 300<sup>Sh</sup>, 404;  $AlCl_3$ : 270, 301, 425;  $AlCl_3/HCl$ : 273, 370, 390; NaOAc: 255, 365, 400; NaOAc/ $H_3BO_3$ : 255, 371.  $C_{21}H_{19}O_{11}$ ; negative ESI-MS  $m/z$  447 [M-H]<sup>-</sup>; MS<sup>2</sup>  $m/z$  285 [M-H- glucosyl moiety (162 amu)]<sup>-</sup>. <sup>1</sup>H NMR (400 MHz,  $d_6$ -DMSO):  $\delta_H$  12.98 (1H, s, OH-5), 9.66 (1H, s, OH-3'), 7.45 (1H, dd,  $J = 8.3$  Hz, H-6'), 7.42 (1H, d, H-2'), 6.91 (1H, d,  $J = 8.3$  Hz, H-5'), 6.79 (1H, d, H-8), 6.45 (1H, d, H-6), 5.08 (1H, d,  $J = 7.1$  Hz, 1''-H), 3.73 – 3.17 (6H, m). <sup>13</sup>C NMR (100 MHz,  $d_6$ -DMSO):  $\delta_c$  182.36 (C-4), 164.94 (C-7), 161.60 (C-5), 163.41 (C-2), 157.41 (C-9), 150.38 (C-4'), 146.24 (C-3'), 103.64 (C-3), 119.64 (C-6'), 121.86 (C-1'), 116.46 (C-5'), 114.03 (C-2'), 105.81 (C-10), 100.36 (C-1''), 100.01 (C-6), 95.20 (C-8), 77.63 (C-5''), 76.86 (C-3''), 73.59 (C-2''), 70.03 (C-4''), 61.09 (C-6'').

**Tellimoside (quercetin-3-O-(6''-O-galloyl)- $\beta$ -D-glucopyranoside)** (9): Brown powder (110 mg).  $R_f$  values: 0.43 ( $S_1$ ), 0.80 ( $S_2$ ) and 0.60 ( $S_3$ ). Color UV dark purple. UV (MeOH):  $\lambda_{max}$  (nm) 263, 295<sup>Sh</sup>, 354; NaOMe: 273, 326, 408;  $AlCl_3$ : 275, 304<sup>Sh</sup>, 429;  $AlCl_3/HCl$ : 270, 300<sup>Sh</sup>, 401; NaOAc: 272, 380; NaOAc/ $H_3BO_3$ : 265, 296<sup>Sh</sup>, 375.  $C_{28}H_{23}O_{16}$ , negative ESI-MS  $m/z$  615 [M-H]<sup>-</sup>; MS<sup>2</sup>  $m/z$  301 [M-H- glucosyl- galloyl moieties (314)]<sup>-</sup>. <sup>1</sup>H NMR (400 MHz,  $d_6$ -DMSO):  $\delta_H$  12.55 (1H, s, OH-5), 9.23 (4H, s, OH-3', 3''', 4''', 5'''), 7.58 (1H, dd,  $J = 8.5$ , 2.0 Hz, H-6'), 7.44 (1H, d,  $J = 1.9$  Hz, H-2'), 6.90 (2H, s, H-2''', 6'''), 6.73 (1H, d,  $J = 8.5$  Hz, H-5'), 6.38 (1H, d,  $J = 1.4$  Hz, H-8), 6.19 (1H, d, H-6), 5.46 (1H, d,  $J = 7.1$  Hz, H-1''), 4.27 (1H, d,  $J = 11.2$  Hz, H-6''b), 4.18 (1H, dd,  $J = 11.7$ , 4.1 Hz, H-6''a), 3.43 – 3.30 (4H, m, H-2'', 3'', 4'', 5''). <sup>13</sup>C NMR (100 MHz,  $d_6$ -DMSO):  $\delta_c$  177.74 (C-4), 166.17 (C-7''), 164.58 (C-7), 161.60 (C-5), 156.94 (C-2), 156.76 (C-9), 148.87 (C-4'), 145.86 (C-3'', 5'), 145.22 (C-3'), 138.85 (C-4''), 133.77 (C-3), 122.34 (C-6'), 121.42 (C-1'), 119.77 (C-1''), 116.22 (C-5'), 115.74 (C-2'), 109.05 (C-2'', 6''), 104.35 (C-10), 101.73 (C-1''), 99.19 (C-6), 94.04 (C-8), 76.71 (C-3'''), 74.68 (C-5'''), 74.49 (C-2''), 70.01 (C-4''), 63.60 (C-6'').

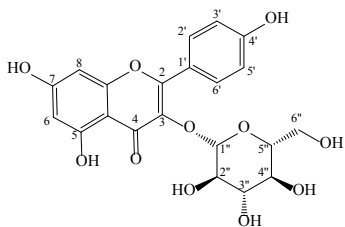
Two aglycones were separated, purified and identified based on the UV-Vis spectral analysis using different diagnostic shift reagents and co-PC, co-TLC with authentic sample which are quercetin (2, 30 mg) and luteolin (6, 30 mg).



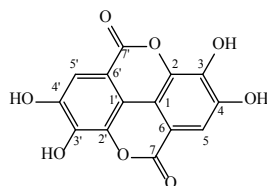
(1)



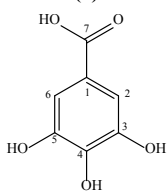
(2)



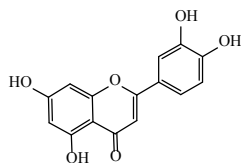
(3)



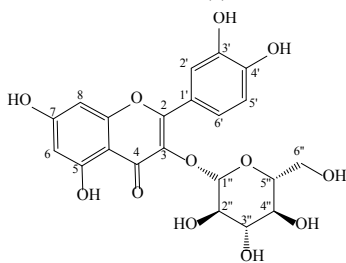
(4)



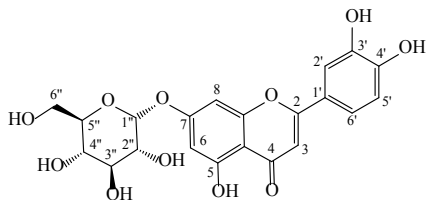
(5)



(6)



(7)



(8)

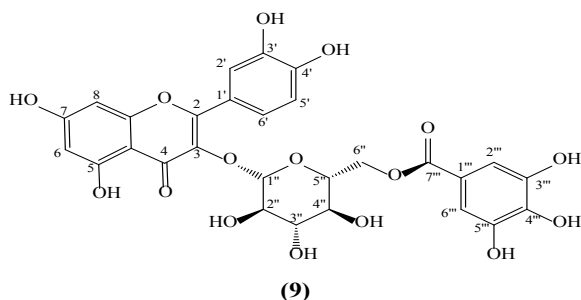


**Figure 2.** Isolated compounds from *A. altissima* leaves

**Table 1.** Pure compounds isolated from *A. altissima* leaves, their retention time and concentration in both methanol extract and derived fraction

| Fraction        | Compound     | R <sub>t</sub> (min) | Conc. (mg/g MeOH extract) | Conc. (mg/g fraction) |
|-----------------|--------------|----------------------|---------------------------|-----------------------|
| EtOAc fraction  | Corilagin    | 16.24                | 5.138                     | 19.17                 |
|                 | Ellagic acid | 32.61                | 0.55                      | 5.96                  |
|                 | Astragalín   | 34.75                | 40.85                     | 133.23                |
|                 | Quercetin    | 45.58                | 0.20                      | 15.51                 |
| n-BuOH fraction | Gallic acid  | 7.31                 | 68.96                     | 26.86                 |
|                 | Tellimoside  | 24.12                | 19.29                     | 20.744                |
|                 | Cynaroside   | 26.16                | 3.62                      | 1.73                  |
|                 | Isoquercetin | 27.58                | 20.29                     | 2.52                  |
|                 | Luteolin     | 51.01                | 0.15                      | 0.18                  |

**Table 2.** Pure compounds isolated from *A. altissima* leaves, their antioxidant potential via DPPH• scavenging activity

| Compound      | DPPH antioxidant activity (SC <sub>50</sub> µg/mL) |
|---------------|--|
| Corilagin     | 4.91±0.032   |
| Ellagic acid  | 2.26±0.027   |
| Astragalín    | 11.28±0.044  |
| Gallic acid   | 4.10±0.059   |
| Tellimoside   | 9.52±0.036   |
| Cynaroside    | 19.83±0.058  |
| Isoquercetin  | 31.83±0.302  |
| Ascorbic acid | 6.44±0.03  |

The results are represented as mean of three analyses ± SD

**Table 3.** Biological properties of compounds isolated from *A. altissima* leaves

| Cpd          | Biological properties  | Ref    |
|--------------|--|--------|
| Corilagin    | Antimicrobial, antitumor, anti-inflammatory, antidiabetic, antihypertensive, hepatoprotective, neuroprotective, cardiovascular protective            | 17     |
| Ellagic acid | Anti-allergic, anti-atherosclerotic, cardioprotective, hepatoprotective, nephroprotective, antitumor, neuroprotective                                | 18     |
| Astragalin   | anti-inflammatory, neuroprotective, cardioprotective, antiobesity, anti-osteoporotic, anticancer, antiulcer, antidiabetic                            | 19     |
| Gallic acid  | Anticancer, anti-inflammatory, cardiovascular protective, neuroprotective, antimicrobial, antiobesity, antidiabetic, hypolipidemic, gastroprotective | 20     |
| Tellimoside  | lipid peroxidation inhibitor   | 21     |
| Cynaroside   | Anticancer, antimicrobial, anti-leishmanial, anti-inflammatory   | 22, 23 |
| Isoquercetin | Anti-inflammatory, anticancer, cardioprotective, antidiabetic, anti-allergic, neuroprotective, antiviral   | 24-26  |

## RESULTS AND DISCUSSION

Nine compounds were chromatographically isolated and purified from *A. altissima* leaves; four compounds from the ethyl acetate and five other compounds from the *n*-butanol fraction derived from the methanol extract of *A. altissima* leaves. Their chemical structures were elucidated based on the collection of different spectroscopic data and their comparison with the previously published one. Compound 1 was isolated as white powder that appeared as a dark purple spot on PC that did not change on spraying with  $\text{AlCl}_3$ . The deprotonated molecule ion  $[\text{M}-\text{H}]^-$  appeared in the negative ion mode ESI-MS spectrum at  $m/z$  633 which is consistent with the molecular formula of  $\text{C}_{27}\text{H}_{23}\text{O}_{18}$ . The molecule ion was further fragmented producing two  $\text{MS}^2$  fragment ions at  $m/z$  482 due to loss of galloyl moiety (152 amu) and at  $m/z$  301 due to loss of galloylglucose (332 amu) which is a characteristic fragmentation pattern of ellagitannins<sup>27</sup>. The  $^1\text{H}$  NMR spectrum ( $d_6$ -DMSO) displayed three singlet signals in the aromatic region; two singlets assigned for the two aromatic protons (3', 3-H) of hexahydroxydiphenoyl (HHDP) which resonate at  $\delta_{\text{H}}$  6.50 and 6.57 ppm, respectively and one sharp singlet at  $\delta_{\text{H}}$  7.02 ppm for the 2'' and 6'' aromatic protons of galloyl moiety. Moreover, seven signals were observed for the protons of glucosyl unit; two singlets at  $\delta_{\text{H}}$  5.82 and 4.60 ppm due to protons attached to  $\text{C}_{3''}$ ,  $\text{C}_{4''}$ , two doublets at  $\delta_{\text{H}}$  6.21 and 3.88 ppm due to protons attached to  $\text{C}_{1''}$ ,  $\text{C}_{2''}$ , with coupling constant 7.2 and 7.3 Hz, respectively, pair of doublet of

doublet that resonate at  $\delta_{\text{H}}$  4.24 and 3.95 ppm due to protons attached to C<sub>6''a</sub>, C<sub>6''b</sub> with coupling constant 11.0, 7.8 and 10.7, 8.8 Hz, respectively and finally one triplet signal at  $\delta_{\text{H}}$  4.36 ppm for 5'''-H with coupling constant 8.1 Hz. The <sup>13</sup>C NMR spectrum of **compound 1** in *d*<sub>6</sub>-DMSO exhibited 25 signals, 14 signals for the carbons of two benzene rings of HHDP, 6 signals for the glucose moiety and 5 signals for the gallic acid unit. Furthermore, the signals at  $\delta_{\text{C}}$  167.62, 167.24 and 165.35 are indicative to the three carbonyl groups of the two benzoyl units of HHDP and that of the galloyl moiety, respectively. Based on the chromatographic and spectral analyses as well as the reported data, **compound 1** was identified as corilagin<sup>28,29</sup>. Corilagin was previously separated from *A. altissima* fruit<sup>8</sup> but it is the first time to be reported from the plant leaves.

**Compound 2** was isolated as yellow amorphous powder that appeared on PC as a yellow spot that remained yellow on spraying with AlCl<sub>3</sub> and was identified as quercetin based on the UV-Vis spectral data, comparison with previous literature and co-PC, co-TLC with authentic sample<sup>30</sup>. Quercetin was isolated before from the leaves of *A. altissima* and *A. excelsa* (Roxb)<sup>31,32</sup>, respectively.

**Compound 3** was isolated as green powder that appeared as a dark purple spot on PC that converted yellow on spraying with AlCl<sub>3</sub>. The molecule ion peak [M-H]<sup>-</sup> appeared in the ESI-MS (negative mode) at *m/z* 447 which matched with the molecular formula of C<sub>21</sub>H<sub>19</sub>O<sub>11</sub>. It was fragmented into a daughter peak of *m/z* 285 [M-H-162]<sup>-</sup> which indicated the loss of hexose unit. The <sup>1</sup>H NMR (DMSO-*d*<sub>6</sub>) exhibited two doublets at  $\delta_{\text{H}}$  6.20, 6.41 corresponding to 6-H, 8-H, respectively and one singlet at  $\delta_{\text{H}}$  12.63 ppm corresponding to 5-OH. Two doublets appeared in the HNMR at  $\delta_{\text{H}}$  (ppm) 6.89 (d, *J* = 8.4 Hz, 2H) and 8.04 (d, *J* = 8.5 Hz, 2H) corresponding to two pairs of *ortho* coupled aromatic protons (3', 5'-H and 2', 6'-H, respectively). The anomeric proton of the glycosyl unit appear as doublet at  $\delta_{\text{H}}$  5.46 ppm with coupling constant 6.1 Hz while the rest protons of the sugar unit appeared as multiplet in the aliphatic region at  $\delta_{\text{H}}$  3.60-3.10 ppm. The carbon signals of the aglycone part matched with the spectral literature of kaempferol. Moreover, the carbon signals of the sugar unit confirmed that it is *O*- $\beta$ -D-glucopyranoside. The downfield shift of both C<sub>-2</sub> and C<sub>-4</sub> as well as the upfield shift of C<sub>-3</sub> proved that the glucose unit is attached to 3-OH of kaempferol aglycone. Based on the mentioned data and reported spectral analyses, **Compound 3** was identified as astragalin<sup>33-35</sup>. Astragalin was previously isolated and identified from *A. altissima* leaves<sup>31</sup>.

**Compound 4** was isolated in the form of green powder that appeared as a violet spot on PC that did not change on spraying with AlCl<sub>3</sub>. The <sup>1</sup>H NMR of the compound dissolved in DMSO-*d*<sub>6</sub> exhibited one singlet signal at  $\delta_{\text{H}}$  7.44

ppm which is corresponding to two symmetrical aromatic protons. The  $^{13}\text{C}$  NMR of the compound in  $\text{DMSO}-d_6$  showed seven signals; one at  $\delta$  159.32 ppm corresponding to carbonyl carbon that appears down fielded due to  $\alpha$ ,  $\beta$ -unsaturated  $\delta$  lactone, the six rest signals are for five aromatic quaternary carbons and one aromatic methine carbon at  $\delta$  148.26, 139.90, 136.47, 112.46, 107.62 and 110.30, respectively. Its deprotonated molecular ion peak  $[\text{M}-\text{H}]^-$  appears at  $m/z$  301 in the negative mode of ESI-MS which is consistent with the molecular formula of  $\text{C}_{14}\text{H}_5\text{O}_8$ . From the supposed molecular formula and the  $^1\text{H}$  and  $^{13}\text{C}$  NMR spectral data the compound was identified as ellagic acid which is known by having  $\text{C}_2$  plane of symmetry that divides the structure into two typical halves each is consisted of seven carbons, primed and unprimed carbon atoms in each half, have the same chemical shift. This data was in complete agreement with the previously published data by <sup>36</sup>. Ellagic acid was one of the phenolic acids existed in the leaves of *A. altissima* <sup>37</sup>.

**Compound 5** was obtained as yellow powder that appeared as a violet spot on PC which converted into dark violet on spraying with  $\text{AlCl}_3$ . The molecular ion peak appears at  $[\text{M}-\text{H}]^-$  appears at  $m/z$  168.90 in the ESI-MS (negative mode) which is conformity with the molecular formula of  $\text{C}_7\text{H}_5\text{O}_5$ . The  $^1\text{H}$  NMR spectrum ( $\text{DMSO}-d_6$ ) exhibited sharp singlet signal at  $\delta$  6.92 ppm which revealed the presence of two identical aromatic protons (H-2 and H-6). The  $^{13}\text{C}$  NMR spectrum ( $\text{DMSO}-d_6$ ) showed five signals corresponding to seven aromatic carbon atoms that resonate at  $\delta_c$  (ppm); 109.36 (C-2, C-6), 121.14 (C-1), 138.61 (C-4), 146.01 (C-3, C-5) and 168.20 (C-7; carbonyl carbon). Compound **5** was identified as 3, 4, 5-trihydroxybenzoic acid (gallic acid) <sup>38</sup>. Gallic acid was previously reported in *A. altissima* leaves <sup>37,5</sup> and *A. altissima* root bark <sup>39</sup>.

**Compound 6** was isolated as brown powder that appeared on PC as dark purple spot that turned yellow on spraying with  $\text{AlCl}_3$ . Compound **6** was identified as luteolin based on UV-Vis spectral data and comparison with published literature <sup>40</sup>. Luteolin was previously reported in *A. altissima* leaves <sup>31,41</sup> and *A. excelsa* (Roxb) leaves <sup>32</sup>.

**Compound 7** was obtained as yellow amorphous powder that appeared as a dark purple spot on PC that turned yellow on complexing with  $\text{AlCl}_3$  spraying agent. The deprotonated molecular ion peak  $[\text{M}-\text{H}]^-$  appeared in the negative mode of ESI-MS at  $m/z$  463 which is conformity with the molecular formula of  $\text{C}_{21}\text{H}_{19}\text{O}_{12}$ . It was further fragmented into two molecule ions of  $m/z$  301  $[\text{M}-\text{H}-162]^-$  and 255 due to loss of glucosyl moiety (162 amu) and subsequent loss of a proton and a carbon dioxide molecule  $[\text{M}-\text{H}-\text{glucosyl}-\text{CO}_2-\text{H}]^-$ . The  $^1\text{H}$  NMR of the compound ( $\text{DMSO}-d_6$ ) showed a downfield singlet at  $\delta_{\text{H}}$  12.63

ppm attributed to 5-OH. Two *meta*-coupled protons appeared as doublets at  $\delta_{\text{H}}$  6.18 and 6.40 ppm with  $J$  1.6 and 1.5 Hz corresponding to 6-H and 8-H. Also, the three aromatic protons of ring B appeared forming an ABX system at  $\delta_{\text{H}}$  (ppm) 6.85 (d,  $J$  = 8.2 Hz, 1H, 5'-H), 7.57 (d,  $J$  = 2.0 Hz, 1H, 2'-H) and 7.59 (dd, 1H, 6'-H) which was overlapped with 2'-H. Moreover, a set of signals that appeared in the region  $\delta_{\text{H}}$  3.58- 3.09 ppm reflected the glycoside unit. The anomeric proton at  $\delta_{\text{H}}$  5.45 ppm which appeared as doublet with  $J$  7.2 Hz together with the  $^{13}\text{C}$  NMR chemical shifts of sugar unit carbons revealed that the sugar unit is *O*- $\beta$ -D-glucopyranoside. The rest signals of  $^{13}\text{C}$  NMR were in complete agreement with those of quercetin aglycone. The downfield shift of both C<sub>4</sub> and C<sub>2</sub> and the upfield shift of C<sub>3</sub> in comparison with the aglycone indicated that the glucosyl moiety is attached to C<sub>3</sub>. **Compound 7** was identified as isoquercetin<sup>42-44</sup> which was previously separated from *A. altissima* fruit<sup>8</sup> but it is the first time to be reported in *A. altissima* leaves.

**Compound 8** was separated as yellow powder that looked as a dark purple spot on PC that converted yellow on spraying with AlCl<sub>3</sub>. The deprotonated molecular ion peak was exhibited at  $m/z$  447 in the negative mode ESI/MS spectrum so that the molecular formula was C<sub>21</sub>H<sub>19</sub>O<sub>11</sub>. It also showed a daughter ion peak at  $m/z$  285 which suggested the loss of glucosyl unit (162 amu). The  $^1\text{H}$  NMR (DMSO-*d*<sub>6</sub>) exhibited the signals of luteolin skeleton with downfield shift of the two *meta*-coupled protons of ring A which resonated at  $\delta_{\text{H}}$  6.45 and 6.79 ppm for 6-H and 8-H, respectively revealing the glycosylation of 7-OH. A sharp singlet appeared at  $\delta_{\text{H}}$  6.75 ppm corresponding to 3-H of ring C. The presence of ABX system at  $\delta_{\text{H}}$  (ppm) 6.91 (d,  $J$  = 8.3 Hz, 1H, 5'-H), 7.42 (d, 1H, 2'-H) and 7.45 (dd,  $J$  = 8.3 Hz, 1H, 6'-H), which was overlapped with 2'-H, characteristic to disubstituted B-ring. The anomeric proton of sugar unit appeared as doublet at  $\delta_{\text{H}}$  5.08 ppm with coupling constant 7.1 Hz revealing that the sugar unit is  $\beta$ -D-glucoside. The  $^{13}\text{C}$  NMR (DMSO-*d*<sub>6</sub>) displayed 21 signals with characteristic carbonyl carbon, four oxygenated carbons and two olefinic carbons at  $\delta_{\text{C}}$  (ppm); 182.36 (C<sub>4</sub>), 163.41, 103.64 (C<sub>2</sub> and C<sub>3</sub>), 164.94, 161.60, 150.38 and 146.24 for C<sub>7</sub>, C<sub>5</sub>, C<sub>4</sub>, and C<sub>3</sub>, respectively. The downfield shift of C<sub>6</sub> and C<sub>8</sub> as well as the upfield shift of C<sub>7</sub> relative to the aglycone spectrum confirmed the glycosylation of 7-OH. **Compound 8** was identified as Cynaroside<sup>45-47</sup> that was separated before from the leaves and branches of *A. altissima*<sup>31</sup> and the leaves of *A. excelsa* (Roxb)<sup>32</sup>.

**Compound 9** was isolated as brown powder that appeared as a dark purple spot on PC that turned yellow on spraying with AlCl<sub>3</sub>. The results of ESI-MS spectrum (negative mode) indicated a molecular ion peak [M-H]<sup>-</sup> at  $m/z$  615

which is consistent with the molecular formula of  $C_{28}H_{23}O_{16}$ . The molecule ion was further fragmented producing a daughter ion at  $m/z$  301  $[M-H-314]^-$  due to loss of glucosyl and galloyl moieties with 162 and 152 amu, respectively. The  $^1H$  NMR spectrum (DMSO- $d_6$ ) displayed a sharp singlet at  $\delta_H$  6.90 ppm attributed to the two aromatic protons of galloyl moiety. Furthermore, five signals were recorded in the aromatic region that were consistent with the skeleton of quercetin 12.55 (s, 1H, 5-OH), 9.23 (s, 4H, 3'-OH), 7.58 (dd,  $J = 8.5, 2.0$  Hz, 1H, 6'-H), 7.44 (d,  $J = 1.9$  Hz, 1H, 2'-H), 6.73 (d,  $J = 8.5$  Hz, 1H, 5'-H), 6.38 (d,  $J = 1.4$  Hz, 1H, 8-H) and 6.19 (d, 1H, 6-H). It also had a distinct doublet at  $\delta_H$  5.46 ppm with  $J$  7.1 Hz which is characteristic for the  $\beta$ -anomeric proton of glucose unit that is attached to C- $_3$  of quercetin. Also, a doublet at 4.27 ppm with  $J$  11.2 Hz and a doublet of doublet at 4.18 ppm with  $J$  11.7 and 4.1 Hz reflected the two protons of glucose methine group whose hydroxyl group is esterified with gallic acid. The rest protons of glucose unit appeared as a multiplet in the region from 3.43 to 3.30 ppm. The  $^{13}C$  NMR spectrum (DMSO- $d_6$ ) contained 26 signals corresponding to 28 C- atoms; 15 carbons for the quercetin nucleus, 6 carbons for the glucosyl moiety and 5 carbons for the galloyl unit. The chemical shift of all signals is in complete agreement with reported data. The downfield shift of C- $_6''$  of glucose unit to 63.60 ppm and the upfield shift of its adjacent C- $_5''$  to 74.68 from their normal positions proved that the galloyl moiety is attached to the hydroxyl group of C- $_6''$  of glucose. Also, the downfield shift of the ortho carbon atoms (C- $_2$  and C- $_4$ ) to 156.94 and 177.74 ppm, respectively as well as the upfield shift of C- $_3$  of aglycone to 133.77 ppm indicated that the glucosyl unit is attached to the hydroxyl group at C- $_3$ . Compound **9** was identified as tellimoside <sup>48</sup>, including the hitherto unknown flavonoids, kaempferol 3-O- $\beta$ -(6''-galloyl)glucopyranoside that was previously reported in *A. altissima* leaves <sup>5</sup> and *A. altissima* fruit <sup>8</sup>.

HPLC-DAD analysis was used to obtain a phytochemical profile of the methanol extract of *A. altissima* leaves, to confirm the purity of the isolated compounds and to identify their concentration in both the crude extract and the fraction from which they were isolated by knowing their retention time and the area under the peak in the obtained chromatograms hence the concentration of the injected pure samples as well as the crude extract and the fractions were known.

HPLC-DAD analyses of the crude extract and the pure isolated compounds were represented in table 1. Corilagin (200  $\mu$ g/mL) was found at 16.24 min and its concentration in the crude extract and the ethyl acetate fraction could be 5.138 mg/g and 19.17 mg/g, respectively. Ellagic acid (200  $\mu$ g/mL) was found at 32.61 min and its concentration in the crude extract and the ethyl acetate fraction could be 0.55 mg/g and 5.96 mg/g, respectively. Astragalgin (1 mg/mL) was found at

34.75 min and its concentration in the crude extract and the ethyl acetate fraction could be 40.85 mg/g and 133.23 mg/g, respectively. Quercetin (1 mg/mL) was found at 45.58 min and its concentration in the crude extract and the ethyl acetate fraction could be 0.20 mg/g and 15.51 mg/g, respectively. Gallic acid (1 mg/mL) was found at 7.31 min and its concentration in the crude extract and the *n*-butanol derived fraction could be 68.96 mg/g and 26.86 mg/g, respectively. Tellimoside (1 mg/mL) was found at 24.12 min and its concentration in the crude extract and the *n*-butanol fraction could be 19.29 mg/g and 20.74 mg/g, respectively. Cynaroside (1 mg/mL) was found at 26.16 min and its concentration in the crude extract and the *n*-butanol fraction could be 3.62 mg/g and 1.73 mg/g, respectively. Isoquercetin (1 mg/mL) was found at 27.58 min and its concentration in the crude extract and the *n*-butanol fraction could be 20.29 mg/g and 2.52 mg/g, respectively. Luteolin (1 mg/mL) was found at 51.01 min and its concentration in the crude extract and the *n*-butanol derived fraction could be 0.15 mg/g and 0.18 mg/g, respectively. The UV spectrum of each pure compound was also recorded which was in complete agreement with our previous UV-analyses and the previously reported data. According to the previously mentioned data, the most abundant phytochemicals in the ethyl acetate fraction are astragalín followed by corilagin and in the *n*-butanol fraction are gallic acid followed by tellimoside. Furthermore, the most predominant phytochemicals in the crude methanol extract are gallic acid followed by astragalín.

The antioxidant potential of the isolated pure compounds was also evaluated through DPPH $\cdot$  scavenging technique. The results were presented in table 2. Ellagic acid exhibited the most potent antiradical activity followed by gallic acid and corilagin with IC<sub>50</sub> values of 2.26 $\pm$ 0.027, 4.10 $\pm$ 0.059, 4.91 $\pm$ 0.032  $\mu$ g/mL against DPPH $\cdot$ , respectively which were stronger than ascorbic acid that scavenged DPPH $\cdot$  with IC<sub>50</sub> value of 6.44 $\pm$ 0.03  $\mu$ g/mL. The potent antioxidant potential of the ethyl acetate derived fraction could be attributed to its richness with ellagic acid and corilagin as well as astragalín which existed in considerable amount (133.23 mg/g fraction) and exhibited strong antioxidant activity (IC<sub>50</sub> = 11.28 $\pm$ 0.044  $\mu$ g/mL). The strong antioxidant activity of the *n*-butanol derived fraction could be attributed to its content of gallic acid. Both ellagic acid and corilagin could be good candidates as potent natural anti-oxidative drugs against oxidative stress induced disorders. In addition to the antioxidant activity, the isolated phytochemicals were previously reported to possess many biological potential that are summarized in table 3<sup>17-26</sup>. These versatile activities provide more evidence for the suitability of the plant derived natural products to serve as drugs and/or drug leads in the treatment of many maladies but more investigations for their pharmacological effects are required first.

## **STATEMENT OF ETHICS**

Not required as no human participants or experimental animals were involved in the study.

## **CONFLICT OF INTERESTS**

The authors declare no conflict of interest.

## **AUTHOR CONTRIBUTIONS**

EAE, MME and ESA conceived and supervised the study. HRM performed the experimental work and wrote the first draft of the manuscript. All authors contributed to data analysis and interpretation, revising the article, gave final approval of the version to be published, and agreed to be accountable for all aspects of the work.

## **FUNDING SOURCES**

This research did not receive any specific grant from funding agencies in the public, commercial or not-for-profit sectors.

## REFERENCES

1. Joshi BC, Sharma RP, Khare A. Quassinoids and Their Chemotaxonomic Significance. *Int J Herb Med.* 2013; 1(2): 200–203.
2. Al-Snafi AE. The Pharmacological Importance of *Ailanthus Altissima*-a Review. *Int J Pharm Rev Res.* 2015; 5(2): 121–129.
3. Kim HM, Lee JS, Sezirahiga J, Kwon J, Jeong M, Lee D. A new canthinone-type alkaloid isolated from *Ailanthus altissima* Swingle. *Molecules.* 2016; 21(5): 1–10. <https://doi.org/10.3390/molecules21050642>
4. Mohamed HR, El-Wakil EA, Abdel-Hameed ES, El-Hashash MM, Shemis M. Evaluation of total phenolics, flavonoids, and antioxidant and cytotoxic potential of *Ailanthus altissima* (Mill.) Swingle leaves. *J Rep Pharm Sci.* 2021; 10(1): 130–136. <https://doi.org/10.4103/jrptps.JRPTPS>
5. Albouchi F, Hassen I, Casabianca H, Hosni K. Phytochemicals, antioxidant, antimicrobial and phytotoxic activities of *Ailanthus altissima* (Mill.) Swingle leaves. *S Afr J Bot.* 2013; 87: 164–174. <http://dx.doi.org/10.1016/j.sajb.2013.04.003>
6. Hong Z, Xiong J, Wu S, Zhu J, Hong J, Zhao Y. Tetracyclic triterpenoids and terpenylated coumarins from the bark of *Ailanthus altissima* (“Tree of Heaven”). *Phytochem.* 2013; 86: 159–167. <http://dx.doi.org/10.1016/j.phytochem.2012.10.008>
7. Wang R, Xu Q, Liu L, Liang X, Cheng L, Zhang M. Antitumour activity of 2-dihydroailanthone from the bark of *Ailanthus altissima* against U251. *Pharm Biol.* 2016; 54(9): 1641–1648. <http://dx.doi.org/10.3109/13880209.2015.1110827>
8. Ni J, Shi J, Tan Q, Chen Q. Phenylpropionamides, Piperidine, and Phenolic Derivatives from the Fruit of *Ailanthus altissima*. *Molecules.* 2017; 22: 1–12. <https://doi.org/10.3390/molecules22122107>
9. Jeong M, Kim HM, Ahn J, Lee K, Jang DS, Choi J. Chemico-Biological Interactions 9-Hydroxycanthin-6-one isolated from stem bark of *Ailanthus altissima* induces ovarian cancer cell apoptosis and inhibits the activation of tumor-associated macrophages. *Chem-Biol Interact.* 2018; 280: 99–108. <https://doi.org/10.1016/j.cbi.2017.12.011>
10. Yan Z-Y, Lv T-M, Wang Y-X, Shi S-C, Chen J-J, Bin-Lin. Terpenylated coumarins from the root bark of *Ailanthus altissima* (Mill.) Swingle. *Phytochem.* 2020; 175(2020): 112361. <https://doi.org/10.1016/j.phytochem.2020.112361>
11. Sánchez-Bonet D, García-oms S, Belda-antolí M, Padrón-Sanz C, Lloris-carsi JM, Cejalvo-Lapeña, D. RP-HPLC-DAD determination of the differences in the polyphenol content of *Fucus vesiculosus* extracts with similar antioxidant activity. *J Chromatogr B.* 2021; 1184(2021): 122978. <https://doi.org/10.1016/j.jchromb.2021.122978>
12. Simirgiotis MJ, Benites J, Areche C, Sepúlveda, B. Antioxidant capacities and analysis of phenolic compounds in three endemic *Nolana* species by HPLC-PDA-ESI-MS. *Molecules.* 2015; 20: 11490–11507. <https://doi.org/10.3390/molecules200611490>
13. Phaniendra A, Jestadi DB, Periyasamy L. Free Radicals: Properties, Sources, Targets, and Their Implication in Various Diseases. *Indian J Clin Biochem.* 2015; 30(1): 11–26. <https://doi.org/10.1007/s12291-014-0446-0>
14. Atta EM, Mohamed NH, Abdelgawad AAM. Antioxidants: an overview on the natural and synthetic types. *Eur Chem Bull.* 2017; 6(8): 365–375. <https://doi.org/10.17628/ecb.2017.6.374-384>

15. Li Z, Lan Y, Miao J, Chen X, Chen B, Liu G. Phytochemicals, antioxidant capacity and cytoprotective effects of jackfruit (*Artocarpus heterophyllus* Lam.) axis extracts on HepG2 cells. *Food Biosci.* 2021; 41(2021): 100933. <https://doi.org/10.1016/j.fbio.2021.100933>
16. El-Sayed MM, El-Hashash MM, Mohamed HR, Abdel-Lateef EE. Phytochemical Investigation and *in vitro* Antioxidant Activity of Different Leaf Extracts of *Salix mucronata* Thunb. *J Appl Pharm Sci.* 2015; 5(12): 80–85. <https://doi.org/10.7324/JAPS.2015.501213>
17. Li X, Deng Y, Zheng Z, Huang W, Chen L, Tong Q. Corilagin, a promising medicinal herbal agent. *Biomed Pharmacother.* 2018; 99(2018): 43–50. <https://doi.org/10.1016/j.biopha.2018.01.030>
18. Sharifi-Rad J, Quispe C, Castillo CMS, Caroca R, Lazo-Vélez MA, Antonyak H. Ellagic Acid: A Review on Its Natural Sources, Chemical Stability, and Therapeutic Potential. *Oxid Med Cell Longev.* 2022; 2022: 3848084. <https://doi.org/10.1155/2022/3848084>
19. Riaz A, Rasul A, Hussain G, Zahoor MK, Jabeen F, Subhani Z. Astragaloside: A Bioactive Phytochemical with Potential Therapeutic Activities. *Adv Pharmacol Sci.* 2018; 2018: 9794625. <https://doi.org/10.1155/2018/9794625>
20. Kakhkeshani N, Farzaei F, Fotouhi M, Alavi SS, Bahramsoltani R, Naseri R. Pharmacological effects of gallic acid in health and diseases : A mechanistic review. *Iran J Basic Med Sci.* 2019; 22: 225–237. <https://doi.org/10.22038/ijbms.2019.32806.7897>
21. Enkhtuya E, Shimamura T, Kashiwagi T, Ukeda H. Antioxidative constituents in the leaves of *Paeonia anomala* grown in Mongolia. *Food Sci Technol Res.* 2017; 23(1): 63–70. <https://doi.org/10.3136/fstr.23.63>
22. Zou Y, Zhang M, Zhang T, Wu J, Wang J, Liu K. Antioxidant and anti-inflammatory activities of cynaroside from *Elsholtzia bodinieri*. *Nat Prod Commun.* 2018; 13(11): 1501–1504. <https://doi.org/10.1177/1934578x1801301122>
23. Tabrez S, Rahman F, Ali R, Alouffi AS, Akand SK, Alshehri BM. Cynaroside inhibits *Leishmania donovani* UDP-galactopyranose mutase and induces reactive oxygen species to exert antileishmanial response. *Biosci Rep.* 2021; 41(1): BSR20203857. <https://doi.org/10.1042/BSR20203857>
24. Valentová K, Vrba J, Bancířová M, Ulrichová J, Křen V. Isoquercitrin: Pharmacology, toxicology, and metabolism. *Food Chem Toxicol.* 2014; 68: 267–282. <https://doi.org/10.1016/j.fct.2014.03.018>
25. Orfali GC, Duarte AC, Bonadio V, Martinez NP, Melo ME, Araújo B. Review of anticancer mechanisms of isoquercitrin. *World J Clin Oncol.* 2016; 7(2): 189–199. <http://dx.doi.org/10.5306/wjco.v7.i2.189>
26. Magar RT, Sohng JK. A Review on Structure, Modifications and Structure-Activity Relation of Quercetin and Its Derivatives. *J Microbiol Biotechnol.* 2020; 30(1): 11–20. <http://dx.doi.org/10.4014/jmb.1907.07003>
27. Dincheva I, Badjakov I, Kondakova V, Dobson P, McDougall G, Stewart D. Identification of the phenolic components in Bulgarian raspberry cultivars by LC-MS. *Int J Agric Sci Res.* 2013; 3(3): 127–138.
28. Nawwar MAM, Hussein SAM, Merfort I. NMR spectral analysis of polyphenols from *Punica granatum*. *Phytochem.* 1994; 36(3): 793–798. [http://dx.doi.org/10.1016/S0031-9422\(00\)89820-9](http://dx.doi.org/10.1016/S0031-9422(00)89820-9)
29. Kochumadhavan A, Mangal P, Kumar LS, Meenakshi BM, Venkanna BU, Muguli G. Corilagin: First Time Isolation from the Whole Plant of *Phyllanthus maderaspatensis* L. *Phar-*

- macog Commun. 2019; 9(4): 135–138. <http://dx.doi.org/10.5530/pc.2019.4.28>
30. Jain SA, Patel AD, Prajapati NK, Prajapati SP. Extraction of flavonoids of seed coat of *Bauhinia tomentosa*. Int J Chem Sci. 2011; 9(2): 657–663.
31. Jin M-I, Bae K-H, Chang H-W, Son, J-K. Anti-inflammatory compounds from the leaves of *Ailanthus altissima*. Biomol Ther. 2009; 17(1): 86–91. <http://dx.doi.org/10.4062/biomolther.2009.17.1.86>
32. Said A, Hawas UW, El-Shenawy S, Nofal SM, Rashed, K. Flavonoids and some biological activities of *Ailanthus excelsa* leaves. IUFJ J Biol. 2010; 69(1): 41–55. <http://dx.doi.org/10.18478/iufj.48603>
33. Xiao ZP, Wu HK, Wu T, Shi H, Hang B, Aisa HA. Kaempferol and quercetin flavonoids from *Rosa rugosa*. Chem Nat Compd. 2006; 42(6): 736–737. <http://dx.doi.org/10.1007/s10600-006-0267-3>
34. Duc LV, Thanh TB, Huu TN. Terpenoids from *Dicliptera chinensis* (L.) Nees Grown in Vietnam and their Anti-inflammatory Activities. Asian J Biomed Pharm Sci. 2018; 8(64): 6–13. <http://dx.doi.org/10.37285/ijpsn.2018.11.2.7>
35. Rezende FM, Ferreira MJP, Clausen MH, Rossi M, Furlan CM. Acylated flavonoid glycosides are the main pigments that determine the flower colour of the Brazilian native tree *Tibouchina pulchra* (Cham.) Cogn. Molecules. 2019; 24(4): 718–734. <http://dx.doi.org/10.3390/molecules24040718>
36. Khallouki F, Haubner R, Hull WE, Erben G, Spiegelhalder B, Bartsch H. Isolation, purification and identification of ellagic acid derivatives, catechins, and procyanidins from the root bark of *Anisophyllea dichostyla* R. Br. Food Chem Toxicol. 2007; 45(3): 472–485. <http://dx.doi.org/10.1016/j.fct.2006.09.011>
37. Luís Â, Gil N, Amaral ME, Domingues F, Duarte AP. *Ailanthus altissima* (Miller) Swingle: A source of bioactive compounds with antioxidant activity. Bioresources. 2012; 7(2): 2105–2120. <http://dx.doi.org/10.15376/biores.7.2.2105-2120>
38. Ghareeb MA, Sobeh M, El-Maadawy WH, Mohammed HS, Khalil H, Botros S. Chemical profiling of polyphenolics in *Eucalyptus globulus* and evaluation of its hepato–renal protective potential against cyclophosphamide induced toxicity in mice. Antioxidants. 2019; 8(9): 4–7. <http://dx.doi.org/10.3390/antiox8090415>
39. Tan Q, Ouyang M, Wu Z. A new seco-neolignan glycoside from the root bark of *Ailanthus altissima*. Nat Prod Res. 2012; 26 (15): 1375–1380. <http://dx.doi.org/10.1080/14786419.2011.587187>
40. Youssef S. Flavonoids from *Onopordon heteracanthum* C.A. Mey. Bull Pharm Sci. 2003; 26(1): 83–89. <http://dx.doi.org/10.21608/bfsa.2003.65472>
41. Zhelev I, Georgiev K, Dimitrova-Dyulgerova I. Carotenoid profile of *Ailanthus altissima* stem bark, *in-vitro* antioxidant and antineoplastic activities. World J Pharm Res. 2016; 5(3): 1816–1825.
42. Liu H, Mou Y, Zhao J, Wang J, Zhou L, Wang M, et al. Flavonoids from *Halostachys caspica* and their antimicrobial and antioxidant activities. Molecules. 2010; 15(11): 7933–7945. <http://dx.doi.org/10.3390/molecules15117933>
43. Manivannan R, Shopna R. Isolation of quercetin and isorhamnetin derivatives and evaluation of anti-microbial and anti-inflammatory activities of *Persicaria glabra*. Nat Prod Sci. 2015; 21(3): 170–175.
44. Aisyah LS, Yun YF, Herlina T, Julaeha E, Zainuddin A, Nurfarida I. Flavonoid com-

pounds from the leaves of *Kalanchoe prolifera* and their cytotoxic activity against P-388 murine leukemia cells. *Nat Prod Sci.* 2017; 23(2): 139–145. <http://dx.doi.org/10.20307/nps.2017.23.2.139>

45. Chiruvella KK., Mohammed A, Dampuri G, Ghanta RG, Raghavan SC. Phytochemical and Antimicrobial Studies of Methyl Angelate and Luteolin-7-O-glucoside Isolated from Callus Cultures of *Soymida febrifuga*. *Int J Biomed Sci.* 2007; 3(4): 269–278.

46. Iwashina T, Setoguchi H, Kitajima J. Flavonoids from the Leaves of *Vitex rotundifolia* (Verbenaceae), and their Qualitative and Quantitative Comparison between Coastal and Inland Populations. *Bull Natl Mus Nat Sci Ser B Bot.* 2011; 37(2): 87–94.

47. Delazar A, Nazemiyeh H, Afshar F, Barghi N, Esnaashari S, Asgharian P. Chemical compositions and biological activities of *Scutellaria pinnatifida* A. Hamilt aerial parts. *Res Pharm Sci.* 2017; 12(3): 187–195. <http://dx.doi.org/10.4103/1735-5362.207199>

48. Güvenalp Z, Demirezer LÖ. Flavonol Glycosides from *Asperula arvensis* L. *Turk J Chem.* 2005; 29(2): 163–169.

49. Nawwar M, Ayoub N, El-Raey M, Zaghoul S, Hashem A, Mostafa E. Acylated flavonol diglucosides from *Ammania auriculata*. *Z Naturforsch C J Biosci.* 2015; 70(1–2) c: 39–43. <http://dx.doi.org/10.1515/znc-2014-4165>



# Development of a liquid chromatographic method to monitorization of medazepam and lorazepam in plasma and its validation

Melike ALPERTENGE<sup>1</sup>, Emrah DURAL<sup>1\*</sup>

<sup>1</sup> Department of Pharmaceutical Toxicology, Faculty of Pharmacy, Cumhuriyet University, 58140 Sivas, Türkiye

## ABSTRACT

This study, it was aimed to develop a simple, sensitive and reliable high-performance liquid chromatographic method for simultaneous analysis of medazepam and lorazepam based on the solid-phase extraction from human blood. For the pretreatment of (500 µL) plasma sample, an efficient extraction method was developed and optimized. Separation was carried out with an ODS reverse phase C18 analytical column (150x4.0mm, 3µm). The composition of 20 mM KH<sub>2</sub>PO<sub>4</sub> buffer and methyl cyanide (6:4, v/v) was employed as the mobile phase in the chromatographic system. The ultraviolet detector was set at 220nm. Determination of coefficients values was found as 0.9928 (r<sup>2</sup>) between 500-2500 ng/mL concentrations for medazepam and 0.9983 between 20-300 ng/mL for lorazepam. It was observed that the method has successful validation test results from accuracy, sensitivity, recovery, precision, and robustness in accordance with ICH Q2R1 guidelines. The method is recommended for monitoring blood levels of lorazepam and medazepam in toxicology laboratories.

**Keywords:** Medazepam, lorazepam, solid-phase extraction, HPLC-UV, method validation

## INTRODUCTION

Medazepam, (7-chloro-2,3-dihydro-1-methyl-5-phenyl-1,4-benzodiazepine), and lorazepam (7-chloro-5-(2-chlorophenyl)-1,3-dihydro-3-hydroxy-2H-1,4-benzodiazepine-2-one) are benzodiazepine group drugs, they are used as a sedative, tranquillizer, anxiolytic, anticonvulsant, hypnotic or muscle-relaxant<sup>1</sup>. Medazepam (Figure 1-a) is metabolised to its active metabolites named

\*Corresponding Author: E-mail: emrahdural@cumhuriyet.edu.tr

ORCID:

Melike ALPERTENGE: 0000-0002-4809-6940

Emrah DURAL: 0000-0002-9320-8008

(Received 20 Jun 2022, Accepted 20 Mar 2023)

diazepam, desmethyldiazepam, and oxazepam by oxidation. The elimination half-life is 2-5 hours. Lorazepam (Figure 1-b) is eliminated by the glucuronide conjugation pathway and its elimination half-life is 10-40 hours<sup>2</sup>.

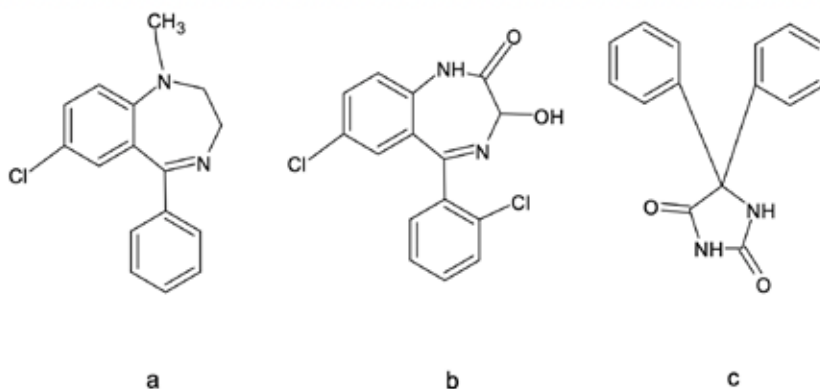


**Figure 1.** Representation of the chemical construction of medazepam (-a), lorazepam (-b) and phenytoin (-c) used as the internal standard.

Medazepam treatment leads to a wide range of toxicologically important effects ranged from enzyme induction-inhibition to genotoxic effects. Its chronic treatment is responsible for reducing human liver CYP2E1 enzyme activity. CYP2E1 inhibition can modulated the toxicity since some clinically used drugs or non-drug xenobiotics are mretabolised by CYP2E1<sup>3</sup>. In addition, the human 20 $\alpha$ -hydroxysteroid dehydrogenase (AKR1C1) inhibition by medazepam treatment was reported<sup>4</sup>. Medazepam treatment is caused to a CYP3A4 induction in the study accomplished in the primary cultures of human hepatocytes in both therapeutics and intoxicated concentrations. Medazepam was found to activate the pregnane X receptor (PXR) in hepatocarcinoma cells<sup>5</sup>. In Chinese hamster cell culture, medazepam treatment produces chromosomal abnormalities and hyperdiploidy, including a dose-dependent reduction in diploid cell count<sup>6</sup>. Chronic exposure to medazepam (5 mg/kg/day, i.p.) resulted in significant reductions in the binding affinity and receptor binding capacity of rats to muscarinic receptors. In contrast, the number of muscarinic receptor binding sites in the hippocampus was decreased<sup>7</sup>. High medazepam concentrations were detected in the plasma of newborn babies whose mothers had been used high doses of medazepam during pregnancy. Thus, placenta seems not to be a strong barrier in the transmission of medazepam. Congenital anomallies behavioral deviations and teratogenic effects have also been found to be associated with the high-dose medazepam use during pregnancy<sup>8</sup>.

In a study, Iakovidou-kritsi et al. (2009), the cytostatic and cytotoxic properties of lorazepam were investigated in human lymphocyte cultures at concentrations equivalent to a daily oral dose of 1-6 mg/day<sup>9</sup>. It was observed that lorazepam caused genotoxic effects at these concentrations<sup>9</sup>. Lorazepam, like other benzodiazepines, has been reported to cause brain dysfunction, prolongation of hospital stay, coma, and even death due to overdose or suicide, and the importance of monitoring plasma drug levels in the treatment of intoxications is important<sup>10</sup>. It has been stated that when lorazepam is used together with sedative herbs such as valerian and passionflower, it may cause intoxications with synergistic effects by increasing the GABA-A receptor activity on the central nervous system<sup>11</sup>. When mouse embryonic stem cell-derived cardiomyocyte cultures and embryonic chick heart micromass (MM) were administered with a range of lorazepam concentrations, the highest lorazepam concentration was observed to cause cytotoxic effects in the embryonic chick heart micromass. It was also observed that lorazepam causes teratogenic effects in mouse embryonic stem cells<sup>12</sup>. Therefore, the development of a reliable, sensitive and simple method for analysis of medazepam and lorazepam is critical in terms of monitoring and treatment of possible intoxication could be considered very serious in terms of public health.

There are some methods for the individual determination of medazepam and lorazepam in the literature. These methods are based on the gas chromatography mass spectrometry (GC-MS)<sup>13</sup>, micellar electrokinetic capillary chromatography (MECC)<sup>14</sup>, electrospray ionization-mass spectrometry (ESI-MS)<sup>15</sup>, and thermal desorption direct analysis real time mass spectrometry (TD-DART-MS)<sup>16</sup>. Additionally, immunoassay<sup>17</sup>, chiral column with UV and circular dichroism (CD) detection<sup>18</sup>, voltametry<sup>19</sup>, fourier transform infrared spectrophotometry (FTIR)<sup>20</sup>, gas chromatography (GC)<sup>21</sup>, high-performance liquid chromatography-electrospray tandem mass spectrometry (HPLC/MS/MS)<sup>22</sup>, liquid chromatography-tandem mass spectrometry (LC-MS/MS)<sup>23,24</sup>, capillary electrophoresis<sup>25</sup> methods were suggested for lorazepam determination. In addition, in the literature, some liquid chromatography-tandem mass spectrometry methods (LC-MS/MS) are recommended for the simultaneous determination of medazepam and lorazepam<sup>26-28</sup>. Described extraction methods are based on liquid-liquid microextraction<sup>29</sup>, solid-phase extraction<sup>30</sup>, and fiber liquid-phase microextraction (LPME)<sup>31</sup>. However, the fact that these are sophisticated instruments make difficult to carry out the relevant analyzes.

Most of these methods may be complicated, time-consuming, non-green and also expensive, that may require special sample preparation techniques and so-

phisticate instruments. HPLC is a relatively simple, repeatable and cost-effective method as compared to the other analysis techniques. Therefore, it not only provides excellent recovery with high sensitivity for a wide range of pharmaceutical compounds, but also provides a good separation opportunity for similar endogenous chemical structures and metabolites. It allows simultaneous determination of both main chemicals and metabolites and endogen metabolic products in biological samples. HPLC allows the separation, identification, quantitative measurement and purification of the components-analytes that make up a mixture that could be a biological, chemical or pharmaceutical sample.

Medazepam and lorazepam are used as benzodiazepine derivatives for different conditions and treatment purposes such as depression, alcohol withdrawal, sleep disorder, anxiety treatment, sedation, skeletal muscle relaxant, antiepileptic, chemotherapy-induced nausea and vomiting. Considering the toxicological risks that may be caused by the intoxications of these active substances, it is thought that it would be important to analyze medazepam and lorazepam together.

In this study, a repeatable, sensitive and reliable high-performance liquid chromatographic method based on solid-phase extraction for the monitoring of medazepam and lorazepam from human blood was developed. The developed method was validated in terms of sensitivity, recovery, linearity, intraday and inter-day repeatability (accuracy and precision were subtitles) and robustness tests according to the International Conference on Harmonization guideline Q2(R1) and subsequent revisions<sup>32</sup>.

## **METHODOLOGY**

### **Chemicals and reagents**

Chemical standards of medazepam and lorazepam were obtained from the Toxicology Department of Ankara University (Ankara, Türkiye) and phenytoin was donated from VEM pharmaceuticals (Istanbul, Türkiye). Analytical grade potassium chloride, sodium chloride, and sodium hydroxide were from obtained from Sigma Aldrich (Missouri, USA). Methyl cyanide ( $\geq 99.9$ ) and methyl alcohol ( $\geq 99.9$ ) were purchased from Riedel de Haen (Seelze, Germany). Di-sodium hydrogen phosphate and potassium dihydrogen phosphate were took from Merck (Darmstadt, Germany). Bovine albumin was provided by Solarbio Life Science (Beijing, China). Carmellose (carboxymethyl cellulose) was taken from Wenda (Izmir, Türkiye). Nylon membrane filter (0.45  $\mu\text{m}$  p.s., 47 mm DIA) was supplied from Millipore (MA, USA). Dionized water was gained from the Water Purification System (Buckinghamshire, UK). The solid-phase  $\text{C}_{18}$  cartridge, Sep-Pac® Vac 1 cc (0.1 g), was purchased from Waters (Dublin, Ireland).

## Instruments and equipments

Pretreatment of the specimens was achieved by a solid-phase extraction vacuum manifold that has 12- cartridge position coupled with an air pump. High-performance liquid chromatography (HPLC) system, Agilent 1100 series (CA, USA) coupled with an ultraviolet detector (G1314A, VWD), a gradient pump (G1311A, QuadPomp), a degasser (G1322A), a port of injection (Rheodyne 7725i) 20  $\mu$ L sample loop and a separation oven (G1316A, Colcom) was used performing analytical separation. Separation was achieved by a C18 (150 x 4.0 mm, 3.0  $\mu$ m particle size) column which was commercially named the ACE 3 (Tokyo, Japan) analytical column. The column oven temperature was set at 40 °C during the chromatographic run. The detection and quantitation was carried out with an ultraviolet detector at 220 nm. The mobile phase was prepared with potassium dihydrogen phosphate buffer (20 mM) pH 2.0 and acetonitrile (6:4, v/v). The phosphoric acid (0.1 and 1 M) solutions were used for pH adjustment of the mobile phase buffer. Mobile phase composition was applied isocratically to the column with 0.5 mL/min flow rate. The result composition of mobile phase solution was filtered with a nylon membrane filtered with a special vacuum system. Following, it was degassed for 20 minutes in an ultrasonic bath MRC ACP (London, UK). The elapsed time between the two analyzes was 5 minutes. The ChemStation® 08.3v software was used in the system control and data integration.

## Stock solutions preparation

Medazepam and lorazepam were prepared as 5 mg/mL, and also phenytoin (Figure 1-c) main stock solutions were prepared as 1 mg/mL by dissolving in methyl alcohol. For this purpose, 50 mg medazepam and lorazepam, and 10 mg phenytoin were dissolved individually in 10 mL flasks. Chemical standards solutions were held at -18 °C during the study.

## Artificial plasma preparation

In order to the preparation of the artificial plasma, 20 mg KCl, 20 mg  $\text{KH}_2\text{PO}_4$ , 180.6 mg  $\text{Na}_2\text{HPO}_4 \cdot 2\text{H}_2\text{O}$ , and 0.8 g NaCl and 4 g bovine albumin were dissolved in 95 mL of deionized water. Then, the solution pH was adjusted with 0.1 M KOH to 7.4 and finally, its volume made up of 100 mL<sup>33</sup>. Finally, the resulting solution was divided into 500  $\mu$ L microtubes and held at -18°C till to the analysis.

## Determination of the internal standard

In order to using as an internal standard in this investigation, clozapine, cinnarizine, chlorpromazine, flunarizine, phenytoin and sodium valproate chemical standards were individually tested. The obtained results at the indicated

chromatographic conditions were explained in the following: It was observed that cinnarizine and clozapine have unfavourable retention times. The peak widths of cinnarizine and clozapine obtained were 3 minutes, with an unsuitable width to cause disruption of the chromatogram. When they were applied to column with medazepam individually, they caused overlapping and chromatographic problems. The sodium valproate peak was not seen in this chromatographic condition, which was thought to be related to the use of the UV wavelength. In addition to this, the peak shape and structure of chlorpromazine and flunarizine were fragmented, so they did not have enough peak sharpness for use as an internal standard.

The retention time of phenytoin in the chromatogram was between the peaks of medazepam and lorazepam. It was not showed any interaction with these peaks. It has a sharp peak structure, and the efficiency obtained in extraction. The best and reproducible recovery values were obtained with phenytoin in extraction applications. Depending of these factors, phenytoin was decided to use as an internal standard in the analysis method.

### **Development of the extraction method**

At the beginning of the sample preparation studies, liquid-liquid extraction and solid-phase extraction methods were applied both STDs and ISTD. In the liquid-liquid extraction method, the human plasma sample (0,5 mL) was treated with 1000  $\mu$ L ethyl acetate. After centrifugation, the organic layer was separated to a clean micro test tube. It was evaporated at room temperature under a stream of nitrogen and redissolved in 100  $\mu$ L mobile phase. Lorazepam did not have the appropriate peak area and peak height compared to the solid-phase extraction method in all liquid-liquid extraction methods that were experimented. In addition, the observed peaks had a shape that was not suitable for quantitative analysis, and they were segmented and not sharp.

The suggested SPE method were optimized in terms of the sampling, cartridge washing, elution and conditioning of the cartridge. In the conditioning step, methanol and ultrapure water application volumes were individually tested from 1 to 5 mL for the determination of the best efficiency value. The borate buffers (pH: 8.0, 8.30 and 9.0) and water were tested for the dilution of plasma samples before application to the solid phase cardridge. Also, water and borate buffers (pH: 8.0, 8.30 and 9.0) were tested for use in the elution step of SPE in volumes ranging from 1 mL to 3 mL.

### **Preparation of the working solutions**

Working solutions of medazepam and lorazepam were prepared weekly from

main stock solutions (5 mg/mL). Medazepam were prepared as 25, 50, 75, 100, 125 µg/mL and lorazepam were prepared as 1, 2.5, 5, 10, 15 µg/mL concentrations. The main stock solution of phenytoin (1 mg/mL) was diluted by methyl alcohol to yield a working solution (50 µg/mL). Validation samples were prepared by taking 10 µL of the working solutions and dissolving them in a 500 µL virtual plasma sample. Following, it was mixed at 1800 rpm for 1 minute. Ultraviolet spectrums of medazepam (a), lorazepam (b), and phenytoin (c) were plotted at concentrations of 1 µg/mL (Figure 2).

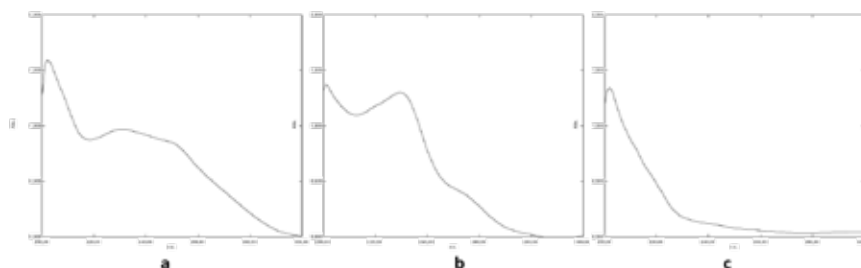


**Figure 2.** Ultraviolet spectrums of medazepam (a), lorazepam (b) and phenytoin (c).

### **Solid-phase extraction**

Initially, samples used in the validation steps were prepared. For this purpose, 10 µL of the aliquot of the working solutions of medazepam, lorazepam and phenytoin were taken separately and transferred to 500 µL of virtual plasma. Then, 0.5 mL of ultrapure water was added into the plasma solutions and this composition were mixed at 3500 rpm for 3 minutes.

Following, these prepared quality control samples were used in the validation steps 1- 4.

*Step-1. Conditioning:* Initially, methanol (3 mL) and then 3 mL ultrapure water were applied appropriately to the cartridge.

*Step-2. Sample loading:* The plasma solution, the preparation of which was described above, was carefully applied to the cartridge.

*Step-3. Washing:* Ultrapure water (2 times x 1 mL) was used for the washing of the cartridge and then it was dried with airflow in the air pump application for 3 minutes.

*Step-4. Elution:* The sample collection tube was settled in the extraction manifold and 1 mL methanol (2 times) was gently applied to the cartridge then it was vacuumed (75 kPa) until reached completely for 3 minutes to recover all liquid.

The elution (2 mL) was collected in test tube and it was placed in the heated block at 40 °C then evaporated to complete dryness with the constant flow of nitrogen (1 kpasca). 200 µL mobile phase was added on the residue. Then it was shaken with the rotative shaker at 3500 rpm for 3 minutes. Finally, the solutions were injected into the liquid chromatography by a manual injection system of 20 µL.

## **RESULTS AND DISCUSSION**

### **Method validation**

The optimum conditions of UV wavelength, mobile phase content and column were determined and plasma samples which containing analytes and internal standard (phenytoin, medazepam and lorazepam) were loaded into the HPLC system under these conditions. The method was validated in accordance with the International Harmonization Conference (ICH) guidelines in terms of the recovery, linearity, accuracy, sensitivity, precision and robustness<sup>32</sup>. A validation protocol was applied, taking into account the reproducibility of the method, to obtain accurate and precise measurements.

Under these chromatographic conditions, analyte-free blank plasma samples were applied to the HPLC system for the determination of endogenous transitions from plasma. A chromatogram sample was given in Figure 3. Retention times of medazepam, phenytoin and lorazepam were 5.2, 6.9 and 8.1 minutes, respectively, under the determined analysis conditions. A sample chromatogram of medazepam (1500 ng/mL), lorazepam (100 ng/mL) and phenytoin (1000 ng/mL) was given in Figure 4. During the analyses, it was observed that the pressure in the system varied between 85-115 bar.

### **Linearity**

After the chromatographic conditions were established, calibration curves for medazepam and lorazepam were formed in concentrations over the range 500 to 2500 ng/mL and 20 to 300 ng/mL versus peak-area ratios to the internal standard (phenytoin). The calibration points (n=5) were 500, 1000, 1500, 2000 to 2500 ng/mL for medazepam and 20, 50, 100, 200 to 300 for lorazepam, and they were prepared in drug-free plasma according to the standard addition method. After extraction procedures were performed, samples were applied to the HPLC system described conditions, and obtained data/values were evaluated and processed.

Calibration curves were constituted at 5 points (n=3) for both medazepam and lorazepam. They were drawn versus the area of phenytoin as an internal stand-

ard by the standard addition method and showed good correlations with  $r^2 = 0.9928$  and  $0.9983$ , respectively.

System suitability parameters were shown that it has a nice selectivity ( $\alpha$ ) and resolution ( $R_s$ ). Theoretical plate number ( $N$ ) and capacity factor ( $k'$ ) showed the good values for a successful determination of medazepam and lorazepam from plasma (Table 1).

**Table 1.** System suitability parameters and chromatographic characteristics of the developed method. Phenytoin was used as the internal standard in the method. For this reason determination coefficient ( $r^2$ ), selectivity factor ( $\alpha$ ), calibration range, calibration equation, and resolution ( $R_s$ ) values belonging to this agent did not be calculated.

| Analyte   | Retention time (tR) | Capacity Factor (k') | Theoretical plate number (N) | Selectivity factor ( $\alpha$ ) | Resolution ( $R_s$ ) | Calibration range (ng/mL) | Calibration equation | Determination coefficient ( $r^2$ ) |
|-----------|---------------------|----------------------|------------------------------|---------------------------------|----------------------|---------------------------|----------------------|-------------------------------------|
| Medazepam | 5.0                 | 1.2                  | 7145                         | 1.6                             | 4.3                  | 500-2500                  | $y=0.9323x+0.1094$   | 0.9928                              |
| Lorazepam | 9.0                 | 2.5                  | 10462                        | 0.3                             | 4.2                  | 20-300                    | $y=2.6179x+0.0135$   | 0.9983                              |
| Phenytoin | 7.1                 | 1.9                  | 8568                         | null                            | null                 | null                      | null                 | null                                |

Abbreviations: Theoretical plate number ( $N$ ) =  $16\left(\frac{tR}{Wt}\right)^2$ ;  $t_R$ : Retention time of the analyte peak;  $t_0$ : retention time of first peak ;  $Wt$ : peak width;

Capacity factor ( $k'$ ) =  $\frac{tR-t_0}{t_0}$ ; Resolution ( $R_s$ ) =  $\frac{\sqrt{N}}{4} \frac{(\alpha-1)}{\alpha} \frac{k}{(k+1)}$  ;

Selectivity factor ( $\alpha$ ) =  $\frac{k_2}{k_1}$ .

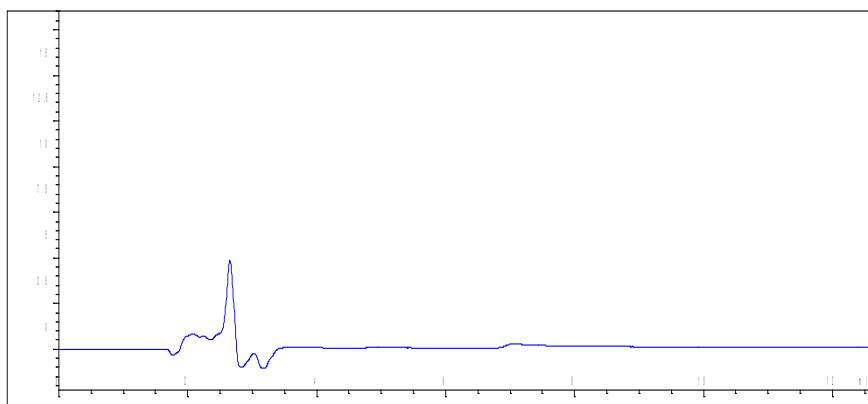


**Figure 3.** Chromatogram of an empty artificial plasma sample extracted by SPE method and prepared for analysis

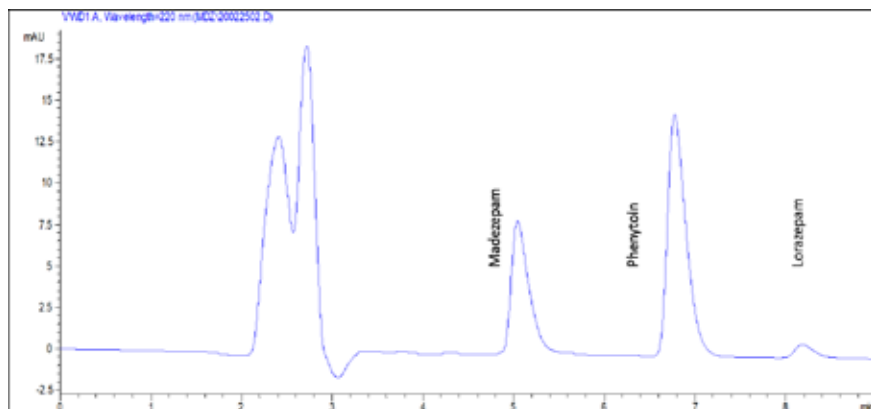


**Figure 4.** A typical chromatogram was obtained from the method exhibited medazepam (1500 ng/mL) phenytoin (1000 ng/mL) and lorazepam (100 ng/mL) peaks, respective

### Sensitivity

The quantification limit (LOQ) and detection limit (LOD) were computed based on the standard deviation of the response and the slope of the calibration graph which according to the ICH recommendation. Calculations were made according to the formulas given below.

$$\text{LOQ} = 10 \sigma/S ; \text{LOD} = 3.3 \sigma/S$$

(S: The slope of calibration curve ;  $\sigma$ : The standard deviation of the response)

The concentration of 20 ng/mL lorazepam and 500 ng/mL medazepam were used as lowest calibration points in the determination of LOD and LOQ. A total of 10 samples prepared as described above were analyzed at the same day.

Results demonstrated that the suggested method has very low sensitivity values. LOQ and LOD values of MDZ and LRZ were calculated to range between 2.86–39.69 ng/mL and 8.67–120.29 ng/mL, respectively (Table 2).

**Table 2.** Sensitivity test data applied of medazepam (500 ng/mL) and lorazepam (20 ng/mL). These results were obtained from individual samples (n=10) prepared as quality control samples in plasma.

| Analyte   | Concentration (ng/mL) | STD/STD |       |       |       | LOD (ng/mL) | LOQ (ng/mL) |
|-----------|-----------------------|---------|-------|-------|-------|-------------|-------------|
|           |                       | Average | SD    | Ratio | RSD%  |             |             |
| Medazepam | 500                   | 0.442   | 0.010 | 0.500 | 2.448 | 39.69       | 120.29      |
| Lorazepam | 20                    | 0.069   | 0.002 | 0.537 | 3.267 | 2.86        | 8.67        |
| Phenytoin | 1000                  | null    | null  | null  | null  | null        | null        |

### Accuracy and precision

The accuracy defined as the relative error (bias%) was carried out with individual replicates (n=5) both in interday and intraday. The precision, defined as the relative standard deviation (RSD%), was calculated by five separate replicate analyses of medazepam and lorazepam both intraday and inter-day. Five replicate spiked samples were assayed intraday and inter-day at the three different concentrations (500, 1500 and 2500 ng/mL for medazepam and 20, 100 and 300 ng/mL for lorazepam) for all analytes.

In order to the observing of the matrix effect, blank-plasma samples were used during the validation tests and validation test samples were prepared with the standard addition method. Accuracy was calculated and presented by the recovery percentage (RE%) and it was found between -1.16 and 4.81%. Relative standard deviations (RSD%) for precision were less than 4.11. These data showed that the method can gain precise and accurate results in plasma analysis of medazepam and lorazepam. Observed results were given in Table 3.

**Table 3.** Confidence parameters of the method include recovery and intraday - inter-day accuracy and precision values. Results were get from individual samples (n=3) prepared as quality control samples in artificial plasma.

| Analyte   | Expected concentration (ng/mL) | Intra-day |   |                  |                | Inter-day |   |                  |                |
|-----------|--------------------------------|-----------|---|------------------|----------------|-----------|---|------------------|----------------|
|           |                                | No. Obs.  | Observed concentration $\bar{x}$ $\pm$ SD (ng/mL) | Precision (RSD%) | Accuracy (RE%) | No. Obs.  | Observed concentration $\bar{x}$ $\pm$ SD (ng/mL) | Precision (RSD%) | Accuracy (RE%) |
| Medazepam | 500                            | 5         | 524.4 $\pm$ 17.2                                  | 2.41             | 4.81           | 5         | 517.2 $\pm$ 5.5                                   | 1.31             | 4.03           |
|           | 1500                           | 5         | 1569.1 $\pm$ 22.6                                 | 1.23             | 4.62           | 5         | 1553.6 $\pm$ 6.9                                  | 4.11             | 4.56           |
|           | 2500                           | 5         | 2557.1 $\pm$ 23.6                                 | 0.84             | 4.25           | 5         | 2553.4 $\pm$ 6.9                                  | 0.37             | 4.13           |
| Lorazepam | 20                             | 5         | 20.4 $\pm$ 0.8                                    | 2.91             | 2.42           | 5         | 20.7 $\pm$ 0.5                                    | 2.02             | 3.57           |
|           | 100                            | 5         | 103.9 $\pm$ 0.6                                   | 0.52             | 3.94           | 5         | 101.9 $\pm$ 2.6                                   | 2.46             | 1.96           |
|           | 300                            | 5         | 296.6 $\pm$ 9.1                                   | 2.78             | -1.16          | 5         | 302.9 $\pm$ 5.5                                   | 2.43             | 1.88           |

## Recovery

The recovery of extraction procedures from simulated plasma was determined by comparing pre-extraction spikes with post-extraction spikes. Individual replicates of spiked samples (n=5) at high, middle and low concentrations of medazepam (2500, 1500 and 500 ng/mL, respectively) and also lorazepam (200, 100 and 20 ng/mL, respectively) were prepared with and without internal standard. The obtained data were evaluated and processed.

Recovery values for medazepam and lorazepam were calculated with 3 replications of samples prepared separately from each other. Recovery values were calculated as between 96.20% and 98.25% for each analyte tabulated in Table 4. Absolute recoveries of medazepam and lorazepam were found as 97.23% and 96.87%, respectively.

**Table 4.** Observed raw recovery data and calculated recovery values of the developed analysis method

| Analyte   | Concentration (ng/mL) | STD/ISTD              |       |      |                    |       |      | Recovery (%) |
|-----------|-----------------------|-----------------------|-------|------|--------------------|-------|------|--------------|
|           |                       | Non-extracted samples |       |      | Extracted samples  |       |      |              |
|           |                       | Mean ( $\bar{x}$ )    | SD    | RSD% | Mean ( $\bar{x}$ ) | SD    | RSD% |              |
| Medazepam | 500                   | 510.22                | 22.59 | 4.84 | 490.85             | 0.016 | 3.13 | 96.20        |
|           | 1500                  | 1472.24               | 39.91 | 2.83 | 1446.51            | 0.122 | 9.39 | 98.25        |
|           | 2500                  | 2544.46               | 46.98 | 4.89 | 2474.64            | 0.081 | 4.44 | 97.25        |
| Lorazepam | 20                    | 21.32                 | 0.003 | 5.45 | 20.57              | 0.001 | 1.85 | 96.48        |
|           | 100                   | 101.63                | 0.011 | 4.18 | 99.21              | 0.005 | 1.87 | 97.61        |
|           | 300                   | 297.77                | 0.016 | 2.07 | 287.41             | 0.042 | 5.36 | 96.52        |

### Robustness

Ultraviolet wavelength value ( $\pm 1$  nm), mobile phase organic solvent component ( $\pm 5\%$ ), buffer pH ( $\pm 0.5$ ) and interpersonal variations did not cause any significant changes in the analysis results (Table 5). In addition, changes in analysts did not lead to significant changes in chromatographic signals, too. Separation robustness experiments demonstrated that the method created data of acceptable precision and accuracy. Robustness results were given in Table 5.

A  $\pm 1$  change in UV wavelength caused a 2.68% (RSD%) change in the quantitative medazepam measurement, and a 0.21% (RSD%) change in the lorazepam measurement. A 5% solvent change in the mobile phase content caused a 1.08% RSD% change in the quantitative medazepam measurement and a 2.30% RSD% change in the lorazepam measurement. A change of 0.5 unit in mobile phase buffer pH caused a 0.72% RSD% change in the quantitative medazepam measurement and a 2.76% RSD% change in the lorazepam measurement. In the robustness test application, where the operator's effect on the method was investigated in the process from sample preparation to sample ejection and calculation, the highest RSD% value for medazepam measurement was  $\leq 3.03\%$  and the highest RSD% value for lorazepam measurement was observed to be  $\leq 4.56\%$ .

**Table 5.** Robustness test results were performed by changing the detector wavelength  $\pm$  1 nm, the mobile phase content  $\pm$  5%, the buffer solution pH  $\pm$  0.5 % and the interpersonal exchange within the standard optimization conditions.

| UV (nm)                | MDZ (Area-AU) | Lorazepam (Area-AU) | MP Comp. (ACN:KH <sub>2</sub> PO <sub>4</sub> v/v) | Medazepam (Area-AU) | Lorazepam (Area-AU) | Buffer pH value        | Medazepam (Area-AU) | Lorazepam (Area-AU) | Inter-personal         | Medazepam |         | Lorazepam |        |
|------------------------|---------------|---------------------|--|---------------------|---------------------|------------------------|---------------------|---------------------|------------------------|-----------|---------|-----------|--------|
|                        |               |                     |  |                     |                     |                        |                     |                     |                        | P1        | P2      | P1        | P2     |
| 219                    | 1456.54       | 97.69               | 55:45  | 1487.80             | 102.41              | pH 1.5                 | 1489.19             | 99.12               | null                   | 1511.57   | 1512.87 | 105.45    | 107.98 |
| 220                    | 1504.29       | 101.78              | 60:40  | 1507.71             | 98.67               | pH 2.0                 | 1513.58.            | 98.45               | null                   | 1512.21   | 1503.69 | 99.42     | 98.54  |
| 221                    | 1536.97       | 103.97              | 65:35  | 1520.11             | 98.31               | pH 2.5                 | 1504.56             | 103.56              | null                   | 1482.52   | 1495.37 | 101.25    | 102.96 |
| Mean (x <sup>̄</sup> ) | 1499.26       | 101.15              | Mean (x <sup>̄</sup> )                             | 1505.21             | 98.48               | Mean (x <sup>̄</sup> ) | 1502.44             | 100.38              | Mean (x <sup>̄</sup> ) | 1506.76   | 1501.97 | 101.70    | 101.46 |
| SD                     | 40.44         | 3.18                | SD   | 16.29               | 2.27                | SD                     | 10.86               | 2.77                | SD                     | 16.95     | 8.75    | 3.09      | 4.72   |
| RSD%                   | 2.68          | 0.21                | RSD%   | 1.08                | 2.30                | RSD%                   | 0.72                | 2.76                | RSD%                   | 1.12      | 0.58    | 3.03      | 4.65   |

Abbreviation: UV: Ultraviolet; MDZ: Medazepam; LRZ: Lorazepam; P1: Person-1; P2: Person-2; MP-Comp.: Mobile Phase Composition; ACN: Acetonitrile; KH<sub>2</sub>PO<sub>4</sub>: Potassium Dihydrogen Phosphate Buffer

An accurate, sensitive, and rapid analytical method was developed to be used for the analysis and separation of two benzodiazepine compounds called medazepam and lorazepam. The chromatographic conditions were as follows: a reverse phase C<sub>18</sub> column was used and the column temperature was set to 40°C; the mobile phase consisted of 40% acetonitrile, and 60% 20 mM potassium dihydrogen phosphate buffer (pH: 2) which was adjusted by adding an phosphoric acid solution (100 mM). The mobile phase flow rate was 0.5 mL/min and the UV detector wavelength was set to 220 nm. Some prominent studies on the subject and their results are given below.

Al-Hawasli et al. (2012) developed a method for the quantitative determination of bromazepam, medazepam and midazolam from the mixture content and in different pharmaceutical preparations. It was used an analytical C<sub>18</sub> column (250 x 4.6 mm, 3  $\mu$ m) for separation and the oven was held at 50°C in the analysis. The mobile phase component was prepared with methyl alcohol: acetonitrile: 50 mM ammonium acetate-pH 9.0 (9:5:6, v/v/v). The UV detector was set to 240 nm. They used a solid phase extraction method in their work. The fact that the working range of medazepam is quite narrow, such as 80-120  $\mu$ g/mL, draws attention in a negative way. On the other hand, the

developed correlation coefficient was calculated as 0.994 ( $r^2$ ). Medazepam's retention time in the chromatogram was as high as  $\geq 8.2$  minutes. The LOD and LOQ were computed as 3.03  $\mu\text{g/mL}$  and 10.12  $\mu\text{g/mL}$ , respectively, which were lower than the sensitivity of our proposed method<sup>34</sup>.

Jinno et al. (1998) was developed an HPLC (SPME/LC) and solid-phase microextraction for simultaneous detection of benzodiazepine, including medazepam, in human urine samples. The benzodiazepine compounds were separated Superiorex ODS column ( $250 \times 1.5$  mm i.d) at 35 °C. Acetonitrile and water (35:65, v/v) were used to form the mobile phase, and the UV wavelength was set to 220 nm for the quantitative determination. The mobile phase flow rate was 1 mL/min. The method calibration was established between concentrations of 20 and 2400 ng/mL and the determination coefficient ( $r^2$ ) was calculated as 0.996. This calibration range represents a very difficult range to be linear. The limit of detection (LOD) was given as 6 ng/mL and the relative standard deviation was calculated as  $<15.0$  (RSD%). In this method, the retention time of medazepam was 125 minutes. This value makes the efficiency of the method controversial in terms of lost mobile phase amount and time<sup>35</sup>.

Muchohi et al. (2005) developed a method based on UV detection-high-performance liquid chromatography for the determination of lorazepam in child plasma. Oxazepam was used as an internal standard. Analytic separation was achieved by a reversed-phase column (150x 4.6 mm, 4  $\mu\text{m}$  i.d.) and acetonitrile and 10 mM (pH 2.4) phosphate buffer (13:7 v/v) was used for the mobile phase. The flow rate was 2.5 mL/min. In the single-step liquid-liquid extraction protocol, n-hexane and dichloromethane (7:3 v/v) were used an organic solvent. Lorazepam-retention time was 11.9 min. A calibration curve was linear between 10 to 300 ng/mL with correlation coefficients higher than 0.99. The limits of detection and quantification were 2.5 and 10 ng/mL, respectively. The relative recoveries of lorazepam were  $84.1 \pm 5.5\%$  ( $n=6$ ) and  $72.4 \pm 5.9\%$  ( $n=7$ )<sup>36</sup>.

In Sreeram et al. (2012) was developed a high-performance liquid chromatographic (HPLC) method for the determination of lorazepam in some pharmaceutical formulations. Chromatographic analysis was performed using reversed phase ODS  $C_{18}$  column in isocratic mode with mobile phase containing methanol: water (13: 7, v/v) was used. The column was kept at ambient temperature. The mobile phase flow was 1.0 mL/min. In the determination, ultraviolet wavelength was held at 230 nm. LOD was found as 35  $\mu\text{g/mL}$  and the LOQ was found as 55  $\mu\text{g/mL}$ . The recovery was higher than 91%. The relative standard deviations (RSD%) was less than 5.0<sup>37</sup>.

Uddin et al (2008) was developed a method based on the ultraviolet detection, reversed-phase high-performance liquid chromatographic method. The UV detector wavelength was set at 240 nm. In the method, they were developed an analytical method for the separation and quantification of alprazolam, bromazepam, clonazepam, diazepam, flunitrazepam, lorazepam from both pharmaceutical and biological matrices. Colchicine was used as internal standard. A Kromasil C8 column (250 × 4 mm, 5 µm i.d), equilibrated with the mobile phase methanol, ammonium acetate and 0.05 M acetonitrile (6:11:3 v/v/v) was used in the study. Mobile phase was applied to the column at the ambient temperature with a gradient flow program. A LC-18 cartridges 500 mg/3 mL and DSC-18 500 mg/3 mL were used in the determination method for the lorazepam. The calibration curve was linear in the range of 0.2 to 15 ng/mL. The correlation coefficient of calibration ( $r^2$ ) was 0.990. Within-day recovery from pharmaceutical/biological samples was between 88-111% and with RSD% in the range of 0.5–11. Between-day recovery from pharmaceutical/biological samples was between 93–110% and RSD values were in the range of 1.0–13%. The LOD and LOQ values for lorazepam were found as 0.2 – 0.5 ng/mL, respectively<sup>38</sup>.

First of all, it should be emphasized that the developed method for the determination of lorazepam (20 – 300 ng/mL) and medazepam (500 - 2500 ng/mL) in human blood is suitable not just only for the determination in the therapeutic range but also for toxic and subtherapeutic ranges of these drugs. The ability to analyze low and high concentrations of lorazepam and medazepam with the method further increased the importance of the data from the validation test in terms of the reliability of the method. The LOD and LOQ data obtained for lorazepam were 2.86 and 8.67 ng/mL, respectively, and 39.69 and 120.29 ng/mL for medazepam, indicating that the developed analysis method could be used safely at subtherapeutic doses. It was observed that the RE% (accuracy) values obtained both intraday and interdays were (-1.16) and 4.56 considering both analytes.

These data, obtained by analyzing the individual prepared samples on five different days (between days) and on the same day (within days), are a clear indication that the proposed method is repeatable and reliable both within and between days. In addition, fast run time (< 9 min), low mobile phase flow (0.5 mL/min) applied to the HPLC system during analysis, high efficiency and ease of application obtained in the extraction application, low volume of organic solvent used during extraction ( $\leq 4$  mL), are other important features that distinguish the study from other chromatographic studies in the literature. It was seen that the yield values between 96.20% and 98.25% obtained from the recovery tests

were directly related to the successful values obtained in the validation parameters such as sensitivity, selectivity, robustness and reproducibility.

The method of applying the mobile phase to the analytical column with isocratic flow has shown very significant positive effects on increasing the intraday and interday repeatability of the method (accuracy and precision). The fact that the intraday and interday precision value was  $\leq 4.11$  (RSD%) and the accuracy value was between -1.16 and 4.81 showed the consistency of the mobile phase content with the analysis performed. The reflections of these positive effects were also observed in the sensitivity (LOD and LOQ) values of the method. At the same time, the isocratic flow prevented the loss of mobile phase between analyzes according to the gradient flow. As it is known, at the end of the gradient flow, the change of the initial mobile phase composition should be balanced and the column should reach the initial mobile phase values again. This situation causes both cost and time consumption in analysis. Isocratic flow showed positive effects in preventing this situation and stabilizing the validation data. The suitability of the mobile phase composition and pH value of the mobile phase for analysis was observed both with the preliminary analyzes performed and with the validation test results obtained.

The analysis method developed and validated and applied to simulated plasma has a practical, economical and environmentally friendly sample preparation method with the use of 0.5 mL plasma and a total of 4 mL organic solvent for extraction, and the total analysis time is less than 8.5 minutes. The method was found to be linear between 0.5 and 2.5  $\mu\text{g/mL}$  for medazepam and between 20 and 300  $\text{ng/mL}$  for lorazepam. Recovery tests ( $n=3$ ) have an average recovery value of 103.7% for medazepam and 100.1% for lorazepam.

The purpose of this study develops a sensitive, sensitive and rapid analytical method. The developed method provided successful separation and detection of medazepam and lorazepam. This RP-HPLC-UV analysis method can be used in toxicological laboratories that make therapeutic and toxicological impressions of medazepam and lorazepam.

#### **STATEMENTS OF ETHICS**

Ethical approval was not required to perform this study.

#### **CONFLICT OF INTEREST STATEMENT**

None of the authors of this article has a personal or financial relationship with any organizations that may inappropriately affect or bias the content of the paper. All authors declare that there is no conflict of interest.

## **AUTHOR CONTRIBUTIONS**

Conception/Design of Study- E.D.; Data Acquisition- E.D.; Data Analysis/Interpretation-E.D., M.A.; Drafting Manuscript- E.D., M.A.; Critical Revision of Manuscript- E.D., M.A.; Final Approval and Accountability- E.D.

## **FUNDING SOURCES**

The authors declare that there are no funding sources of interest regarding the publication.

## **ACKNOWLEDGMENTS**

The authors kindly thank the Toxicology Department of Forensic Sciences Institute of Ankara University and VEM Pharmaceuticals (Tekirdağ, Türkiye) for donating analytical standards, medazepam and lorazepam, and phenytoin, respectively. In addition, the authors appreciate to “*Cumhuriyet University-Medical School Research Center*” (CUTFAM) for their open collaboration in this reasearch.

## REFERENCES

1. Papoutsis II, Athanaselis SA, Nikolaou PD, Pistos CM, Spiliopoulou CA, Maravelias CP. Development and validation of an EI-GC-MS method for the determination of benzodiazepine drugs and their metabolites in blood: Applications in clinical and forensic toxicology. *J Pharm Biomed Anal.* 2010;52(4):609–14. <https://doi.org/10.1016/j.jpba.2010.01.027>
2. Dailly E, Bourin M. The use of benzodiazepines in the aged patient: Clinical and pharmacological considerations. *Pak J Pharm Sci.* 2008;21(2):144–50.
3. Tassaneeyakul W, Birkett DJ, Miners JO. Inhibition of human hepatic cytochrome P450E1 by azole antifungals, CNS-active drugs and nonsteroidal anti-inflammatory agents. *Xenobiotica.* 1998;28(3):293–301. <https://doi.org/10.1080/004982598239579>
4. El-Kabbani O, Dhagat U, Hara A. Inhibitors of human 20 $\alpha$ -hydroxysteroid dehydrogenase (AKR1C1). *J Steroid Biochem Mol Biol.* 2011;125(1–2):105–11. <https://doi.org/10.1016/j.jsbmb.2010.10.006>
5. Vrzal R, Kubsova K, Pavek P, Dvorak Z. Benzodiazepines medazepam and midazolam are activators of pregnane X receptor and weak inducers of CYP3A4: Investigation in primary cultures of human hepatocytes and hepatocarcinoma cell lines. *Toxicol Lett.* 2010;193(2):183–8. <https://doi.org/10.1016/j.toxlet.2010.01.004>
6. Lafi A, Parry JM. A study of the induction of aneuploidy and chromosome aberrations after diazepam, medazepam, midazolam and bromazepam treatment. *Mutagenesis.* 1988;3(1):23–7. <https://doi.org/10.1093/mutage/3.1.23>
7. Popova J, Petkov V V., Tokuschieva L. The effect of chronic diazepam and medazepam treatment on the number and affinity of muscarinic receptors in different rat brain structures. *Gen Pharmacol.* 1988;19(2):227–31. [https://doi.org/10.1016/0306-3623\(88\)90066-3](https://doi.org/10.1016/0306-3623(88)90066-3)
8. Gidai J, Ács N, Bánhidly F, Czeizel AE. A study of the effects of large doses of medazepam used for self-poisoning in 10 pregnant women on fetal development. *Toxicol Ind Health.* 2008;61–8. <https://doi.org/10.1177/0748233708089016>
9. Iakovidou-kritsi Z, Akritopoulou K, Ekonomopoulou MT, Mourelatos D. *In vitro* genotoxicity of two widely used benzodiazepines: alprazolam and lorazepam. *Aristotle Univ Med J.* 2009;36:39–44.
10. Pandharipande PP, Pun BT, Herr DL, Maze M, Girard TD, Miller RR, et al. Effect of sedation with dexmedetomidine vs lorazepam on acute brain dysfunction in mechanically ventilated patients: The MENDS randomized controlled trial. *J Am Med Assoc.* 2007;298(22):2644–53. <https://doi.org/10.1001/jama.298.22.2644>
11. Jang MH, Piao XL, Kim JM, Kwon SW, Park JH. Inhibition of cholinesterase and amyloid- $\beta$  aggregation by resveratrol oligomers from *Vitis amurensis*. *Phyther Res.* 2008;22(4):544–549. <https://doi.org/10.1002/ptr.2406>
12. Ahir BK, Pratten MK. Association of anxiolytic drugs diazepam and lorazepam, and the antiepileptic valproate, with heart defects—Effects on cardiomyocytes in micromass (MM) and embryonic stem cell culture. *Reprod Toxicol.* 2011;31(1):66–74. <https://doi.org/10.1016/j.reprotox.2010.09.008>
13. Scott KS, Nakahara Y. A study into the rate of incorporation of eight benzodiazepines into rat hair. *Forensic Sci Int.* 2003;133(1–2):47–56. [https://doi.org/10.1016/s0379-0738\(03\)00049-5](https://doi.org/10.1016/s0379-0738(03)00049-5)
14. Hancu G, Gáspár A, Gyéresi Á. Separation of 1,4-benzodiazepines by micellar electrokinetic capillary chromatography. *J Biochem Biophys Methods.* 2007;69(3):251–9. <https://doi.org/10.1016/j.jbmb.2007.03.006>

doi.org/10.1016/j.jbbm.2006.02.003

15. Figueiredo EC, Sparrapan R, Sanvido GB, Santos MG, Zezzi Arruda MA, Eberlin MN. Quantitation of drugs via molecularly imprinted polymer solid phase extraction and electrospray ionization mass spectrometry: Benzodiazepines in human plasma. *Analyst*. 2011;136(18):3753–7. <https://doi.org/10.1039/c1an15198c>

16. Jones S, Sisco E, Marginean I. Analysis of benzodiazepines by thermal desorption direct analysis in real time mass spectrometry (TD-DART-MS). *Anal Methods*. 2020;12(45):5433–41. <https://doi.org/10.1039/DoAY01650K>

17. Smink BE, Mathijssen MPM, Lusthof KJ, De Gier JJ, Egberts ACG, Uges DRA. Comparison of urine and oral fluid as matrices for screening of thirty-three benzodiazepines and benzodiazepine-like substances using immunoassay and LC-MS(-MS). *J Anal Toxicol*. 2006;30(7):478–85. <https://doi.org/10.1093/jat/30.7.478>

18. Kanazawa H, Kunito Y, Matsushima Y, Okubo S, Mashige F. Stereospecific analysis of lorazepam in plasma by chiral column chromatography with a circular dichroism-based detector. *J Chromatogr A*. 2000;871(1–2):181–8. [https://doi.org/10.1016/S0021-9673\(99\)01244-3](https://doi.org/10.1016/S0021-9673(99)01244-3)

19. Norouzi P, Ganjali MR, Meibodi ASE. A novel adsorptive square wave voltammetric method for pico molar monitoring of lorazepam at gold ultra microelectrode in a flow injection system by application of fast Fourier transform analysis. *Anal Lett*. 2008;41(7):1208–24. <https://doi.org/10.1080/00032710802052601>

20. Konož E, Sarrafi AHM, Samadzadeh M, Boreiri S. Quantitative analysis of lorazepam in pharmaceutical formulation through FTIR spectroscopy. *E-Journal Chem*. 2012;9(4):2232–8. <https://doi.org/10.1155/2012/914974>

21. Perez ER, Knapp JA, Horn CK, Stillman SL, Evans JE, Arfsten DP. Comparison of LC-MS-MS and GC-MS analysis of benzodiazepine compounds included in the drug demand reduction urinalysis program. *J Anal Toxicol*. 2016;40(3):201–7. <https://doi.org/10.1093/jat/bkv140>

22. Zhu H, Luo J. A fast and sensitive liquid chromatographic-tandem mass spectrometric method for assay of lorazepam and application to pharmacokinetic analysis. *J Pharm Biomed Anal*. 2005;39(1–2):268–74. <https://doi.org/10.1016/j.jpba.2005.02.024>

23. Goucher E, Kicman A, Smith N, Jickells S. The detection and quantification of lorazepam and its 3-O-glucuronide in fingerprint deposits by LC-MS/MS. *J Sep Sci*. 2009;32(13):2266–72. <https://doi.org/10.1002/jssc.200900097>

24. Turfus SC, Braithwaite RA, Cowan DA, Parkin MC, Smith NW, Kicman AT. Metabolites of lorazepam: Relevance of past findings to present day use of LC-MS/MS in analytical toxicology. *Drug Test Anal*. 2011;3(10):695–704. <https://doi.org/10.1002/dta.305>

25. Baldacci A, Thormann W. Analysis of lorazepam and its 3O-glucuronide in human urine by capillary electrophoresis: Evidence for the formation of two distinct diastereoisomeric glucuronides. *J Sep Sci*. 2006;29(1):153–63. <https://doi.org/10.1002/jssc.200500268>

26. Moretti M, Freni F, Tomaciello I, Vignali C, Groppi A, Visonà SD, et al. Determination of benzodiazepines in blood and in dried blood spots collected from post-mortem samples and evaluation of the stability over a three-month period. *Drug Test Anal*. 2019;11(9):1403–11. <https://doi.org/10.1002/dta.2653>

27. Morini L, Vignali C, Polla M, Sponta A, Groppi A. Comparison of extraction procedures for benzodiazepines determination in hair by LC-MS/MS. *Forensic Sci Int*. 2012;218(1–3):53–6. <https://doi.org/10.1016/j.forsciint.2011.10.013>

28. Kim J, Lee S, In S, Choi H, Chung H. Validation of a simultaneous analytical method for the detection of 27 benzodiazepines and metabolites and zolpidem in hair using LC-MS/MS and its application to human and rat hair. *J Chromatogr B Anal Technol Biomed Life Sci.* 2011;879(13–14):878–86. <https://doi.org/10.1016/j.jchromb.2011.02.038>
29. Molaei K, Asgharinezhad AA, Ebrahimzadeh H, Shekari N, Jalilian N, Dehghani Z. Surfactant-assisted dispersive liquid-liquid microextraction of nitrazepam and lorazepam from plasma and urine samples followed by high-performance liquid chromatography with UV analysis. *J Sep Sci.* 2015;38(22):3905–13. <https://doi.org/10.1002/jssc.201500586>
30. Lemmer P, Schneider S, Mühe A, Wennig R. Quantification of lorazepam and lormetazepam in human breast milk using GC-MS in the negative chemical ionization mode. *J Anal Toxicol.* 2007;31(4):224–6. <https://doi.org/10.1093/jat/31.4.224>
31. de Bairros AV, de Almeida RM, Pantaleão L, Barcellos T, Silva SM e., Yonamine M. Determination of low levels of benzodiazepines and their metabolites in urine by hollow-fiber liquid-phase microextraction (LPME) and gas chromatography-mass spectrometry (GC-MS). *J Chromatogr B Anal Technol Biomed Life Sci.* 2015;975:24–33. <https://doi.org/10.1016/j.jchromb.2014.10.040>
32. ICH I. Q2 (R1): Validation of analytical procedures: text and methodology. In: International Conference on Harmonization, Geneva. 2005.
33. Mercolini L, Mandrioli R, Amore M, Raggi MA. Separation and HPLC analysis of 15 benzodiazepines in human plasma. *J Sep Sci.* 2008;31(14):2619–26. <https://doi.org/10.1002/jssc.200800212>
34. Al-Hawasli H, Al-Khayat MA, Al-Mardini MA. Development of a validated HPLC method for the separation and analysis of a Bromazepam, Medazepam and Midazolam mixture. *J Pharm Anal.* 2012;2(6):484–91. <https://doi.org/10.1016/j.jpha.2012.05.001>
35. Jinno K, Taniguchi M, Hayashida M. Solid phase micro extraction coupled with semi-microcolumn high performance liquid chromatography for the analysis of benzodiazepines in human urine. *J Pharm Biomed Anal.* 1998;17(6–7):1081–91. [https://doi.org/10.1016/S0731-7085\(98\)00074-0](https://doi.org/10.1016/S0731-7085(98)00074-0)
36. Muchohi SN, Obiero K, Kokwaro GO, Ogutu BR, Githiga IM, Edwards G, et al. Determination of lorazepam in plasma from children by high-performance liquid chromatography with UV detection. *J Chromatogr B Anal Technol Biomed Life Sci.* 2005;824(1–2):333–40. <https://doi.org/10.1016/j.jchromb.2005.07.040>
37. Sreeram V, Basaveswara Rao M, Nagendrakumar A, Sivanath M, K S. Validated RP-HPLC Method for the estimation of lorazepam in pharmaceutical formulation. *J Pharm Sci Innov.* 2012;1(6):5–8.
38. Uddin MN, Samanidou VF, Papadoyannis IN. Development and validation of an HPLC method for the determination of six 1,4-benzodiazepines in pharmaceuticals and human biological fluids. *J Liq Chromatogr Relat Technol.* 2008;31(9):1258–82. <https://doi.org/10.1080/10826070802019574>



# Biological activity and chemical composition of the essential oil from the fruits of *Ferula rigidula* Fisch. ex DC.

Gökalp İŞCAN<sup>1\*</sup>, Mine KÜRKÇÜOĞLU<sup>1</sup>, Fatma TOSUN<sup>2</sup>, Mahmut MİSKİ<sup>3</sup>

<sup>1</sup> Anadolu University, Faculty of Pharmacy, Department of Pharmacognosy, Eskişehir, Türkiye

<sup>2</sup> Istanbul Medipol University, School of Pharmacy, Department of Pharmacognosy, Istanbul, Türkiye

<sup>3</sup> Istanbul University, Faculty of Pharmacy, Department of Pharmacognosy, Istanbul, Türkiye

## ABSTRACT

The hydro-distilled essential oils of the fruits of *F. rigidula* Fisch. ex DC. was analyzed by Gas Chromatography (GC) and Gas Chromatography/Mass Spectrometry (GC/MS) systems at the same time. Thirty-one compounds were characterized representing 98.2% of the essential oils. The main components of the oil were determined as  $\alpha$ -pinene and camphene (24% and 20%, respectively). The anticandidal and antibacterial effects of the essential oil were determined by using partly modified CLSI protocols M27-A2 and M7-A7, respectively. The essential oil of the dried fruits showed several inhibitory effects on the tested bacteria panel (MIC, 62.5 to 2000  $\mu\text{g/mL}$ ) and *Candida* species (MIC, 125 to 1000  $\mu\text{g/mL}$ ).

**Keywords:** Antibacterial; anticandidal; *Ferula rigidula*; essential oil; GCMS

## INTRODUCTION

*Ferula* L., one of the largest genera in Apiaceae, has more than 220 species<sup>1</sup> and is found from central Asia to the Mediterranean region and northern Africa<sup>2</sup>. The genus is represented by 26 species, 15 of which are endemic in the Flora of Turkey<sup>3-4</sup>. *Ferula rigidula* Fisch. ex DC. is distributed throughout Türkiye's Central and Eastern Anatolia regions and adjacent areas of neighboring countries<sup>3</sup>. *F. rigidula* is known as "Çağsır, Çakşır". Leaves of *F. rigidula* have been used as vegetable and food products in Türkiye<sup>5</sup>. Aerial parts of *F. rigidu-*

\*Corresponding author: E-mail: giscan@anadolu.edu.tr

ORCIDs:

Gökalp İşcan: 0000-0003-1210-0490

Mine Kürkçüoğlu: 0000-0002-9375-0294

Fatma Tosun: 0000-0003-2533-5141

Mahmut Miski: 0000-0003-2653-0563

(Received 27 Feb 2023, Accepted 20 Mar 2023)

*la* have been used in traditional medicine to treat diabetes and hypercholesterolemia in Anatolia<sup>6</sup>. Different parts of *F. elaeochytris* Korovin<sup>6,7</sup>, *F. orientalis* L.<sup>6,8</sup>, *F. capsica* M. Bieb.<sup>6</sup>, and *F. longipedunculata* Peşmen<sup>9</sup> have been used in traditional medicine as an aphrodisiac, immunostimulant, antidiabetic, and for treatment of gastric pain and gynecologic diseases in Türkiye. Several *Ferula* species have been used in folk medicine to treat neurological disorders, stomachache, hysteria, epilepsy, infant colitis, rheumatism, headache, asthma, inflammations, dysentery, digestive disorders, dizziness, bronchitis, influenza, and arthritis and as a tranquilizer, antidiabetic, antipyretic, muscle relaxant, and antispasmodic<sup>10,11</sup>.

Recent studies have shown various species of *Ferula*, and their constituents have hypotensive, gastroprotective, neuroprotective, anti-oxidant, hepatoprotective, memory-enhancing, antimicrobial, anti-obesity, anticarcinogenic and anthelmintic effects<sup>11-14</sup>. Biological and pharmacological studies indicate that the extracts and compounds of the genus *Ferula* have various biological activities, such as antibacterial<sup>14,15</sup>, antiparasitic<sup>15</sup>, anti-inflammatory<sup>16,17</sup>, antioxidant<sup>17</sup>, antihypertensive<sup>18</sup>, antiviral<sup>19,20</sup>,  $\alpha$ -amylase and  $\alpha$ -glucosidase inhibitory activity<sup>21</sup> and cytotoxic<sup>15, 22-24</sup>.

The main phytochemical components in the genus *Ferula* are coumarins, coumarin ethers, sesquiterpenes, sesquiterpene lactones, sesquiterpene esters, monoterpenes, monoterpene coumarins, prenylated coumarins, sulfur-containing compounds, phytoestrogen, flavonoids, and carbohydrates<sup>16,25</sup>.

Several bioactivities of the different *Ferula* species essential oils have been reported, such as insecticidal, antimicrobial, immunomodulator, anti-acetylcholinesterase, antispasmodic, neuroprotective, anti-oxidant, anxiolytic,  $\alpha$ -amylase and tyrosinase inhibitory, antileishmanial and cytotoxic,<sup>21, 26-32</sup>.

Previously daucane esters<sup>33</sup> and humulane<sup>34</sup> complex esters from the hexane extract of *Ferula rigidula* roots have been reported.

A previous study reported that the aerial parts methanol extract of *F. rigidula* exhibited antibacterial, antifungal, antioxidant,  $\alpha$ -amylase,  $\alpha$ -glucosidase, cytotoxic, tyrosinase and cholinesterase inhibitory activity and total phenolic and total flavonoid contents<sup>35</sup>.

In the present study, hydrodistilled essential oil of *Ferula rigidula* fruits was analyzed by GC and GC-MS systems simultaneously and evaluated for their antibacterial and antifungal activity by using broth micro-dilution methods.

## METHODOLOGY

### Plant material

The plant material was collected from Hasan Mountain in Aksaray, Türkiye in July 2012. A voucher specimen identified by Prof. Dr. H. Duman (Gazi University, Ankara) is kept at the Herbarium of Gazi University in Ankara, Türkiye (GAZI 9898000001575).

### Isolation of the essential oil

Dried and crushed fruits of *F. rigidula* were subjected to hydro-distillation for 3 h using a Clevenger-type apparatus. The oil yield of the fruits was 0.8 % on a moisture-free basis. The oil was dried over anhydrous sodium sulfate and stored in sealed vials in the dark, at 4°C, ready for GC and GC/MS analyses and antimicrobial testing.

### GC and GC/MS conditions

The oil was analyzed by capillary GC and GC/MS using an Agilent GC-MSD system (Agilent Technologies Inc., Santa Clara, CA).

**GC/MS:** The GC/MS analysis was carried out with an Agilent 5975 GC-MSD system. Innowax FSC column (60m x 0.25mm, 0.25µm film thickness) was used with helium as carrier gas (0.8 mL/min.). GC oven temperature was kept at 60°C for 10 min and programmed to 220°C at a rate of 4°C/min, and kept constant at 220°C for 10 min and then programmed to 240°C at a rate of 1°C/min. Split ratio was adjusted 40:1. The injector temperature was at 250°C. MS were taken at 70 eV. Mass range was from  $m/z$  35 to 450.

**GC:** The GC analysis was done with an Agilent 6890N GC system fitted with a FID detector set at a temperature of 300 °C. To obtain the same elution order with GC/MS, simultaneous auto-injection was done on a duplicate of the same column applying the same operational conditions. Relative percentage amounts of the separated compounds were calculated from FID chromatograms.

### Identification of compounds

The components of essential oil were identified by comparison of their mass spectra with those in the Baser Library of Essential Oil Constituents, Wiley GC/MS Library, Adams Library, Mass Finder Library and confirmed by comparison of their retention indices. Alkanes were used as reference points in the calculation of relative retention indices (RRI). Relative percentage amounts of the separated compounds were calculated from FID chromatograms. The results of the analysis are shown in Table 1.

## Antimicrobial assay

Antibacterial and anticandidal effects of the samples were evaluated by using partly modified CLSI (formerly NCCLS) microdilution broth methods M7-A7 and M27-A2, respectively<sup>41,42</sup>. Different from the protocol essential oil solution were diluted between the concentration of 8000 to 15.6 µg/mL in DMSO.

*Escherichia coli* NRRL B-3008, *Pseudomonas aeruginosa* ATCC 27853, *Salmonella typhimurium* ATCC 13311, *Bacillus cereus* NRRL B-3711, *B. subtilis* NRRL B-4378, *Serratia marcescens* NRRL B-2544, *Staphylococcus epidermidis* ATCC 12228, *E. coli* O157:H7 RSSK 234 (RSSK; RSHM National Type Culture Collection Strains of Bacteria), two different strains of *Candida albicans* (clinically isolated, Osmangazi University, Faculty of Medicine, Department of Microbiology and ATCC 90028), *C. utilis* NRRL Y-12968, *C. krusei* NRRL Y-7179, *C. glabrata* (clinically isolated, Osmangazi University, Faculty of Medicine, Department of Microbiology and ATCC 90028) were used as the test microorganisms. Chloramphenicol (Merck), Ampicillin (Merck), Amphotericin-B (Sigma-Aldrich), and Ketoconazole (Sigma-Aldrich) were used as standard antimicrobial agents.

## RESULTS AND DISCUSSION

Hydrodistilled essential oil yield was 0.8% (v/w on dry weight basis). According to GC and GC/MS analysis results thirty-one compounds representing 98.2% of the oil were characterized and given in Table 1 with their relative percentages. The essential oil yield obtained was 0.8% (v/w).  $\alpha$ -Pinene (23.8%), camphene (19.6%), germacrene D-4-ol (8.1%) and  $\delta$ -cadinene (5.6%) were the main components.

About 60.0% of the essential oil consisted of monoterpene hydrocarbon compounds ( $\alpha$ -pinene 23.8%; camphene 19.6%; limonene 4.1%; myrcene 3.6%;  $\beta$ -pinene 2.7%; sabinene 2.5%), followed by sesquiterpenes hydrocarbons and oxygenated sesquiterpenes 18.5% ( $\delta$ -cadinene 5.6%; germacrene B 3.7%; germacrene D 2.8%; bicyclogermacrene 2.3%) and 15.7% (germacrene D-4-ol 8.1%;  $\alpha$ -cadinol 4.7%; T-muurolol 1.7%) respectively (Table 1).

**Table 1.** The Chemical composition of the essential oils of *F. rigidula*

| RR1a | RR1b  | Compounds                 | %    | IM                  |
|------|---|---------------------------|------|---------------------|
| 1032 | 1032 <sup>36</sup><br>1008-1039 <sup>37</sup>     | $\alpha$ -Pinene          | 23.8 | t <sub>R</sub> , MS |
| 1076 | 1076 <sup>36</sup><br>1043-1086 <sup>37</sup>     | Camphene                  | 19.6 | t <sub>R</sub> , MS |
| 1100 | 1100 <sup>40</sup>                                | Undecane                  | 0.4  | MS                  |
| 1118 | 1118 <sup>36</sup><br>1085-1130 <sup>37</sup>     | $\beta$ -Pinene           | 2.7  | t <sub>R</sub> , MS |
| 1132 | 1132 <sup>36</sup><br>1098-1140 <sup>37</sup>     | Sabinene                  | 2.5  | t <sub>R</sub> , MS |
| 1159 | 1122-1169 <sup>37</sup><br>1159 <sup>38</sup>     | d-3-Carene                | 0.8  | t <sub>R</sub> , MS |
| 1174 | 1174 <sup>36, 38</sup><br>1140-1175 <sup>37</sup> | Myrcene                   | 3.6  | t <sub>R</sub> , MS |
| 1203 | 1203 <sup>36, 38</sup><br>1178-1219 <sup>37</sup> | Limonene                  | 4.1  | t <sub>R</sub> , MS |
| 1210 | 1188-1233 <sup>37</sup>                           | $\beta$ -Phellandrene     | 1.1  | t <sub>R</sub> , MS |
| 1255 | 1255 <sup>36, 38</sup><br>1222-1266 <sup>37</sup> | $\gamma$ -Terpinene       | tr   | t <sub>R</sub> , MS |
| 1280 | 1280 <sup>36, 38</sup><br>1246-129 <sup>37</sup>  | $p$ -Cymene               | 0.5  | t <sub>R</sub> , MS |
| 1290 | 1290 <sup>36</sup><br>1261-1300 <sup>37</sup>     | Terpinolene               | 1.3  | t <sub>R</sub> , MS |
| 1497 | 1497 <sup>36</sup><br>1462-1522 <sup>37</sup>     | $\alpha$ -Copaene         | 0.2  | MS                  |
| 1549 | 1549 <sup>36</sup>                                | $\beta$ -Cubebene         | 0.3  | t <sub>R</sub> , MS |
| 1590 | 1592 <sup>36</sup><br>1549-1597 <sup>37</sup>     | Bornyl acetate            | 3.6  | t <sub>R</sub> , MS |
| 1600 | 1565-1608 <sup>37</sup>                           | $\beta$ -Elemene          | 0.2  | MS                  |
| 1612 | 1612 <sup>36</sup>                                | $\beta$ -Caryophyllene    | 1.0  | t <sub>R</sub> , MS |
| 1650 | 1650 <sup>36</sup>                                | $\gamma$ -Elemene         | 0.7  | t <sub>R</sub> , MS |
| 1694 | 1722 <sup>39</sup>                                | Bicyclosesquiphellandrene | 0.1  | MS                  |
| 1726 | 1726 <sup>36</sup><br>1676-1726 <sup>37</sup>     | Germacrene D              | 2.8  | MS                  |
| 1740 | 1740 <sup>36</sup>                                | $\alpha$ -Muurolene       | 0.9  | t <sub>R</sub> , MS |
| 1755 | 1755 <sup>36</sup><br>1692-1757 <sup>37</sup>     | Bicyclogermacrene         | 2.3  | t <sub>R</sub> , MS |
| 1772 | 1773 <sup>36, 38</sup><br>1722-1774 <sup>37</sup> | d-Cadinene                | 5.6  | t <sub>R</sub> , MS |

|                             |  |                   |      |                     |
|-----------------------------|--|-------------------|------|---------------------|
| 1776                        | 1776 <sup>36</sup><br>1735-1782 <sup>37</sup>    | g-Cadinene        | 0.7  | t <sub>R</sub> , MS |
| 1854                        | 1778-1854 <sup>37</sup>                          | Germacrene B      | 3.7  | MS                  |
| 1904                        | 1854-1928 <sup>37</sup>                          | Epicubebol        | 0.2  | MS                  |
| 1957                        | 1884-1964 <sup>37</sup>                          | Cubebol           | 0.2  | MS                  |
| 2069                        | 2000-2070 <sup>37</sup>                          | Germacrene D-4-ol | 8.1  | MS                  |
| 2187                        | 2136-2200 <sup>37</sup><br>2187 <sup>38</sup>    | T-Cadinol         | 0.8  | MS                  |
| 2209                        | 2205 <sup>36</sup><br>2153-2209 <sup>37</sup>    | T-Muurolol        | 1.7  | t <sub>R</sub> , MS |
| 2255                        | 2255 <sup>36</sup><br>2180-2255 <sup>37,38</sup> | α-Cadinol         | 4.7  | t <sub>R</sub> , MS |
| Monoterpene hydrocarbons    |  |                   | 60.0 |                     |
| Sesquiterpenes hydrocarbons |  |                   | 18.5 |                     |
| Oxygenated sesquiterpenes   |  |                   | 15.7 |                     |
| Others                      |  |                   | 4.0  |                     |
| Total %                     |  |                   | 98.2 |                     |
| Number of compounds         |  |                   | 31   |                     |

RRI<sup>a</sup>: RRI Relative retention indices experimentally calculated against *n*-alkanes; RRI<sup>b</sup>: RRI from literature <sup>36-40</sup> for polar column values; % calculated from FID data; t; Trace (<0.1 %); IM: Identification Method: t<sub>R</sub>, Identification based on comparison with co-injected with standards on a HP Innowax column; MS, identified on the basis of computer matching of the mass spectra with those of the libraries.

Previously, the fruit essential oil of another three population (Ankara, *Çubuk Dam*; Malatya, *Sürgü-Erkenek* and Malatya, *Doğanşehir-Polat* in 2002) of *Ferula rigidula* were analyzed. Fruits essential oils were characterized by the presence of camphene (15%), α-pinene (13%), δ-cadinene (13%), α-cadinol (10%) and germacrene D-4-ol (10%) from Ankara; α-pinene (60%), β-pinene (14%), tricyclene (8%), naphthalene (6%) and eremophilene (3%) from Malatya, *Sürgü-Erkenek*; α-pinene (68%), tricyclene (9%) and β-pinene (4%) from Malatya, *Doğanşehir-Polat*<sup>43</sup>.

According to microdilution broth assays the essential oil of *F. rigidula* fruits was demonstrated weak to moderate antimicrobial effects having MIC values of 62.5 to 2000 mg/ml when compared to standard agents. Interestingly *B.*

*subtilis* was the most susceptible strain that inhibited at the concentration of 62.5 mg/ml of the oil (Table 2). *B. subtilis* has been associated with foodborne illness with vomiting and diarrhea was also frequently reported<sup>44</sup>.

**Table 2.** Antibacterial effect of *F. rigidula* essential oil (MIC, µg/mL)

| Microorganisms                    | E0   | S1   | S2   |
|-----------------------------------|------|------|------|
| <i>Escherichia coli</i>           | 2000 | 3.9  | 1    |
| <i>Pseudomonas aeruginosa</i>     | 1000 | 62.5 | 15.6 |
| <i>Salmonella typhimurium</i>     | 1000 | 3.9  | 1    |
| <i>Bacillus cereus</i>            | 1000 | 7.8  | 1    |
| <i>Bacillus subtilis</i>          | 62.5 | 1.9  | 1    |
| <i>Serratia marcescens</i>        | 1000 | 15.6 | 15.6 |
| <i>Staphylococcus epidermidis</i> | 2000 | 3.9  | 1    |
| <i>E. coli</i> O157:H7            | 2000 | 3.9  | 1    |

**EO:** Dried fruits essential oil of *F. rigidula*, **S1:** Chloramphenicol, **S2:** Ampicillin

Tested *Candida* species were inhibited by the essential oil in the range of 125 to 2000 mg/ml. *C. albicans* and *C. utilis* were the most susceptible strains in the test panel (Table 3). To our knowledge, no previous study has been published about the antimicrobial effects of *F. rigidula* essential oil. In a previous study, methanol extract of the roots of *F. rigidula* was evaluated for its antimicrobial activity against 7 different pathogenic bacteria and 8 fungi<sup>45</sup>. Minimal inhibitory concentrations of the extract were 270 to 1500 mg/ml against bacteria panel while the antifungal growth inhibition doses were between the 100 to 750 mg/ml.

**Table 3.** Anticandidal effect of *F. rigidula* essential oil (MIC, µg/mL)

| Microorganisms            | E0   | S1   | S2   |
|---------------------------|------|------|------|
| <i>Candida albicans</i> * | 125  | 0.05 | 0.1  |
| <i>Candida utilis</i>     | 125  | 1.6  | 0.05 |
| <i>Candida tropicalis</i> | 2000 | 0.2  | 0.2  |
| <i>Candida krusei</i>     | 500  | 1.6  | 0.2  |
| <i>Candida albicans</i>   | 1000 | 0.1  | 0.2  |
| <i>Candida glabrata</i>   | 500  | 3.2  | 0.2  |

**EO:** Dried fruits Essential Oil of *F. rigidula*, **S1:** Ketoconazole, **S2:** Amphotericin-B, \*: Clinically isolated strain,

Essential oils appear to be a possible antimicrobial agents and option for synthetic substances, based on the so many research papers and reviews. There is a huge demand for the new bioactive natural alternatives for pharmaceutical and food industries<sup>46-51</sup>.

In the present study, antibacterial and anticandidal potential of the essential oil obtained from the fruits of *F. rigidula* were evaluated for the first time here. As a foodborne pathogen *B. subtilis* was the most susceptible strain in the test panel. Further studies with various human and foodborne pathogens will demonstrate the therapeutic properties of this oil.

## REFERENCES

1. Plants of the World Online- Royal Botanical Gardens, Kew. <https://powo.science.kew.org/taxon/30105171-2#publications>
2. Pimenov MG, Leonov MV. The Asian Umbelliferae biodiversity database (ASIUM) with particular reference to South-West Asian taxa. *Turk J Bot.* 2004; 28: 139–145.
3. Peşmen H. *Ferula* L. In *Flora of Turkey and the East Aegean Islands*. Davis, PH Ed., Edinburgh University Press, Edinburgh, 1972; Vol.4, pp 440-453.
4. Tuncay HO, Akalın E, Doğru-Koca A, Eruçar FM, Miski M. Two new *Ferula* (Apiaceae) species from central Anatolia: *Ferula turcica* and *Ferula latialata*. *Horticulturae*. 2023; 9(2), 144. <https://doi.org/10.3390/horticulturae9020144>
5. Baytop T. *Therapy with Medicinal Plants in Turkey-Past and Present*. Nobel Tip Kitabevleri, Istanbul, 1999; pp. 348–349.
6. Altundag E, Ozturk M. Ethnomedicinal studies on the plant resources of east Anatolia, Turkey. *Proc Soc Behav Sci.* 2011; 19: 756–777. <http://dx.doi.org/10.1016/j.sbspro.2011.05.195>
7. Güzel Y, Güzelşemme M., Miski M. Ethnobotany of medicinal plants used in Antakya: a multicultural district in Hatay Province of Turkey. *J Ethnopharmacol.* 2015; 174: 118–152. [doi.org/10.1016/j.jep.2015.07.042](https://doi.org/10.1016/j.jep.2015.07.042).
8. Mükemre M, Behçet L, Çakılcıoğlu U. Ethnobotanical study on medicinal plants in villages of Çatak (Van-Turkey). *J Ethnopharmacol.* 2015; 166: 361–374. [doi.org/10.1016/j.jep.2015.03.040](https://doi.org/10.1016/j.jep.2015.03.040).
9. Demirci S, Özhatay N. An ethnobotanical study in Kahramanmaraş (Turkey); wild plants used for medicinal purpose in Andırın, Kahramanmaraş. *Turk J Pharm Sci.* 2012; 9(1): 75–92.
10. Iranshahi M, Iranshahi M. Traditional uses, phytochemistry and pharmacology of asafoetida (*Ferula assa-foetida* oleo-gum-resin) A review. *J Ethnopharmacol.* 2011; 134(1): 1-10. <https://doi.org/10.1016/j.jep.2010.11.067>
11. Pavlović I, Radenković M, Branković S, Milenković MT, Niketić M, Ušjak L, et al. Spasmolytic, gastroprotective and antioxidant activities of dry methanol extract of *Ferula heuffelii* underground parts. *Chem Biodiversity.* 2022; 19(5): e202200047. <https://doi.org/10.1002/cbdv.202200047>
12. Latifi E, Mohammadpour AA, Hafshejani BF, Nourani H. *Ferula assa-foetida* oleo gum resin ethanolic extract alleviated the pancreatic changes and antioxidant status in streptozotocin-induced diabetic rats: A biochemical, histopathological, and ultrastructural study. *J Food Biochem.* 2022; 46:e 14191. <https://doi.org/10.1111/jfbc.14191>
13. Zahra G, Ramin R, Mohammad RA, Mohammad HB. Anti-inflammatory, antioxidant, and immunomodulatory activities of the genus *Ferula* and their constituents: a review. *Iran J Basic Med Sci.* 2021; 24:1613-1623. <https://doi.org/10.22038/ijbms.2021.59473.13204>
14. Arjmand Z, Hamburger Z, Dastan D. Isolation and purification of terpenoid compounds from *Ferula haussknechtii* and evaluation of their antibacterial effects. *Nat Prod Res.* 2022; [doi.org/10.1080/14786419.2022.2103558](https://doi.org/10.1080/14786419.2022.2103558)
15. Zhou Y, Xin F, Zhang G, Qu H, Yang D, Han X. Recent advances on bioactive constituents in *Ferula*. *Drug Dev Res.* 2017; 78(7): 321-331. [doi.org/10.1002/ddr.21402](https://doi.org/10.1002/ddr.21402)

16. Li Q, Li J-J, Bao X-H, Zhang S-Y, Luo Q, Li K-M. Unusual sesquilignans with anti-inflammatory activities from the resin of *Ferula sinkiangensis*. *Bioorg Chem*, 2022; 127: 105986. <https://doi.org/10.1016/j.bioorg.2022.105986>
17. Askari VR, Baradaran Rahimi V, Assaran A, Iranshahi M, Boskabady MH. Evaluation of the anti-oxidant and anti-inflammatory effects of the methanolic extract of *Ferula szowitsiana* root on PHA-induced inflammation in human lymphocytes. *Drug Chem Toxicol*. 2020; 43(4): 353-360. <https://doi.org/10.1080/01480545.2019.1572182>
18. Kazemi F, Mohebbati R, Niazmand S, Shafei MN. Antihypertensive effects of standardized Asafoetida: Effect on Hypertension Induced by Angiotensin II. *Adv Biomed Res*. 2020; 9(77): 1-6 [https://doi.org/10.4103/abr.abr\\_106\\_20](https://doi.org/10.4103/abr.abr_106_20)
19. Doğan HH, Duman R. The anti HRSV activity of *Ferula halophila* Peşmen aqueous and methanol extract by MTT assay. *Trak Univ J Nat Sci*. 2021; 22(1): 43-48. <https://doi.org/10.23902/trkjnat.805545>
20. Perera WPRT, Liyanage JA, Dissanayake KGC, Gunathilaka H, Weerakoon WMTDN, Wanigasekara DN. Antiviral potential of selected medicinal herbs and their isolated natural products. *Bio Med Res Int*. 2021; 7872406. <https://doi.org/10.1155/2021/7872406>
21. Singh G. *In silico* screening and pharmacokinetic properties of phytoconstituents from *Ferula asafoetida* H. Karst. (Heeng) as potential inhibitors of  $\alpha$ -amylase and  $\alpha$ -glucosidase for Type 2 Diabetes Mellitus, *J Diabetes Metab Disord*. 2022; 21(2): 1339-1347. doi: 10.1007/s40200-022-01064-6
22. Iranshahi M, Rezaee R, Najafi MN, Haghbin A, Jamal Kasaian J. Cytotoxic activity of the genus *Ferula* (Apiaceae) and its bioactive constituents, *Avicenna J Phytomed*, 2018; 8 (4): 296-312.
23. Yi X, Li Z, Zheng Q, Sang R, Li H, Gao G. Three new tetrahydrobenzofuran derivatives from *Ferula sinkiangensis* K.M. Shen and their cytotoxic activities. *Nat Prod Res*. 2022; 1-5. <https://doi.org/10.1080/14786419.2022.2075361>
24. Abutaha N, Nasr FA, Al-Zharani M, Alqahtani AS, Noman OM, Mubarak M. Effects of hexane root extract of *Ferula hermonis* boiss. On human breast and colon cancer cells: an *in vitro* and *in vivo* study. *Bio Med Res Int*. 2019; 3079895. doi. org/10.1155/2019/3079895
25. Shomirzoeva O, Xu MY, Sun ZJ, Li C, Nasriddinov A, Muhidinov Z. Chemical constituents of *Ferula seravschanica*. *Fitoterapia*. 2021; 149:104829. doi.org/10.1016/j.fitote.2021.104829.
26. Arjmand Z, Dastan D. Chemical characterization and biological activity of essential oils from the aerial part and root of *Ferula haussknechtii*. *Flavour Frag J*. 2020; 35(1): 114-123. <http://dx.doi.org/10.1002/ffj.3544>
27. Topdas EF, Sengul M, Taghizadehghalehjoughi A, Hacimuftuoglu A. Neuroprotective potential and antioxidant activity of various solvent extracts and essential oil of *Ferula orientalis* L. *J Essent Oil Bear Pl*. 2020; 23: 121-138. doi.org/10.1080/0972060X.2020.1729247
28. Sonigra P, Meena M. Metabolic profile, bioactivities, and variations in the chemical constituents of essential oils of the *Ferula* genus (Apiaceae). *Front Pharmacol*. 2021; 11:608649. <https://doi.org/10.3389/fphar.2020.608649>
29. Youssef FS, Mamatkhanova MA, Mamadalieva NZ, Zengin G, Aripova SF, Alshammari E, et al. Chemical profiling and discrimination of essential oils from six *Ferula*

species using GC analyses coupled with chemometrics and evaluation of their antioxidant and enzyme inhibitory potential. *Antibiotics*. 2020; 9(8): 518. doi.org/10.3390/antibiotics9080518.

30. Mahmoudvand H, Yadegari JG, Khalaf AK, Hashemi MJ, Dastyarhaghghi S, Salimikia, I. Chemical composition, antileishmanial, and cytotoxic effects *Ferula macrecolea* essential oil against *Leishmania tropica*. *Parasite Epidemiol Control*. 2022; 19: e00270. <https://doi.org/10.3390%2Fbiom11020272>

31. Ahmadi Koulaei S, Hadjiakhoondi A, Delnavazi MR, Tofighi Z, Ajani Y, Kiashi, F. Chemical composition and biological activity of *Ferula aucheri* essential oil. *Res J Pharmacogn*. 2020; 7(2): 21-31. <https://doi.org/10.22127/rjp.2020.210354.1537>

32. Han R, Sun Y, Ma R, Wang D, Sun J, Zhao S, et al. The inhibitory effect and mechanism of *Ferula akitschkensis* volatile oil on gastric cancer. *Evid Based Complementary Altern Med*. 2022; 2022: 5092742. <https://doi.org/10.1155%2F2022%2F5092742>

33. Miski M, Jakupovic J. Daucane esters from *Ferula rigidula*. *Phytochemistry*. 1990; 29(1): 173-178 <https://doi.org/10.1021/np50053a009>

34. Akhmedov DM, Mir-Babaev NF, Aleskerova AN, Serkerov SV, Knight D, Salan Y. Humulane esters from *Ferula rigidula*. *Chem Nat Comp*. 1993; 29(2): 248-248.

35. Zengin G, Sinan KI, Ak G, Mahomoodally MF, Paksoy MY, Picot-Allain C, et al. Chemical profile, antioxidant, antimicrobial, enzyme inhibitory, and cytotoxicity of seven Apiaceae species from Turkey: A comparative study. *Ind Crops Prod*. 2020; 153: 112572. <http://dx.doi.org/10.1016/j.indcrop.2020.112572>

36. Süzgeç-Selçuk S, Özek G, Meriçli AH, Baser KHC, Haliloglu Y, Özek T. Chemical and Biological Diversity of the Leaf and Rhizome Volatiles of *Acorus calamus* L. from Turkey, *TEOP* 2017; 20(3): 646 – 661. <http://dx.doi.org/10.1080/0972060X.2017.1331142>

37. Babushok VI, Linstrom PJ and Zenkevich IG. Retention indices for frequently reported compounds of plant essential oils. *J Phys Chem Ref Data*, 2011; 40: 043101-1-043101-47. <http://dx.doi.org/10.1063/1.3653552>

38. Karahisar E, Kose YB, Iscan G, Kurkuoglu M, Tugay O. Chemical Composition and Anticandidal Activity of Essential Oils Obtained from Different Parts of *Prangos heyneae* H. Duman & MF. Watson, *Rec Nat Prod*, 2022; 16(1): 74-83. <http://doi.org/10.25135/rnp.246.21.02.1971>

39. Polatoglu K, Demirci F, Demirci B, Goren, N; and Baser, KHC. Essential Oil Composition and Antibacterial Activity of *Tanacetum argenteum* (Lam.) Willd. ssp. *argenteum* and *T. densum* (Lab.) Schultz Bip. ssp *amani* Heywood from Turkey, *J Oleo Sci*, 2010; 59(7) 361-367. <https://doi.org/10.5650/jos.59.361>

40. Kose YB, Iscan G, Kurkuoglu M and Kucuk S. Anticandidal Activity of *Hypericum elongatum* var. *elongatum* Essential Oil, *Fresen Environ Bull*, 2018; 27 (12): 8481-8485.

41. CLSI (NCCLS) M7-A7, Methods for Dilution Antimicrobial Susceptibility Tests for Bacteria That Grow Aerobically; Approved Standard, Seventh Edition, 2006.

42. CLSI (NCCLS) M27-A2 Reference Method for Broth Dilution Antifungal Susceptibility Testing of Yeasts; Approved Standard-Second Edition; Vol.22, No. 15, 2002.

43. Başer KHC, Demirci B, Sagioglu M, Duman H. Essential oil of *Ferula* species of Turkey. In Proceedings of the 38th International Symposium on Essential Oils, Graz, Austria, 9–12 September 2007.

44. Logan, NA. *Bacillus* and relatives in foodborne illness. *J App Microbiol*, 2012;

112(3), 417-429. doi.org/10.1111/j.1365-2672.2011.05204.x

45. Zengin G, Sinan KI, Ak G, Mahomoodally MF, Paksoy MY, Picot-Allain C, Custodio L. Chemical profile, antioxidant, antimicrobial, enzyme inhibitory, and cytotoxicity of seven Apiaceae species from Turkey: A comparative study. *Ind Crop Prod*. 2020; 153: 112572. doi.org/10.1016/j.indcrop.2020.112572,

46. Wińska K, Mączka W, Łyczko J, Grabarczyk M, Czubaszek A, Szumny A. Essential oils as antimicrobial agents—myth or real alternative? *Molecules*. 2019; 24(11): 2130. <https://doi.org/10.3390%2Fmolecules24112130>

47. İşcan G. Antibacterial and anticandidal activities of common essential oil constituents, *Rec Nat Prod*. 2017; 11(4): 374-388.

48. Adorjan B, Buchbauer G. (2010). Biological properties of essential oils: an updated review. *Flavour Frag J*. 25(6): 407-426. doi.org/10.1002/ffj.2024

49. Bajpai VK, Baek KH. Biological efficacy and application of essential oils in foods—a review. *J Essent Oil Bear Pl*. 2016; 19(1): 1-19. <http://dx.doi.org/10.1080/0972060X.2014.935033>

50. Abers M, Schroeder S, Goelz L, Sulser A, St Rose T, Puchalski K, et al. Antimicrobial activity of the volatile substances from essential oils. *BMC Complement Altern Med*. 2021; 21(1): 1-14. <https://doi.org/10.1186/s12906-021-03285-3>

51. Swamy MK, Akhtar MS, Sinniah UR. Antimicrobial properties of plant essential oils against human pathogens and their mode of action: an updated review. *Evid Based Complement Alternat Med*. 2016; 2016: 1-21. <https://doi.org/10.1155/2016/3012462>

# Chemical composition, antimicrobial and antioxidant activity of a “lipid phase” from *Zanthoxylum pistaciifolium* Griseb leaves

Yamilé HEREDIA DÍAZ<sup>1\*</sup>, Julio C. ESCALONA ARRANZ<sup>1</sup>, Ania OCHOA PACHECO<sup>1</sup>, Rosalia GONZÁLEZ FERNÁNDEZ<sup>2</sup>, Pedro L. BATISTA CORBAL<sup>2</sup>, Paul COS<sup>3</sup>, Alexandra ESCALONA CAPARROS<sup>1</sup>

<sup>1</sup> Pharmacy Department, Faculty of Natural and Exact Sciences, Oriente University, Avenue Patricio Lumumba s/n, 90500 Santiago de Cuba, Cuba

<sup>2</sup> Medical Toxicology Centre (TOXIMED), Medical Sciences University, Highway km 1½, CP 90400. Santiago de Cuba, Cuba

<sup>3</sup> Laboratory for Microbiology, Parasitology and Hygiene (LMPH), Faculty of Pharmaceutical, Biomedical and Veterinary Sciences, University of Antwerp, Belgium

## ABSTRACT

The present research aimed is to carry out the phytochemical analysis and to evaluate the antimicrobial and antioxidant activity, of the lipid phase from Cuban endemic plant *Zanthoxylum pistaciifolium* Griseb leaves. The total extract was fractioned by Column Chromatography, while its lipid fractions were analyzed by Nuclear Magnetic Resonance and Gas Chromatography-Mass Spectrometry. Antimicrobial activity versus a strain panel of two bacteria and six yeast was tested by microdilution method. Antioxidant activity was evaluated as the scavenging property on DPPH and ABTS<sup>+</sup> radicals. For the first time 31 compounds are informed, among which fatty acid derivatives and sesquiterpenes prevail. Ethyl palmitate and geranylinalool emerge as the main compounds. Good anti-*Candida* activity as well as a moderate radical scavenging property were demonstrated. The cell viability determined reflects a slight toxicity over Vero cells (IC<sub>50</sub> in 34.9 ± 0.78 µg/mL). The investigation reveals that lipid phase has an interesting potential for pharmaceutical applications.

**Keywords:** Antimicrobial activity, ethyl palmitate, gas chromatography-mass spectrometry, geranylinalool, radical scavenging

\*Corresponding Author: E-mail: yherediad@gmail.com

ORCID:

Yamilé HEREDIA DÍAZ: 0000-0003-3863-0668

Julio C. ESCALONA ARRANZ: 0000-0003-3609-4451

Ania OCHOA PACHECO: 0000-0001-9069-6897

Rosalía GONZÁLEZ FERNÁNDEZ: 0000-0001-8268-2428

Pedro L. BATISTA CORBAL: 0000-0001-7733-7638

Paul COS: 0000-0003-4361-8911

Alexandra ESCALONA CAPARROS: 0000-0003-4344-7315

(Received 02 Nov 2022, Accepted 24 March 2023)

## INTRODUCTION

*Zanthoxylum* genus belongs to the Rutaceae family. Compiled by Linné in 1757, it comprises about 573 species distributed worldwide mainly in tropical and temperate regions<sup>1</sup>. Species of this genus stand out due to their economic importance as source of edible fruits, oils, wood, raw materials for industries, and for having ornamentals, culinary and medicinal applications<sup>2</sup>. With such applications diversity, it constitutes one of the most remarkable genera not only within its family but also the plant kingdom. From a chemical point of view, this genus is characterized by a high production of various types of alkaloids, lignans, coumarins and amides, all of which present chemotaxonomic relevance to the genre. Furthermore, other metabolite types such as flavonoids, sterols and terpenes have been isolated<sup>3</sup>.

*Zanthoxylum pistaciifolium* Griseb is one of the species that grows in Cuba. Known as “palo vencedor”, “pensador” or “bálsamo”, it is a common shrub in arid coastal lands of Cuba, mainly in the Eastern region. Ethnobotanic reports refer that this plant has been used for aromatic baths<sup>4</sup>, pulmonary infections and other associated diseases (particularly cold)<sup>5</sup>, ear pain and others<sup>6</sup>. The species is traditionally used as an oily extract obtained from the leaf in the treatment of earaches and there are yet no reports that justify it. One of the most common infections affecting the human ear is otomycosis, also known as external fungal otitis, which occurs due to fungal growth of *Candida* spp. This fungal growth associates with bacteria and cause more complex harder to treat ear infections.

From a chemical point of view there is scarce information about the composition of this plant, only the presence of volatile compounds as  $\alpha$ -pinene (12.35%), linalool (6.68%), 2,6-dimetil-2,4,6-octatriene (6.50%), limonene (6.19%) and phytol (6.06%) have been reported before<sup>7</sup>. On the other hand, no precedent of pharmacologic studies has been found, therefore, there are not enough scientific evidence to support its ethnopharmacological use as antifungal and antibacterial by the Cuban population. Considering the lack of such precedents, this work aims to investigate the chemical profile of the lipid fractions of *Z. pistaciifolium* leaves, as well as to determine their antimicrobial and antioxidant activity.

## METHODOLOGY

### Collection of the plant material

Leaves from *Zanthoxylum pistaciifolium* were collected in October 2017 at “El Palenque”, close to Siboney neighborhood, Santiago de Cuba, Cuba. Botanical specimens were identified by Professor Félix Acosta Cantillo, and a voucher specimen (No. 21660) was deposited in the Herbarium of the Eastern Center of Ecosystems and Biodiversity.

## Extraction, separation and structural analysis of the lipid fraction compounds

A total extract in ethanol 95% was prepared with dry and milled leaves using percolation methodology. Once prepared, the extract was left to repose, filtered, and dried using a vacuum rotator evaporator (IKA-Werke, Germany) at 40°C. The obtained 60 grams were defatted using a liquid-liquid extraction with hexane to be later chemically characterized and evaluated in their biological activity. The hexane phase (lipid phase, LP) was dried and prepared for a column chromatographic separation, using gel silica 60 (0.063-0.2 mm/70-230 Mesh ASTM, Macherey-Nagel, Germany) as stationary phase. A gradient elution starting with n-hexane followed by mixtures of hexane: dichloromethane (95:5 - 5:95), pure dichloromethane, dichloromethane: ethyl acetate (95:5 - 5:95), pure ethyl acetate and ethyl acetate: methanol (95:5 - 50:50) was used.

In accordance to their behavior on the Thin Layer Chromatography (TLC), the fractions derived from previous separation were joined. Glass plates (20 x 20 cm) with internal fluorescence indicator were used, which were revealed with an UV-lamp (Biosystems, Brazil) at 254 and 365 nm and iodine vapors. The fractions that appeared as pure or non-complex were analyzed by Nuclear Magnetic Resonance (NMR), and afterwards by Gas Chromatography and Mass Spectrometry (GC-MS).

The NMR spectra was recorded in a VARIAN apparatus (USA) operated at 200 MHz (<sup>1</sup>H). The chemical shifts were analyzed with MestRenova software version: 6.1.0-6224 of 2010. Deuterated chloroform (Cambridge Isotope Laboratories, Inc. USA) was used as solvent. The GC-MS was performed using a SHIMADZU GC/MS-QP2010 apparatus with an auto-injector AOC-20i (Japan), composed by a Mega 2 series chromatography coupled to a quadrupolar spectrometer of positive electronic impact (70e<sup>-</sup>V) as ionization mode and a mass range between 13 and 500 *m/z*. A validated program for the separation of fatty compounds was used, consisting of an Rtx-5 MS capillary column (30 m x 0.25 mm x 0.25 μm) and helium as carrier gas with a flow rate of 1 mL min<sup>-1</sup>. The injection port temperature was 250°C while the ion trap and transfer-line temperatures were 250°C. The oven temperature was programmed at 60°C (3 minutes) increasing by 40°C min<sup>-1</sup> until reaching 140°C, to continue with a ramp temperature of 4°C min<sup>-1</sup> until completion at 300°C.

Linear retention indexes were calculated in relation to homologous series of n-alkanes (C8-C24). Percentages of constituents were determined based on their GC-FID peak areas, using the normalization procedure without corrections for

response factor (EZChrom v 6.7 software). Compounds were identified as far as possible by comparing fragmentation patterns in their mass spectra with those stored on the National Institute of Standards and Technology (NIST) library<sup>8</sup> and with literature data<sup>9</sup>. Identity was confirmed in many compounds by means of their Kovacts retention indexes. To process spectra, the software GC/MS solution version 2.70 of 2010 was used, in its “postrun analysis” option.

### **Microorganisms and reference drugs**

The antimicrobial activity of the lipid phase was tested facing it to three bacteria and six yeast strains supplied by the Laboratory for Microbiology, Parasitology and Hygiene (LMPH), University of Antwerp, Belgium. *Candida albicans* ATCC B59630 (Azole Resistant), *Candida glabrata* ATCC B63155, *Candida kefyr* ATCC B46120, *Candida krusei* ATCC B68404, *Candida parapsilosis* ATCC J941058 and *Candida tropicalis* CDC49 were the yeast strain used while *Staphylococcus aureus* ATCC 6538, *Escherichia coli* ATCC 8739 and *Pseudomonas aeruginosa* ATCC 9027 were the bacteria ones. Miconazole and ampicillin (Sigma-Aldrich, USA) were used as reference drugs for fungi and bacteria, respectively.

### ***In vitro* antimicrobial activity**

*In vitro* antibacterial and antifungal activity was determined by the microdilution method with resazurin (redox indicator) in sterile 96-well microplates<sup>10</sup>. In each well 10  $\mu$ L of the sample were added together with 190  $\mu$ L bacteria inoculum ( $5 \times 10^5$  CFU/mL) and yeast inoculum ( $5 \times 10^3$  CFU/mL). Untreated control wells (100% cell growth) and medium-control wells (0% cell growth) were included in the microplates. Later on, the microplates were incubated at 37°C for 17 hours (for bacteria) and 24 hours (for yeast). Afterwards, 20  $\mu$ L of resazurin (Sigma-Aldrich, USA) at 50  $\mu$ g mL<sup>-1</sup> per well were added and the microplates were incubated under the same temperature conditions (bacteria: 30 min and yeast: 4 hours). Microbial growth was determined by fluorimetry method ( $\lambda_{ex}$  = 550 nm,  $\lambda_{em}$  = 590 nm) using a microplate reader (Tecan, Mechelen, Belgium). The product was classified as active when the bacterial growth inhibition (%) was greater than 50%. The results are expressed as percentage reduction in bacterial growth/viability compared to control wells. To accomplish this, LPs were dried and solved in dimethyl sulfoxide (DMSO) at 1 g mL<sup>-1</sup>. Serial dilutions in pure water were made to obtain five levels of concentrations corresponding to: 4.0, 2.0, 1.0, 0.5, 0.25 mg mL<sup>-1</sup>. Each concentration was screened by triplicate and the results were reflected as mean  $\pm$  standard deviation.

### **Scavenging activity facing the radicals 2,2-azino-bis- (3-ethyl benzothiazoline-6-sulfonic acid) (ABTS<sup>•+</sup>) and 2,2 diphenyl -1-picrylhydrazyl (DPPH)**

The scavenging capacity on ABTS<sup>•+</sup> (Merck, KGaA, Darmstadt, Germany) radical was developed according to the methodology described in the literature<sup>11</sup>. Different concentration of the LP (solutions of 62.5 to 1 000 µg/mL based on the extract's dry weight) were added to 3 mL of diluted ABTS<sup>•+</sup> solution and after 90 min the absorbance was measured at 734 nm. Ascorbic acid (Fluka, 99 % pure, Germany) at a concentration of (1 mg/mL) was considered as positive control. The radical quenching activity was determined by calculating the percent inhibition of the radical. The ABTS<sup>•+</sup> radical scavenge of *Z. pistaciifolium* extracts were estimated as a function of the extract concentration capable to quench the 50 % of the radical (IC<sub>50</sub>) obtained by interpolation in the curve constructed from the five evaluated concentrations. All experiments were repeated three times.

The scavenging capacity on DPPH (Merck, KGaA, Darmstadt, Germany) radical was developed according to the methodology described in the literature<sup>12</sup>. In short: A solution of 0.1 mM of DPPH<sup>•</sup> was prepared using 0.00394 g dissolved in 100 mL of ethanol. A total of 0.25 mL of the LP (solutions of 62.5 to 1 000 µg/mL based on the phase dry weight) were placed in test tubes, where were added 1.5 mL of the DPPH<sup>•</sup> solution. The mix was shaken in a vortex (Heidolph REAX 2000, Germany) and kept in the dark for 20 min. The absorbance was measured in spectrophotometer (T60 UV-Visible Spectrophotometer) at 517 nm. The positive control was an ascorbic acid solution at 1 mg/mL. The radical sequestration ability was determined by calculating the percent inhibition of the radical. The antioxidant capacity against these radicals was expressed as a function of the half inhibitory concentrations (IC<sub>50</sub>) of the tested extracts obtained by interpolation in the calibration curve constructed. All the experiments were developed by triplicate.

### **Cell viability**

Cellular proliferation and viability were assessed in Vero cells (green monkey kidney cells) purchased from ATCC (American Type Culture Collection). Cells were incubated at 37°C in 5% CO<sub>2</sub> atmosphere, seeded in sterile 96-well microtiter plates on a Dulbecco's Modified Eagle Medium (DMEM) (Sigma-Aldrich, USA) and supplemented with 10% inactivated fetal calf serum (FCS) (Sigma-Aldrich, USA), 2% of L-glutamine and D-glucose (4.5 g L<sup>-1</sup>)<sup>10</sup>.

Cell viability was measured as follow: 200  $\mu\text{L}$  of cell inoculum ( $5 \times 10^5$  cell/well) were added in 96 well microplates and incubated by 24 hours at 37 °C in 5 %  $\text{CO}_2$  atmosphere. The old medium was removed, and the wells were washed twice with fresh Saline Dulbecco's Phosphate Buffer, so that 100  $\mu\text{L}$  of the LP at concentrations from 8 to 256  $\mu\text{g mL}^{-1}$  could be added later. The microplates were incubated for another 72 hours under the same conditions. Next, a volume of 50  $\mu\text{L}$  of resazurin was added to each well and the plates were incubated against for 4 hours at 37°C, 5%  $\text{CO}_2$  to complete the assessment of cellular viability. This was performance by measuring the fluorescence at  $\lambda_{\text{ex}}$  550 nm,  $\lambda_{\text{em}}$  590 nm with a microplate reader (Tecan, Mechelen, Belgium) and using tamoxifen (Sigma-Aldrich, USA) as a reference drug (positive control, from 3.6 to 114  $\mu\text{M}$ )<sup>13</sup>. Untreated-control wells were used as solvent control. The results were expressed as percent reduction in cell viability as compared to untreated-control wells; the 50% cytotoxic concentration ( $\text{CC}_{50}$ ) was determined.

### Statistical analysis

All analyses were performed using the software SPSS v.19 by ANOVA analysis. Bonferroni test was performed to indicate significant differences between groups with  $p \geq 0.05$ . Results were reflected as mean  $\pm$  standard deviation.

## RESULTS AND DISCUSSION

### Chromatographic separation and structural characterization

Eight grams of the lipid phase were fractioned using Colum Chromatography with gel-silica 60 as stationary phase. The column was eluted with an increasing polarity gradient of different mixtures of n-hexane and dichloromethane. The 56 fractions generated were grouped according to their behavior on TLC on iodine vapors and ultraviolet light at two wavelengths (254 and 365 nm) to get four main fractions ( $\text{FH}_1$ ,  $\text{FH}_2$ ,  $\text{FH}_3$ ,  $\text{FH}_4$ ).

**Fraction 1 ( $\text{FH}_1$ ):** This fraction was obtained as a colorless semisolid and eluted with hexane and shows multiple signal from  $\delta_{\text{H}}$  0.77 to 0.89 ppm at NMR  $^1\text{H}$  (200 MHz,  $\text{CDCl}_3$ ) spectra, indicating terminal methyl groups. Additionally, signals from 1.26 to 2.05 ppm were observed, which indicate the presence of  $\text{CH}_2$  groups from a saturated hydrocarbon chain. Signals at  $\delta_{\text{H}}$  2.32, 2.42, 2.99 and 3.88 ppm suggest *ortho*- $\text{CH}_3$  groups from a different pattern of substitution on cyclic hydrocarbons exist, which are commonly present in essential oils. The double triplet at  $\delta_{\text{H}}$  5.15 can be associated to an olefin ( $\text{sp}^2$ ) proton. Those appreciations are confirmed by the results of GC/MS (see Table 1) where four non-aromatic sesquiterpenes were identified (56.96%), nine saturated hydrocarbons (29.82%) and an unsaturated triterpene squalene

(7.48%). This kind of composition has been informed before for other *Zanthoxylum* species. The hexane extract of *Z. naranjillo* was rich on sesquiterpenes including  $\beta$ -selinene, while the most abundant hydrocarbon was nonacosane (13.22%), compound that also appears in *Z. guilletii*<sup>14,15</sup>.

Table 1. Relative abundance in the lipid phase of *Z. pistaciifolium* identified by GC-MS

| N <sup>o</sup>                     | Compound              | Rt <sup>a</sup> | PI <sup>b</sup> | A <sup>c</sup> (%) |
|------------------------------------|-----------------------|-----------------|-----------------|--------------------|
| <b>Fraction 1 (FH<sub>1</sub>)</b> |                       |                 |                 |                    |
| FH <sub>1-1</sub>                  | $\alpha$ -Himachalene | 1449            | 1449            | 3.63               |
| FH <sub>1-2</sub>                  | Selina-4,11-diene     | 1474            | 1476            | 5.99               |
| FH <sub>1-3</sub>                  | $\beta$ -selinene     | 1492            | 1492            | 23.92              |
| FH <sub>1-4</sub>                  | $\alpha$ -selinene    | 1500            | 1501            | 23.42              |
| FH <sub>1-5</sub>                  | Octadecane            | 1799            | 1800            | 2.49               |
| FH <sub>1-6</sub>                  | Nonadecane            | 1898            | 1900            | 2.20               |
| FH <sub>1-7</sub>                  | Eicosane              | 1999            | 2000            | 2.30               |
| FH <sub>1-8</sub>                  | Heneicosane           | 2099            | 2100            | 2.35               |
| FH <sub>1-9</sub>                  | Docosane              | 2199            | 2200            | 2.43               |
| FH <sub>1-10</sub>                 | Tricosane             | 2296            | 2300            | 2.67               |
| FH <sub>1-11</sub>                 | Unknown               | 2354            |                 | 5.74               |
| FH <sub>1-12</sub>                 | Tetracosane           | 2397            | 2400            | 2.16               |
| FH <sub>1-13</sub>                 | Squalene              | 2837            | 2836            | 7.48               |
| FH <sub>1-14</sub>                 | Nonacosane            | 2898            | 2900            | 13.22              |
| <b>Total identified (%)</b>        |                       |                 |                 | 92.9               |
| Hydrocarbon compounds              |                       |                 |                 | 94.26              |
| Non terpene                        |                       |                 |                 | 29.82              |
| Sesquiterpenes                     |                       |                 |                 | 56.96              |
| Triterpenes                        |                       |                 |                 | 7.48               |
| <b>Fraction 2 (FH<sub>2</sub>)</b> |                       |                 |                 |                    |
| FH <sub>2-1</sub>                  | Ethyl tetradecanoate  | 1795            | 1794            | 1.82               |
| FH <sub>2-2</sub>                  | Ethyl palmitate       | 1999            | 1993            | 86.38              |
| FH <sub>2-3</sub>                  | Ethyl heptadecanoate  | 2095            | 2097            | 1.90               |
| FH <sub>2-4</sub>                  | Oleic acid            | 2171            | 2171            | 3.25               |
| FH <sub>2-5</sub>                  | Ethyl stearate        | 2196            | 2197            | 6.65               |
| <b>Total identified (%)</b>        |                       |                 |                 | 100                |
| Oxygenated compounds               |                       |                 |                 | 100                |
| Fatty acid and it derivatives      |                       |                 |                 | 100                |
| <b>Fraction 3 (FH<sub>3</sub>)</b> |                       |                 |                 |                    |
| FH <sub>3-1</sub>                  | Pentadecane           | 1497            | 1500            | 1.16               |
| FH <sub>3-2</sub>                  | Ethyl 9-oxononanoate  | 1508            | 1507            | 2.49               |

|                                    |   |      |      |       |
|------------------------------------|---|------|------|-------|
| FH <sub>3-3</sub>                  | Hexadecane  | 1597 | 1600 | 2.31  |
| FH <sub>3-4</sub>                  | Heptadecane   | 1696 | 1700 | 1.96  |
| FH <sub>3-5</sub>                  | Benzyl Benzoate   | 1785 | 1789 | 5.40  |
| FH <sub>3-6</sub>                  | Benzyl salicylate   | 1889 | 1886 | 2.33  |
| FH <sub>3-7</sub>                  | Ethyl palmitate   | 1992 | 1993 | 24.57 |
| FH <sub>3-8</sub>                  | Methyl 10-octadecenoate   | 2100 | 2100 | 1.16  |
| FH <sub>3-9</sub>                  | Ethyl-9,12-octadecadienoate   | 2165 | 2166 | 23.73 |
| FH <sub>3-10</sub>                 | Oleic acid  | 2172 | 2171 | 29.96 |
| FH <sub>3-11</sub>                 | Ethyl stearate  | 2191 | 2197 | 2.14  |
| FH <sub>3-12</sub>                 | Phytol acetate  | 2216 | 2212 | 2.79  |
| <b>Total identified (%)</b>        |   |      |      | 100   |
| Hydrocarbon compounds              |   |      |      | 5.43  |
| Non terpene                        |   |      |      | 5.43  |
| Oxygenated compounds               |   |      |      | 86.84 |
| Fatty acid and it derivatives      |   |      |      | 81.56 |
| Terpenes                           |   |      |      | 2.79  |
| Others                             |   |      |      | 2.49  |
| Aromatic compounds                 |   |      |      | 7.73  |
| <b>Fraction 4 (FH<sub>4</sub>)</b> |   |      |      |       |
| FH <sub>4-1</sub>                  | (5Z)-6,10-Dimethyl-5,9-undecadien-2-one                               | 1453 | 1450 | 1.73  |
| FH <sub>4-2</sub>                  | 3-Cyclohexene-1-carboxaldehyde, 4-(4-methyl-3-pentenyl)               | 1535 | 1534 | 1.91  |
| FH <sub>4-3</sub>                  | Selin-6-en-4 $\alpha$ -ol   | 1639 | 1636 | 10.94 |
| FH <sub>4-4</sub>                  | 1,3,6,10-Cyclotetradecatetraene, 3,7,11-trimethyl-14-(1-methylethyl)- | 1922 | 1923 | 3.23  |
| FH <sub>4-5</sub>                  | Geranylinalool  | 2036 | 2034 | 65.99 |
| FH <sub>4-6</sub>                  | Hexadecane, 5-octyl   | 2273 | 2270 | 2.60  |
| FH <sub>4-7</sub>                  | Bis(2-ethylhexyl) phthalate   | 2555 | 2552 | 9.45  |
| FH <sub>4-8</sub>                  | Hexacosane, 8 methyl  | 2630 | 2634 | 1.99  |
| FH <sub>4-9</sub>                  | Nonacosane  | 2903 | 2900 | 2.16  |
| <b>Total identified (%)</b>        |   |      |      | 100   |
| Hydrocarbon compounds              |   |      |      | 9.98  |
| Non terpene                        |   |      |      | 6.75  |
| Terpene                            |   |      |      | 3.23  |
| Oxygenated compounds               |   |      |      | 90.02 |
| Sesquiterpenes                     |   |      |      | 10.94 |
| Diterpenes                         |   |      |      | 65.99 |
| Others                             |   |      |      | 13.09 |
| <b>Total compounds</b>             |   |      |      | 36    |

<sup>a</sup>Calculated retention index, <sup>b</sup>Reported retention index, <sup>c</sup>Relative area

**Fraction 2 (FH<sub>2</sub>):** This fraction was obtained as an intense yellow semisolid and eluted with hexane: dichloromethane (45:55 v/v), it shows a singlet at  $\delta_H$  0.82 and 0.86 ppm, which is characteristic of terminal CH<sub>3</sub>; as well as one at  $\delta_H$  1.23 which characterizes CH<sub>2</sub> from aliphatic hydrocarbons. Nevertheless, a singlet at 2.01 and a triplet at 2.26 ppm indicate unsaturation and/or  $\alpha$ -carbonyl CH<sub>2</sub> group. The multiplet at 4.10 ppm can be associated to substitutions type O-CH<sub>2</sub>, while the doublet at  $\delta_H$  5.23 ppm is related to olefinic proton (CH). (Figure 1). Altogether, this fraction looks like a mixture of free or esterified saturated or un-saturated fatty acids. The GC-MS analysis (Table 1) confirmed a 96.75% of esterified fatty acid plus the oleic acid (3.25%) in agreement with the suggestions derived from NMR experiment. Fragments *m/z* 88 and 101 are the most abundant in most of them corresponding to alpha and beta carbonyl bond-breaking (Figure 2). Molecular ions were identified at *m/z* 228,

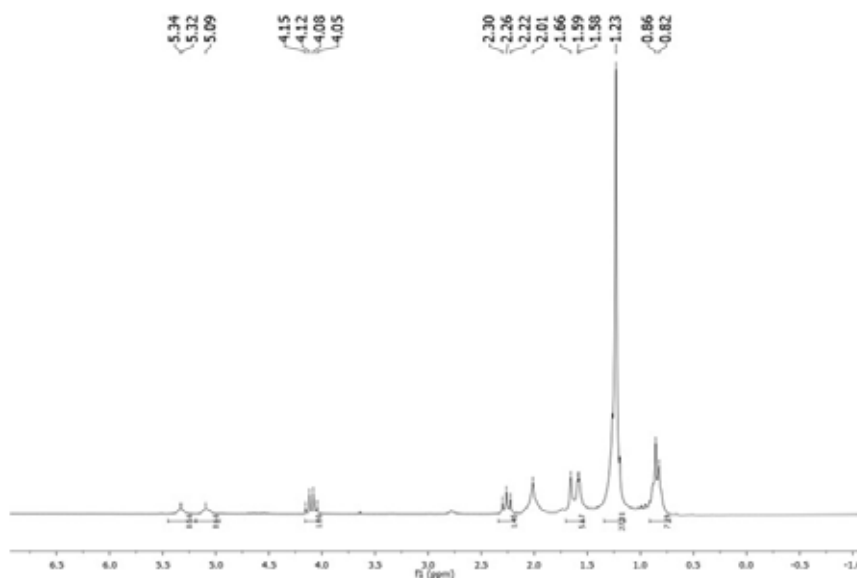


**Figure 1.** NMR 1H spectrum (CDCl<sub>3</sub>, 500 MHz) for FH<sub>2</sub> fraction

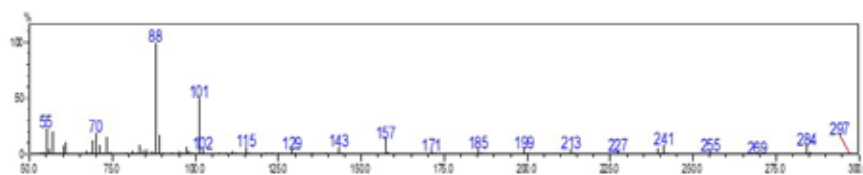


**Figure 2.** Mass spectra for the ethyl palmitate (FH<sub>2-2</sub>) (positive electronic impact)



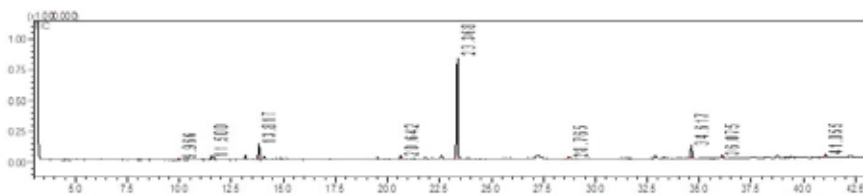


**Figure 4.** GC-MS chromatogram obtained for FH<sub>4</sub> fraction

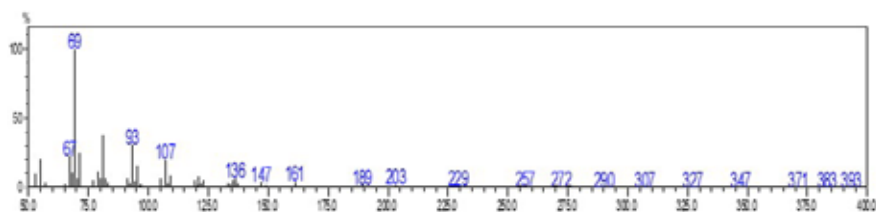


**Figure 5.** Mass spectra for geranylinalool (FH<sub>4.5</sub>) (positive electronic impact)

In general, this phytochemical procedure allowed to identify 35 compounds that represent 97.22% of all the peaks. In the fraction 1, thirteen compounds were identified, of which  $\beta$ -selinene and  $\alpha$ -selinene were the most abundant. Five compounds were identified for fraction 2, ethyl palmitate was the most abundant. On the other hand, for fraction 3 the oleic acid was it the majorities of the twelve total compounds. Of the nine metabolites recognized in fraction 4, geranylinalool was the most abundant. Four substances were identified in more than one fraction: ethyl palmitate, ethyl stearate, oleic acid (Fractions 2 and 3) and nonacosane (Fractions 1 and 4).

Ethyl palmitate looks like the most abundant one of all compounds. Many chemically different types of compounds were identified: 14 non-terpene hydrocarbons, eight fatty acid derivatives, five sesquiterpenes, two diterpenes, two aromatic compounds and others. A low level of free fatty acid was observed as well as the absence of steroids. This chemical composition matches reports of hexane extracts prepared from other species for the genre as *Z. armatum*, *Z. dipetalum*, *Z. kauaense* and *Z. hawaiiense* in which the terpene substances are common, as well as saturated or unsaturated hydrocarbons<sup>16,17</sup>. Nevertheless, the relative abundance and diversity of fatty acids is higher than the one previously informed for the *Zanthoxylum* genre<sup>18</sup>.

Sesquiterpenes were the third most abundant metabolite type, which matches previous reports of chemical composition for *Z. naranjillo* in which  $\beta$ -selinene was also identified<sup>14</sup>. Essential oil studies of other *Zanthoxylum* species refer to an abundance of this kind of compounds, such is the case of *Z. schinifolium*

in which a 46.45% was informed with  $\beta$ -selinene as main compound<sup>19</sup>. The species in study (*Z. pistaciifolium*) is not an exception, as our research group once again reports  $\beta$ -selinene in its composition, together with selin-4,11-diene, and  $\alpha$ -selinene (main compounds)<sup>7</sup>.

These results enrich the knowledge about *Z. pistaciifolium* leaves' chemical composition, considering that 31 of the identified compounds are reported for the first time in this plant.

### ***In vitro* antibacterial and antifungal activity**

Table 2 shows the concentration in which 50% or more of the microbial growth is inhibited. A good of activity against some yeast as *Candida albicans*, *Candida glabrata*, *Candida kefyr*, *Candida krusei*, *Candida parapsilosis* and *Staphylococcus aureus* bacteria can be observed. The antifungal activity of *Zanthoxylum* spp. extracts reports are quite common, but not those of lipid nature. The activity of petroleum ether extracts from *Z. acanthopodium* against *C. albicans* and *C. krusei* as well as the hexane extract of *Z. armatum* facing *T. longifusus* and *M. canis* can be considered as the exception<sup>20,21</sup>.

**Table 2.** Antimicrobial activity of the lipid phase from *Z. pistaciifolium* extract

| Microorganism                        | Concentration (mg mL <sup>-1</sup> ) | Inhibition $\pm$ SD <sup>a</sup> (%) |
|--------------------------------------|--------------------------------------|--------------------------------------|
| <b>Yeast</b>                         |                                      |                                      |
| <i>C. albicans</i> (azole resistant) | < 0.25                               | 93.78 $\pm$ 0.01                     |
| <i>C. glabrata</i>                   | < 0.25                               | 90.96 $\pm$ 0.71                     |
| <i>C. kefyr</i>                      | < 0.25                               | 96.12 $\pm$ 1.50                     |
| <i>C. krusei</i>                     | < 0.25                               | 95.03 $\pm$ 0.08                     |
| <i>C. parapsilosis</i>               | < 0.25                               | 94.45 $\pm$ 0.30                     |
| <i>C. tropicalis</i>                 | < 1.0                                | 77.61 $\pm$ 1.30                     |
| <b>Bacteria</b>                      |                                      |                                      |
| <i>E. coli</i>                       | NA <sup>b</sup>                      | NA                                   |
| <i>P. aeruginosa</i>                 | NA                                   | NA                                   |
| <i>S. aureus</i>                     | < 0.25                               | 54.98 $\pm$ 2.95                     |

<sup>a</sup>Standard deviation, <sup>b</sup>Non-activity

It is a general consent that the antimicrobial potential of *Zanthoxylum* species is related to the presence of terpene compounds<sup>22-25</sup>. Due to this, the antimicrobial activity observed for this lipid phase of *Z. pistaciifolium* leaves can be associated with the presence of those kinds of compounds, specifically with the

presence of geranylinalool, an oxygenated diterpene which has been proven to have a high antimicrobial and insecticide activity<sup>26,27</sup>. Nevertheless, other metabolites isolated in this extract of *Z. pistaciifolium* leaves as ethyl palmitate and other fatty acid derivatives, can also contribute to the measured activity<sup>28</sup>.

### DPPH<sup>•</sup> and ABTS<sup>•+</sup> scavenging activity

Results associated to scavenging activity are displayed in Figure 6. The IC<sub>50</sub> observed for DPPH<sup>•</sup> radical was moderate, considering the statistic difference ( $p < 0.05$ ) between the IC<sub>50</sub> values of lipid phase ( $0.31 \pm 0.009$  mg/mL) and ascorbic acid ( $0.042 \pm 0.003$  mg/mL). On the contrary, for the ABTS<sup>•+</sup> radical the activity can be considered as good, even when statistic difference was present, but in this case, closer IC<sub>50</sub> values for the lipid phase ( $0.42 \pm 0.03$  mg/mL) regarding the standard antioxidant compound ( $0.35 \pm 0.01$  mg/mL) can be observed.

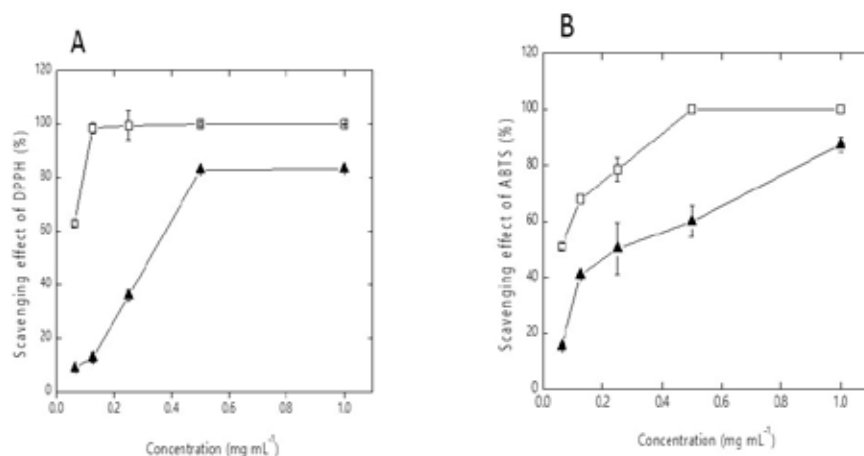


**Figure 6.** Scavenging activity of the lipid phase (□) from *Z. pistaciifolium* extract and the reference ascorbic acid (▲). 6A) DPPH<sup>•</sup> scavenging, 6B) ABTS<sup>•+</sup> scavenging

Acceptable scavenging activity demonstrated for the lipid phase of *Z. pistaciifolium* leaves extract can also be related to the presence of terpenoids, which have been reported in the literature as good scavengers, mainly monoterpene and sesquiterpene types<sup>29</sup>. Once again, fatty acid and its derivatives can also contribute to this determined activity.

### Cell viability

The cell viability results demonstrated that even when the IC<sub>50</sub> is not too high which is expected for a natural extract, the value of  $34.9 \pm 0.78$  μg/mL is higher than that of tamoxifen reference ( $3.59$  μg/mL). Other studies refer higher IC<sub>50</sub> values when lipid fractions are faced to Vero cells, as is the case of *Z. rhoifo-*

*lium*<sup>30,31</sup>. Nevertheless, the scarce number of reports using this cell line makes a deeper analysis hard. Because of this, further *in vivo* and/or *in vitro* experiments will be necessary.

Antimicrobial and scavenging activity was demonstrated for the lipid phase from *Z. pistaciifolium* leaves extract, most importantly the activity against *Candida* spp. and ABTS<sup>+</sup> radical. Both activities were associated to the presence of several types of terpene substances as well as fatty acid and its derivatives. This phytochemical study allows us to report 35 compounds of different chemical profile. These findings justify for the first time that *Z. pistaciifolium* species could be a potential candidate for the treatment of ear diseases in ethno-botanical practices.

#### **CONFLICT OF INTEREST**

The authors declare that there is no conflict of interest regarding the publication and dissemination of the information provided here in.

#### **FUNDING SOURCES**

The authors declare that there is no funding sources of interest regarding the publication.

## REFERENCES

1. The Plant List. [Internet]. 2013. Available from: <http://www.theplantlist.org/> [Accessed 2020/10/24].
2. Yang G, Chen D. Alkaloids from the roots of *Zanthoxylum nitidum* and their antiviral and antifungal effects. *Chem Biodivers*. 2008;5(9):1718-1722. <https://doi.org/10.1002/cbdv.200890160>.
3. Patiño LOJ, Prieto RJA, Cuca SLE. *Zanthoxylum* Genus as potential source of bioactive compounds. In: Rasooli I, editor. *Bioactive compounds in phytomedicine* Rijeka, Croatia: InTech, 2012,184-218.
4. Roig JT. *Plantas medicinales, aromáticas o venenosas de Cuba*. La Habana: Editorial Científico-Técnica; 2012. p. 736.
5. Heredia YD, Tuentner E, García JD, Ochoa AP, Cos P, Pieters L, et al. Novel flavonol-3-O-methylethers from *Zanthoxylum pistaciifolium* Griseb. (Rutaceae). *Nat Prod Res*. 2022;36(19):4869-4878. <https://doi.org/10.1080/14786419.2021.1906240>
6. Martínez J. Yerberos de Cuba. La Habana: Fundación Fernando Ortiz; 2013. p. 32
7. Heredia Y, González R, Escalona J, García J, de la Vega J. Influencia del medio de extracción en la composición de sustancias volátiles de las hojas de *Zanthoxylum pistaciifolium* Griseb. *Rev Cub Quím*. 2016;28(1):490-506.
8. National Institute of Standards and Technology. [Internet]. 2020. Available from: <https://www.nist.gov/srd/nistia.cfm> [Accessed 2020/12/22].
9. Adams RP. Identification of essential oil components by Gas Chromatography/Mass Spectrometry. Illinois: Allured Publishing Corporation; 2007. p.15.
10. Cos P, Vlietinck AJ, Berghe DV, Maes L. Anti-infective potential of natural products: How to develop a stronger *in vitro* 'proof-of-concept'. *J Ethnopharmacol*. 2006;106(3):290-302. doi:10.1016/j.jep.2006.04.003
11. Choi Y, Lee SM, Chun J, Lee HB, Lee J. Influence of the heat treatment on the antioxidant activities and polyphenolic compounds of Shiitake (*Lentinus edodes*) mushroom. *Food Chem*. 2006;99(2):381-387. doi:10.1016/j.foodchem.2005.08.004
12. Shimada K, Fujikawa K, Yahara K, Nakamura T. Antioxidative properties of xanthan on the autoxidation of soybean oil in cyclodextrin emulsion. *J Agric Food Chem*. 1992;40(6): 945-948. <https://doi.org/10.1021/jf00018a005>
13. McMillian MK, Li L, Parker JB, Patel L, Zhong Z, Gunnett JW, et al. An improved resazurin-based cytotoxicity assay for hepatic cells. *Cell Biol Toxicol*. 2002;18:157-173. <https://doi.org/10.1023/A:1015559603643>
14. Bastos JK, Gottlieb OR, Sartia SJ, Filho DS. Isolation of lignans and sesquiterpenoids from leaves of *Zanthoxylum naranjillo*. *Nat Prod Lett*. 1996;9(1):65-70. <https://doi.org/10.1080/10575639608043580>
15. Ombito OJ, Matasyoh CJ, Vulule MJ. Chemical composition and larvicidal activity of *Zanthoxylum gillettii* essential oils against *Anopheles gambiae*. *Afr J Biotechnol*. 2014;13(21):75-80. <https://doi.org/10.5897/AJB2014.13711>
16. Kumar V, Reddy SGE, Chauhan U, Kumar N, Singh B. Chemical composition and larvicidal activity of *Zanthoxylum armatum* against diamondback moth, *Plutella xylostella*. *Nat Prod Res*. 2015;30(6):689-692. <https://doi.org/10.1080/14786419.2015.1036270>
17. Marr KL, Tangs CS. Volatile insecticidal compounds and chemical variability of hawai-

ian *Zanthoxylum* (Rutaceae) species. *Biochem Syst Ecol.* 1992;20(3):209-217. [https://doi.org/10.1016/0305-1978\(92\)90055-I](https://doi.org/10.1016/0305-1978(92)90055-I)

18. Xia L, You J, Li G, Sun Z, Suo Y. Compositional and antioxidant activity analysis of *Zanthoxylum bungeanum* seed oil obtained by supercritical CO<sub>2</sub> fluid extraction. *J Am Oil Chem Soc.* 2010;88(1):23-32. <https://doi.org/10.1007/s11746-010-1644-4>

19. Wang CF, Yang K, Zhang HM, Cao J, Fang R, Liu ZL, et al. Components and insecticidal activity against the maize weevils of *Zanthoxylum schinifolium* fruits and leaves. *Molecules.* 2011;16(4):3077-3088. <https://doi.org/10.3390/molecules16043077>

20. Devi OZ, Rao KS, Bidalia A, Wangkheirakpam R, Mukherjee OS. GC-MS Analysis of phytocomponents and antifungal activities of *Zanthoxylum acanthopodium* DC. Collected from Manipur, India. *European J Med Plants.* 2015;10(1):1-9. <https://doi.org/10.9734/EJMP/2015/19353>

21. Alam F, Saqib QN. Evaluation of *Zanthoxylum armatum* Roxb for *in vitro* biological activities. *J Tradit Complement Med.* 2017;7(4):515-518. <https://doi.org/10.1016/j.jtcme.2017.01.006>

22. Vuuren SF, Viljoen AM. Antimicrobial activity of limonene enantiomers and 1,8-cineole alone and in combination. *Flavour Fragr J.* 2007;22(6):540-544. <https://doi.org/10.1002/ffj.1843>

23. Park SN, Lim YK, Freire MO, Cho E, Jin D, Kook JK. Antimicrobial effect of linalool and a-terpineol against periodontopathic and cariogenic bacteria. *Anaerobe.* 2012;18(3):369-372. <https://doi.org/10.1016/j.anaerobe.2012.04.001>

24. Dai J, Zhu L, Yang L, Qiu J. Chemical composition, antioxidant and antimicrobial activities of essential oil from *Wedelia prostrata*. *Excli J.* 2013;12:479-490. <https://doi.org/https://www.ncbi.nlm.nih.gov/pmc/articles/PMC4669986/>

25. Pejcin B, Savic A, Sokovic M, Glamoclija J, Ciric A, Nikolic M, et al. Further *in vitro* evaluation of antiradical and antimicrobial activities of phytol. *Nat Prod Res.* 2014;28(6):372-376. <https://doi.org/10.1080/14786419.2013.869692>

26. Jirovetz L, Buchbauer G, Schmidt E, Stoyanova AS, Denkova Z, Nikolova R, et al. Purity, antimicrobial activities and ol factoric evaluations of geraniol/nerol and various of their derivatives. *J Essent Oil Res.* 2007;19(3):288-291. <https://doi.org/10.1080/10412905.2007.9699283>

27. Zatlá AT, Dib MEA, Djabou N, Tabti B, Meliani N, Costa J, et al. Chemical variability of essential oil of *Daucus carota* subsp. *sativus* from Algeria. *J Herbs Spices Med Plant.* 2017;23(3):216-230. <https://doi.org/10.1080/10496475.2017.1296053>

28. Kujumgiev A, Bankova V, Ignatova A, Popov, S. Antibacterial activity of propolis, some of its components and their analogs. *Pharmazie* 1993; 48(10):785-786.

29. Chandra M, Prakash O, Kumar R, Kumar RB, Bhushan B, Kumar M, et al.  $\beta$ -selinene-rich essential oils from the parts of *Callicarpa macrophylla* and their antioxidant and pharmacological activities. *Medicines.* 2017;4(3):52. <https://doi.org/10.3390/medicines4030052>

30. Melo NB, Leitão JM, Oliveira LG, Santos SE, Carneiro SM, Rodrigues KA, et al. Inhibitory effects of *Zanthoxylum rhoifolium* Lam. (Rutaceae) against the infection and infectivity of macrophages by *Leishmania amazonensis*. *An Acad Bras Cienc.* 2016;88(3):1851-1861. <https://doi.org/10.1590/0001-3765201620150131>

31. Moura-Costa GF, Nocchi SR, Ceole LF, de Mello JC, Nakamura CV, Dias FB et al. Antimicrobial activity of plants used as medicinals on an indigenous reserve in Rio das Cobras, Parana. *Brazil J Ethnopharmacol.* 2012;143(2):631-638. <https://doi.org/10.1016/j.jep.2012.07.016>

# Formulation and evaluation of atorvastatin tablets by solid dispersion technique

Reza GOUDARZI<sup>1</sup>, Mohammad Mehdi MAHBOOBIAN<sup>1\*</sup>

<sup>1</sup> Department of Pharmaceutics, School of Pharmacy, Hamadan University of Medical Sciences, Hamadan, Iran

---

## ABSTRACT

Atorvastatin (ATR) is a low water-soluble drug with a low oral bioavailability. In the present study, the solid dispersion (SD) technique was used to develop a high-soluble formulation of the ATR by the appropriate carrier and then formulated into a tablet. The atorvastatin solid dispersion (ATR-SD) was developed using the polyvinyl-pyrrolidone K30 (PVP-K30) as a carrier in various ratios by the conventional solvent evaporation method. Dissolution studies were done with the select of the optimum drug:polymer ratio. Tablets were prepared by direct compression using various excipients in different ratios to obtain optimum formulation. The highest dissolution rate was obtained for ATR:PVP-K30 ratio of 1:1, which showed a significant increase in dissolution efficiency after 1 hour. Saturated solubility indicated 1.6-fold enhancement for optimum SD formulation compared to the untreated drug. DSC, XRD, and FTIR analysis proved complete amorphization during SD processes. This study provided a new tablet formulation of ATR with enhanced dissolution characteristics by utilizing the SD technique.

**Keywords:** Atorvastatin, solid dispersion, PVP-K30, dissolution rate, direct compression

---

## INTRODUCTION

Atorvastatin (ATR) as a 3-hydroxy-3-methylglutaryl-coenzyme A (HMG-CoA) reductase inhibitor is the most preferred statin to treatment hyperlipidemia by decreasing serum levels of cholesterol, triglyceride, low-density lipoprotein, and increasing level of high-density lipoprotein<sup>1,2</sup>. ATR has solubility and dissolution rate-limited step for absorption. These characteristics lead to low oral bioavailability (12%) and cause to classify in Biopharmaceutical Classification

---

\*Corresponding author: E-mail: m.mahboobian@umsha.ac.ir

ORCID:

Reza Goudarzi: 0000-0001-6105-1512

Mohammad Mehdi Mahboobian: 0000-0003-1395-1457

(Received 20 Dec 2022, Accepted 08 Feb 2023)

System (BCS) as class II drug<sup>3</sup>. This characteristic can lead to increasing the daily dose of ATR up to 80 mg to achieve appropriate therapeutic efficiency, which can cause more side effects, especially in the case of polypharmacy<sup>4</sup>. Thus, enhancement in ATR dissolution rate is challenging due to its late release induced by insufficient solubility<sup>5</sup>. Among various approaches used to enhance drug dissolution, solid dispersion (SD) is very popular due to the simple steps of the process and economic efficiency<sup>6</sup>. In SD processes, the drug disperses highly in the hydrophilic carrier. It causes increasing dissolution rate and solubility by different mechanisms such as increase in surface area by decreasing in particle size<sup>7</sup>, improvement in drug wettability by direct contact with the hydrophilic carrier and changing in drug crystallinity<sup>8</sup>. SDs can develop by different methods. Among them, solvent evaporation and melting are the most common techniques due to convenience and need of simple facilities<sup>9</sup>. On the other hand, each method has some limitations depending on the physicochemical properties of selected drug and carriers. For instance, the melting method usually happens at high temperatures, which can predispose the drug or carrier to decomposition or in the solvent evaporation method, the drug and carrier dissolve in an organic solvent, and choosing a suitable solvent that could dissolve both the carrier and the drug may be problematic<sup>9,10</sup>.

Various grades of polyvinyl-pyrrolidone (PVP) are one of the most hydrophilic carriers to prepare SD formulations<sup>11</sup>. Polyvinyl-pyrrolidone K30 (PVP-K30) with an amorphous state is employed successfully to enhance the solubility of several poor water-soluble drugs such as toltrazuril<sup>12</sup>, indomethacin<sup>13</sup>, celecoxib<sup>14</sup>, gliclazide<sup>15</sup> and meloxicam<sup>16</sup>. Since high glass transition and melting temperature restrict the usage of this polymer for preparing SD by melting method<sup>11</sup>. Therefore, in this study, the solvent evaporation method was selected for preparing atorvastatin solid dispersions (ATR-SDs). Furthermore, different tablet formulations were prepared to evaluate the effect of various excipients on optimum SD formulation and preparation a suitable tablet with satisfactory dissolution efficiency characteristics.

Since tablets are the most common dosage form for oral drug delivery, the direct compression (DC) technique is the shortest and least complex way to fabricate tablets by rightly blending active pharmaceutical ingredient (API) with the suitable excipients and then compressing them into the tablet. DC technique has many advantages comparing wet/dry granulation, including being suitable for thermosensitive, solvent labile, or hydrolysis susceptible drugs and fewer manufacturing steps. On the other hand, considering the importance of flowability and compressibility of excipients in the DC method to certify uni-

form die filling compared to the granulation processes, the selection of excipient types and their amounts in the final formulation is so critical<sup>17,18</sup>.

As stated, this study aimed to prepare ATR-SDs by PVP-K30 as the carrier in various drug:carrier ratios. Based on *in vitro* dissolution studies, an optimum ratio was selected for physicochemical characterization and tableting. Tablet formulations contain different excipients and SD powders were designed for DC. Finally, tablets were analyzed for hardness, friability, disintegration time, and dissolution behavior.

## **METHODOLOGY**

### **Materials**

Atorvastatin calcium trihydrate was obtained from Sobhan Pharmaceutical Co. (Tehran, Iran). PVP-K30, Talc, and Carboxymethyl cellulose (Croscarmellose sodium) were purchased from Samchun Pure Chemical Co., Ltd (Seoul, Korea). Sodium starch glycolate was provided by Blulux laboratories Reagent, Ltd (India). Magnesium stearate was purchased from Acros Organics (Belgium). Colloidal silicon dioxide (Aerosil) and Microcrystalline cellulose (Avicel PH-102) were purchased from Evonik Degussa (Germany) and Boehringer Mannheim (Germany), respectively. All other chemicals were of pharmaceutical grades.

### **Preparation of ATR-SDs**

For the preparation of PVP-K30 based SDs by the solvent evaporation method, the calculated amount of drug and carrier (ATR:PVP-K30) in various weight ratios (1:1, 1:3, 1:5, and 1:7) were dissolved in the minimum amount of methanol with constant stirring for 30 min<sup>19</sup>. The obtained solution was kept in the oven (MMM-group, Germany) for 48 h at 45 °C for solvent evaporation and then in a desiccator for 48 h at room temperature to ensure no solvent remained in the mixture. Finally, the residue was sieved through No 100 mesh to get uniformly sized particles.

### **Preparation of physical mixture**

For investigation of the influence of SD processes apart from the polymer effect, the physical mixture (PM) of the best formulation was prepared by homogenous mixing of drug and carrier, in the selected ratio, which were previously sieved through mesh No 100<sup>20</sup>.

### ***In vitro* dissolution analysis**

The pure drug, SD formulations, and PM, each equivalent to 20 mg ATR, were

subjected to dissolution test for one h in 250 mL phosphate buffer solution (pH=6.8) at  $37\pm 0.5^{\circ}\text{C}^{21}$  for one h and rotating speed of 75 rpm, using a basket dissolution test apparatus (USP dissolution tester apparatus I)<sup>22,23</sup>. At various intervals, 2 mL of the sample was withdrawn and replaced with 2 mL of fresh buffer to keep the sink condition. Then samples were centrifuged (13000 rpm, 10 min), diluted, and spectrophotometrically (Specord 210 plus, Germany) assayed for ATR content at 242 nm<sup>24</sup>. The dissolution efficiency (DE) was deliberate as the area under the dissolution curve up to 60 min and was measured by the trapezoidal method and expressed as a percentage of the area at maximum dissolution.

### **Saturated solubility analysis**

Saturated solubility was assayed by adding an excess amount of pure ATR, optimum SD, and relative PM to 1 mL of distilled water in a test tube. Samples were agitated for 72 h at  $25\pm 0.5^{\circ}\text{C}$  at a rotating speed of 120 rpm using a shaker incubator (Heidolph Unimax 1010, Germany)<sup>25</sup>. Then they were centrifuged, and the supernatant was separated, diluted, and assayed for ATR content by using UV spectrophotometer at 242nm.

### **X-ray powder diffraction analysis (XRD)**

The XRD patterns of PVP-K30, ATR, SD, and PM were recorded using an X-ray diffractometer (Malvern PANalytical BV, Netherlands) to investigate the sample crystallinity modification during processes. Samples were subjected to nickel filtered  $\text{CuK}\alpha$  radiation ( $K=1.5406\text{ \AA}$ ), generating at 40 mA and 40 kV and scanned from  $2\theta$  angles of  $2^{\circ}$  to  $70^{\circ}$  with a step size of  $0.026^{\circ}$ <sup>26</sup>.

### **Differential scanning calorimetry analysis (DSC)**

Thermal analyses of SD, PM, pure ATR, and polymer were performed using DSC200 F3Maia (Germany). Samples were weighed and sealed in aluminum pans and were subjected to heat at a temperature rate of  $10^{\circ}\text{C}/\text{min}$  from  $32^{\circ}\text{C}$  to  $250^{\circ}\text{C}$ . Nitrogen gas purge was used throughout the analysis to keep an inert atmosphere. A sealed empty aluminum pan was used as a reference<sup>27</sup>.

### **Fourier transform infrared spectroscopy analysis (FTIR)**

FTIR analysis was done using an FTIR spectrometer (Bruker alpha, tensor 27, Germany). For this purpose, 2 mg of each sample (pure ATR, SD, PM, and PVP-K30) was triturated with 200 mg potassium bromide (KBr) and then compressed into a transparent disk under pressure. The FTIR spectrum of each sample was recorded over a wavenumber range of  $4000\text{--}400\text{ cm}^{-1}$  and a resolution of  $2.0\text{ cm}^{-1}$ <sup>28</sup>.

## Preparation of the SD tablets

In order to prepare SD tablets by direct compression method in various formulas, API and excipients were first sieved. Selected SD powder (equivalent to 20 mg ATR) was blended with carboxymethyl cellulose sodium (Croscarmellose sodium), or sodium starch glycolate in 1% and 2% w/w for 10 min as superdisintegrants, and then microcrystalline cellulose (Avicel PH-102) as filler was added to the mixture. Talc or Colloidal silicon dioxide (Aerosil) in various w/w ratios was added as glidant as well. Finally, the mixture was lubricated with magnesium stearate. The tablets were compressed by a single punch tablet press machine (Kavosh Co., Iran). Tablet weight theoretically was 200 mg. The composition of 8 tablet formulations is presented in Table 1.

**Table 1.** Composition of prepared ATR-SD tablets.

| Formulation code               | F1  | F2  | F3  | F4  | F5  | F6  | F7  | F8  |
|--------------------------------|-----|-----|-----|-----|-----|-----|-----|-----|
| ATR-PVP-K30 (mg)               | 40  | 40  | 40  | 40  | 40  | 40  | 40  | 40  |
| Sodium starch glycolate (mg)   | 2   | 4   | -   | -   | 2   | -   | 4   | -   |
| Croscarmellose sodium (mg)     | -   | -   | 2   | 4   | -   | 2   | -   | 4   |
| Talc (mg)                      | 2   | 2   | 2   | 2   | -   | -   | -   | -   |
| Colloidal silicon dioxide (mg) | -   | -   | -   | -   | 2   | 2   | 2   | 2   |
| Magnesium stearate (mg)        | 2   | 2   | 2   | 2   | 2   | 2   | 2   | 2   |
| Avicel PH 102 (mg)             | 154 | 152 | 154 | 152 | 154 | 154 | 152 | 152 |
| Total weight (mg)              | 200 | 200 | 200 | 200 | 200 | 200 | 200 | 200 |

## **Physical properties of the SD tablets**

In order to evaluate SD tablets physical properties, they were analyzed for hardness, friability, and disintegration time.

### **Hardness**

10 tablets from each formulation were tested using a hardness tester (Erweka, Germany), and breaking strength of each tablet was measured<sup>29</sup>.

### **Friability**

This test was carried out using friability tester (Erweka, Germany). 20 tablets from each formulation were loaded in the drum with speed of 25 rpm for 4 min. The whole weight of tablets before and after test was measured. The friability was calculated as a percentage of weight loss due to abrasion<sup>30</sup>.

### **Disintegration time**

Tablet disintegration test apparatus (Kavosh Co., Iran) was employed to determination of disintegration time of each formulation. The 900 mL of water at a temperature of  $37^{\circ}\text{C}\pm 2^{\circ}\text{C}$  was selected as a disintegration medium. Six tablets at once placed in the apparatus and time taken for all tablets to disintegrate completely was recorded<sup>31</sup>.

### **Dissolution test**

Tablets were also subjected to a dissolution test using USP type II (paddle) dissolution test apparatus with the same condition as previously explained for SD powders<sup>21</sup>. Finally, results were compared with the control tablet (containing untreated ATR by the same tablet formulation as the optimum tablet).

### **Statistical analysis**

In the present study, data were statistically analyzed by using GraphPad Prism 7 and one-way analysis of variance (ANOVA) followed by Tukey's test was applied. A *P* value less than 0.05 was served to be statistically significant.

## **RESULTS AND DISCUSSION**

### ***In vitro* dissolution studies**

To determine the optimum ratio for further analysis, the dissolution study was first done. Figure 1 illustrates dissolution profiles obtained for intact drug, SDs formulated in various ratios, and corresponding PMs. For all SD formulations containing PVP-K 30 as a hydrophilic carrier, a higher dissolution profile was obtained compared to the intact drug. As shown in Table 2, the maximum dis-

solution efficiency value during 60 min ( $DE_{60}$ ) was obtained for 1-1 drug-carrier ratio, which showed about 32% increases compare to the intact drug, while there was no significant difference between 1-1 and 1-3 ratios ( $P$  value > 0.05). It was noteworthy that by increasing carrier concentration to 7-fold,  $DE_{60}$  was decreased either for SD formulations or PMs. This confirms that the use of PVP-K30 as a water-soluble carrier can highly increase the dissolution rate of the drug. The hydrophilic nature and solubilization capacity of PVP-K30, cause a reduction in interfacial tension between the drug and dissolution medium, which results in drug wettability improvement<sup>14,32</sup>. On the other hand, applying further concentrations of PVP-K30 did not affect as much as lower concentrations (for both SD and PM) due to the generation of a viscous matrix around drug particles, which could hinder drug release by decreasing diffusion coefficient. As shown in Figure 1, in all SD formulations, the dissolution rate was significantly higher than the corresponding PM. Especially for 1-3, 1-5, and 1-7 ratios, the dissolution rates from physical mixtures were approximately like untreated ATR. It confirms that the SD method can remarkably increase the dissolution characteristic of the poorly water-soluble drug through several mechanisms, including the decrease in particle size and accumulation that lead to an increase in surface area and higher drug wettability<sup>7</sup>.

**Table 2.** Dissolution efficiency ( $DE_{60}$ ) of various samples (Mean $\pm$ SD, n=3)

| Samples (ATR:PVP-K30 ratio) | $DE_{60}$ (%)    |
|-----------------------------|------------------|
| ATR Powder                  | 49.56 $\pm$ 3.61 |
| 1-1 SD                      | 81.92 $\pm$ 1.95 |
| 1-3 SD                      | 80.89 $\pm$ 2.23 |
| 1-5 SD                      | 73.73 $\pm$ 6.8  |
| 1-7 SD                      | 65.69 $\pm$ 3.28 |
| 1-1 PM                      | 67.27 $\pm$ 2.82 |
| 1-3 PM                      | 55.34 $\pm$ 4.49 |
| 1-5 PM                      | 57.75 $\pm$ 0.75 |
| 1-7 PM                      | 55.88 $\pm$ 5.51 |

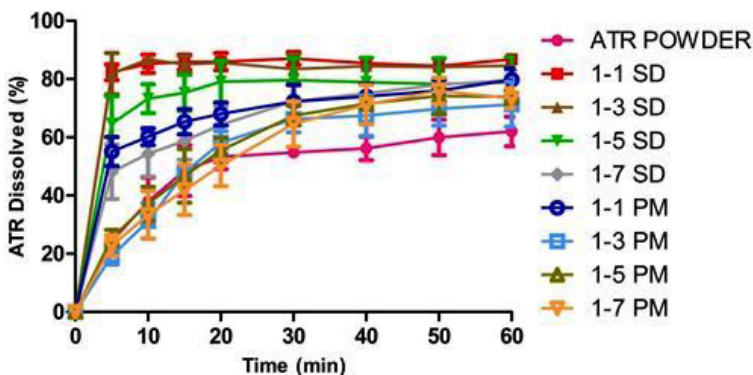


**Figure 1.** Dissolution graph of ATR-SD samples and related PMs (Mean $\pm$ SD, n=3).

### Saturated solubility studies

Saturated solubility studies were done for formulations that consist of drug-PVP-K30 ratio equal to 1-1, which was the optimum ratio. The saturated solubility of pure ATR in distilled water was  $141.02 \pm 3.35$   $\mu\text{g/mL}$ , which was increased to  $171.02 \pm 6.34$   $\mu\text{g/mL}$  and  $229.08 \pm 3.61$   $\mu\text{g/mL}$  for PM and SD samples, respectively. This solubility enhancement in the presence of a hydrophilic carrier could be associated with intermolecular hydrogen bonding formation between ATR and PVP-K30<sup>33</sup>. As mentioned, PVP-K30 causes a solubilizing effect by decreasing interfacial tension between ATR and release medium<sup>32</sup>. Higher saturated solubility for SD formulation than PM is another evidence for a greater dissolution rate of SD preparation compared to PM.

### X-ray powder diffraction analysis (XRD)

X-ray diffraction patterns of untreated ATR, PVP-K30, optimum SD formulation, and relative PM are presented in Figure 2. PVP-K30 did not show any sharp peak, which indicates its amorphous nature. The XRD pattern of intact ATR showed characteristic peaks at  $2\theta$  values of 9.1, 10.31, 12.23, 16.90, 17.09, 19.49, 21.64, and 23.74 that are related to its crystalline nature<sup>4,27,34</sup>. Completely disappearing of these peaks in SD formulation proves amorphization occurred completely. Whereas in PM diffractogram, ATR characteristic peaks were still presented although with a reduced intensity, which indicated that the crystalline structure of the pure drug still exists with slight amorphization (measured about 7%). Based on the results, high amorphization during SD processes could be the main mechanism for extra elevation in the dissolution rate of the SD formulation compared to the PM<sup>4</sup>.

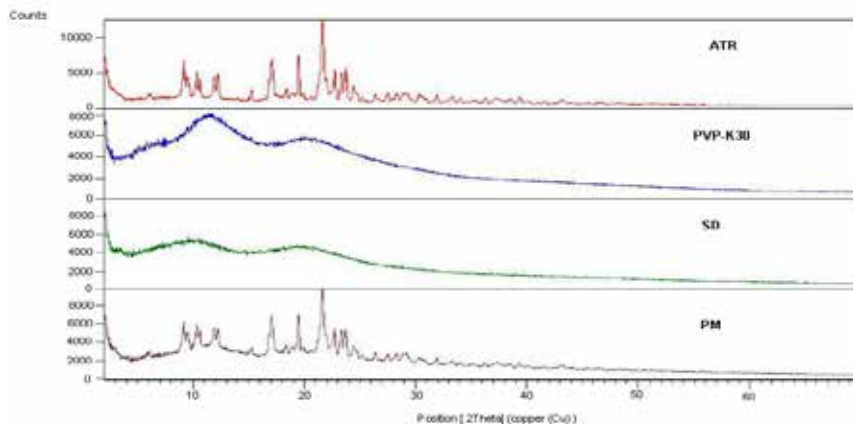


**Figure 2:** XRD patterns of the untreated drug (ATR), PVP-K30, optimum SD and PM.

### Differential scanning calorimetry analysis (DSC)

The results of DSC analysis for SD and PM and components are illustrated in Figure 3. The ATR thermal curve displayed three broad endothermic peaks at 63.63 °C, 99.98 °C, and 125.34 °C related to three step water loss (due to tri-hydrate form), and the fourth endothermic peak at 157.98 °C is related to the melting point of ATR<sup>24</sup>. PVP-K30 thermogram showed only a broad endothermic peak from 32 °C to 70 °C, corresponding to the loss of water because of the hygroscopic structure of PVP-K30<sup>35</sup>. The absence of any other peaks confirms the total amorphous structure for PVP-K30. No peak was recorded around the ATR melting point in the SD thermogram that confirms entire amorphization. In the corresponding PM thermogram, ATR endothermic peaks were recorded but with extremely low intensity, which proves amorphization occurred not as much as SD sample. In consequence, there was a precise correlation between DSC and XRD studies.

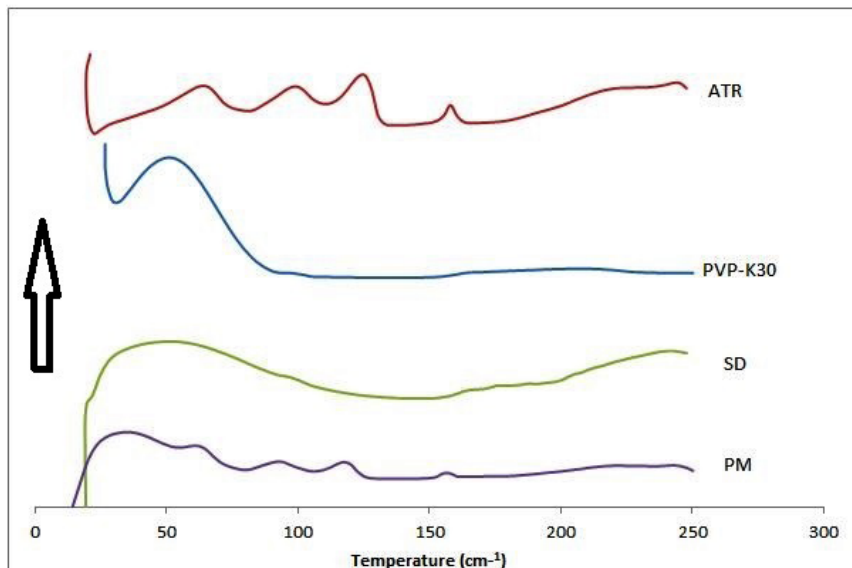


**Figure 3.** DSC thermograms of the untreated drug (ATR), PVP-K30, optimum SD and PM (□ : endothermic peak direction).

### Fourier transform infrared spectroscopy analysis (FTIR)

Figure 4 exhibited the FTIR spectra of ATR, carrier, SD and PM preparation. The PVP-K30 spectrum showed characteristic peaks at  $2953.50\text{ cm}^{-1}$  corresponding to the C-H stretching vibration and  $1665.99\text{ cm}^{-1}$  related to the C=O band. A broad band at  $3467.61\text{ cm}^{-1}$ , ascribed to O-H stretching vibration was recorded, due to water presence as DSC finding affirmed<sup>36</sup>. The bulk ATR showed sharp characteristic peaks at  $3669.7\text{ cm}^{-1}$  and  $3364.5\text{ cm}^{-1}$ , corresponding to O-H and N-H stretching, respectively. The C=O asymmetry and symmetry stretching bonds were seen at  $1650.5\text{ cm}^{-1}$  and  $1579.3\text{ cm}^{-1}$ , respectively. The stretching of aromatic C-C bonds were represented at  $1552\text{ cm}^{-1}$ ,  $1510.5\text{ cm}^{-1}$ , and  $1435.8\text{ cm}^{-1}$ . The sharp bonds at  $1435.86\text{ cm}^{-1}$  related to C-N stretching, and at  $1216.51\text{ cm}^{-1}$  linked to C-F stretching vibration. Finally, the C-O stretching bond was recorded at  $1159.5\text{ cm}^{-1}$ . As it is clear in Figure 4, PM spectra showed the principal characteristic peak of the component with a comparatively sharp appearance, in contrast in the SD sample all characteristic peaks were considerably broadened that attributed to full drug amorphization during SD preparation, confirming DSC and XRD results. Another reason for broader peaks in the SD sample than PM could be related to hydrogen bonding formation between the O-H or N-H group of ATR and the C=O group of PVP-K30 as reported by other researchers for SD development of various drugs with PVP-K30<sup>37,38</sup>.

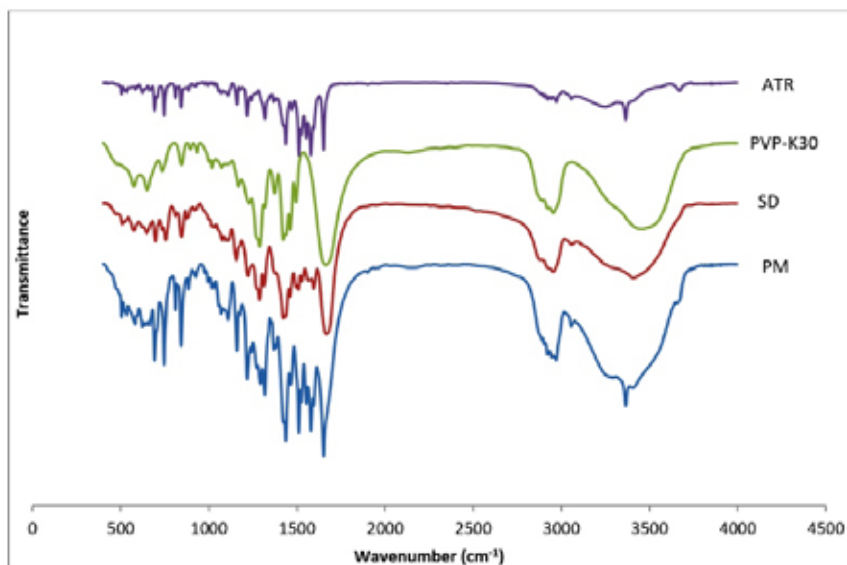


**Figure 4:** FTIR spectra of the untreated drug (ATR), PVP-K30, optimum SD and PM.

## Tableting properties

### Hardness

As shown in Table 3, changes in the type of disintegrants and, also glidants could affect hardness. F3 and F4 formulations in which croscarmellose sodium (CRS) was used as superdisintegrant showed slightly higher hardness than tablets F1 and F2 in which sodium starch glycolate (SSG) was used instead. However, talc was used in all of them as a glidant. But this increase in hardness was contrary in the presence of Aerosil as a glidant, which could be understood by comparing F7 and F8 formulations. In the F7 formulation applying SSG showed significantly higher hardness than applying CRS in the F8 formulation. The same results were obtained for F5 and F6, which are the same in 1% Aerosil. The F5 formulation showed more hardness by use of SSG. By comparison of F2 and F7 formulations, which differed only in the type of glidant, it can be concluded that Aerosil causes tablets to be about two times harder than those prepared by talc. In conclusion, higher hardness values were recorded for formulations containing Aerosil than formulations containing talc. Moreover, in the presence of Aerosil, higher hardness values were measured for those containing SSG.

**Table 3.** Physical properties of prepared tablets (Mean±SD)

| Formulation | Hardness (kp)<br>(n=10) | Friability (%)<br>(n=20) | Disintegration<br>time (min) (n=6) | DE <sub>60</sub> (%)<br>(n=3) |
|-------------|-------------------------|--------------------------|------------------------------------|-------------------------------|
| F1          | 4.68±0.42               | 0.72                     | < 1                                | 88.13±0.17                    |
| F2          | 4.92±0.33               | 0.77                     | < 1                                | 78.88±1.3                     |
| F3          | 5.21±0.40               | 0.50                     | > 15                               | 71.38±1.43                    |
| F4          | 5.08±0.23               | 0.58                     | > 15                               | 61.68±3.08                    |
| F5          | 8.67±0.88               | 0.12                     | > 30                               | -                             |
| F6          | 7.62±0.9                | 0.04                     | > 30                               | -                             |
| F7          | 8.04±0.94               | 0.10                     | 15 << 30                           | 36.99±.62                     |
| F8          | 6.51±0.79               | 0.36                     | 15 << 30                           | 15.93±3.61                    |
| Control     | 9.9±0.39                | 0.09                     | < 1                                | 48.96±0.64                    |

Kp: kilopond

min: minute

### Friability

Friability is another factor for evaluating the tablet's physical strength over mechanical stress during the development procedure and transportation<sup>39</sup>. Although the high hardness of the tablet is not always the reason for its low attrition due to the possibility of capping, our funding revealed a logical correlation between hardness and friability (Table 3). However, the friability percentages for all formulations were lower than 0.8%, which met commercial requirements<sup>30</sup>.

### Disintegration time

The disintegration time of formulated tablets was analyzed as a distinguished test to guide formulation selection for further analysis. As shown in Table 3, the fastest disintegration time was observed in F1 and F2 by using SSG in 1% w/w and 2% w/w ratios, respectively. There was no significant difference between F1 and F2 formulations. So, control tablet was formulated by the same formulation as F1 (optimum formulation with the lowest percentage of excipients) for better comparison of the effects. It should be noted that the use of talc as a glidant, also helps the tablet to disintegrate easily, even with a lower percentage of superdisintegrant, either SSG or CRS. But in general, SSG showed

better disintegration activity than CRS<sup>40</sup>. It could be concluded that while PVP-K30 (which acts as a binder) is present in the formulation, CRS is not a suitable disintegrant. Also, Aerosil should not use in combination with PVP-K30, due to its moisture adsorbent and thickening agent, which makes the tablet difficult to break up and needs more time to disintegrate<sup>41</sup>. Also, SSG in the concentration of 1% w/w could not disintegrate tablets formulated by Aerosil, while in 2% w/w, it could slowly disintegrate tablets within a long time. The result obtained from the comparison of F3 and F4 formulations was noteworthy. By increasing the CRS ratio, disintegration time did not change significantly, as reported by other researchers to albumin tannate tableting<sup>42</sup>. Finally, maximum disintegration times were shown for F5 and F6 formulations, which took more than 30 minutes to disintegrate, so they were rejected for subjecting to the dissolution test.

### **Tablets dissolution properties**

Acquired dissolution profiles for various tablet formulations are represented in Figure 5. The maximum drug dissolution rate was obtained for F1 formulation that showed 90% drug dissolved within 15 min. The Control Tablet that contained untreated ATR with the exact formulation of F1 showed approximately half the dissolution rate of the F1 formulation. It proves that drug dispersion in a suitable carrier (SD preparation) could become a promising strategy in new formulation development that shows a higher dissolution rate. By comparison of F1 against F2 and F3 against F4, it can assume that when the tablet disintegrates well in a lower percentage of disintegrant, increasing in concentration of disintegrant results in a lower dissolution rate and haven't any benefit on disintegration time. At higher concentrations, a thick barrier rises at the release medium around the tablet due to the high viscosity of the superdisintegrant, which could hinder the disintegration or dissolution of tablet components<sup>41</sup>. As shown in Table 3, the  $DE_{60}$  values obtained for F7 and F8 formulations weren't desirable due to their long disintegration time (more than 20 min). It can conclude that Aerosil is not a suitable glidant for the formulation containing PVP-K30, which acts as a strong binder, because of the high rigidity created for the formulation that could hinder tablet disintegration and drug dissolution.

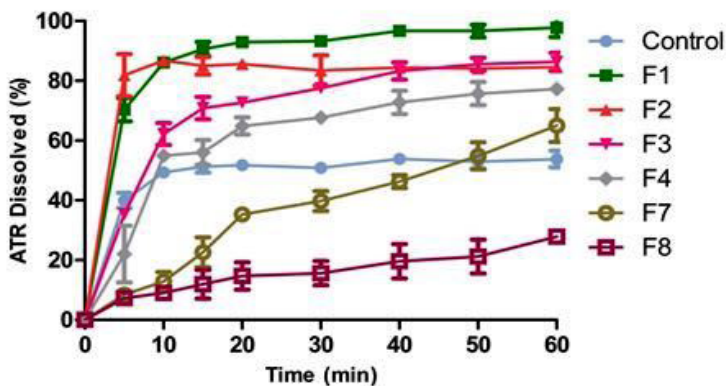


**Figure 5.** Dissolution graph of ATR tablets (Mean $\pm$ SD, n=3).

## CONCLUSIONS

The present study exhibited that the SD technique, developed by solvent evaporation method and PVP-K30 as a carrier, could improve the dissolution characteristic of ATR effectively, as a poor-soluble drug. It was found that using PVP-K30 in the least ratio, which is in equal proportion to the ATR, causes the maximum increase in the dissolution rate (up to 80%) in the first 10 min. It seems that in addition to the selection of the appropriate polymer, choosing the correct concentration has a great effect on increasing the dissolution rate over a period of time. Also, more than 60% elevation of ATR saturated solubility was obtained by using this method of preparation. The findings of the solid-state characterizations revealed that the total amorphization of ATR-PVP-K30 SD could be the key factor for this dissolution rate enhancement. Furthermore, to formulate an efficient tablet from optimum ATR-PVP-K30 SD (1:1 ratio), SSG at 1% w/w as a disintegrant, talc at 1% w/w for lubrication, and magnesium stearate at 1% w/w besides Avicel PH 102 were found to be suitable components to formulate SD based tablets of ATR.

## STATEMENT OF ETHICS

None.

## CONFLICT OF INTEREST

The authors report no conflicts of interests.

## AUTHOR CONTRIBUTIONS

Reza Goudarzi; Investigation, Writing - Original Draft. Mohammad Mehdi Mahboobian; Conceptualization, Supervision.

## **ACKNOWLEDGMENT**

This work was supported financially (Grant No. 9706273738) by the deputy of research and technology, Hamadan University of Medical Sciences, Hamadan, Iran.

## REFERENCES

1. Shamsuddin MF, Ansari SH, Ali J. Atorvastatin solid dispersion for bioavailability enhancement. *J Adv Pharm Technol Res.* 2016;7(1):22. <https://doi.org/10.4103/2231-4040.169873>.
2. Fayed ND, Goda AE, Essa EA, El Maghraby GM. Chitosan-encapsulated niosomes for enhanced oral delivery of atorvastatin. *J Drug Deliv Sci Technol.* 2021;66:102866. <https://doi.org/10.1016/j.jddst.2021.102866>.
3. Sharma M, Mehta I. Surface stabilized atorvastatin nanocrystals with improved bioavailability, safety and antihyperlipidemic potential. *Sci Rep.* 2019;9(1):1-11. <https://doi.org/10.1038/s41598-019-52645-0>.
4. Shaker MA, Elbadawy HM, Shaker MA. Improved solubility, dissolution, and oral bioavailability for atorvastatin-Pluronic® solid dispersions. *Int J Pharm.* 2020;574:118891. <https://doi.org/10.1016/j.ijpharm.2019.118891>.
5. Dong W, Su X, Xu M, Hu M, Sun Y, Zhang P. Preparation, characterization, and *in vitro/vivo* evaluation of polymer-assisting formulation of atorvastatin calcium based on solid dispersion technique. *Asian J Pharm Sci.* 2018;13(6):546-54. <https://doi.org/10.1016/j.ajps.2018.08.010>.
6. Liu Y, Wang T, Ding W, Dong C, Wang X, Chen J, et al. Dissolution and oral bioavailability enhancement of praziquantel by solid dispersions. *Drug Deliv Transl Res.* 2018;8(3):580-90. <https://doi.org/10.1007/s13346-018-0487-7>.
7. Jermain SV, Brough C, Williams III RO. Amorphous solid dispersions and nanocrystal technologies for poorly water-soluble drug delivery—an update. *Int J Pharm.* 2018;535(1-2):379-92. <https://doi.org/10.1016/j.ijpharm.2017.10.051>.
8. Bhujbal SV, Mitra B, Jain U, Gong Y, Agrawal A, Karki S, et al. Pharmaceutical amorphous solid dispersion: A review of manufacturing strategies. *Acta Pharm Sin B.* 2021;11(8):2505-36. <https://doi.org/10.1016/j.apsb.2021.05.014>.
9. Singh G, Kaur L, Gupta GD, Sharma S. Enhancement of the solubility of poorly water soluble drugs through solid dispersion: a comprehensive review. *Indian J Pharm Sci.* 2017;79(5):674-87. <https://doi.org/10.4172/pharmaceutical-sciences.1000279>.
10. Paudwal G, Rawat N, Gupta R, Baldi A, Singh G, Gupta PN. Recent advances in solid dispersion technology for efficient delivery of poorly water-soluble drugs. *Curr Pharm Des.* 2019;25(13):1524-35. <https://doi.org/10.2174/1381612825666190618121553>.
11. Nair AR, Lakshman YD, Anand VS, Sree KN, Bhat K, Dengale SJ. Overview of extensively employed polymeric carriers in solid dispersion technology. *AAPS Pharm Sci Tech.* 2020;21(8):1-20. <https://doi.org/10.1208/s12249-020-01849-z>
12. Sun W, Pan B. Effect of micro-environment modification and polymer type on the in-vitro dissolution behavior and in-vivo performance of amorphous solid dispersions. *Eur J Pharm Sci.* 2017;104:240-54. <https://doi.org/10.1016/j.ejps.2017.04.007>.
13. Li J, Fan N, Wang X, Li C, Sun M, Wang J, et al. Interfacial interaction track of amorphous solid dispersions established by water-soluble polymer and indometacin. *Eur J Pharm Sci.* 2017;106:244-53. <https://doi.org/10.1016/j.ejps.2017.05.067>.
14. Motallae S, Taheri A, Homayouni A. Preparation and characterization of solid dispersions of celecoxib obtained by spray-drying ethanolic suspensions containing PVP-K30 or isomalt. *J Drug Deliv Sci Technol.* 2018;46:188-96. <https://doi.org/10.1016/j.jddst.2018.05.020>.
15. Febriyenti F, Rahmi S, Halim A. Study of gliclazide solid dispersion systems using PVP

K-30 and PEG 6000 by solvent method. *J Pharm Bioallied Sci.* 2019;11(3):262. [https://doi.org/10.4103/jpbs.JPBS\\_87\\_18](https://doi.org/10.4103/jpbs.JPBS_87_18).

16. Shi X, Huang W, Xu T, Fan B, Sheng X. Investigation of drug–polymer miscibility and solubilization on meloxicam binary solid dispersion. *J Pharm Innov.* 2020;15(1):125-37. <https://doi.org/10.1007/s12247-019-09378-4>.

17. Schmidt PC, Rubensdörfer CJ. Evaluation of Ludipress as a “multipurpose excipient” for direct compression: Part I: Powder characteristics and tableting properties. *Drug Dev Ind Pharm.* 1994;20(18):2899-925. <https://doi.org/10.3109/03639049409042687>.

18. de Backere C, De Beer T, Vervaeke C, Vanhoorne V. Effect of binder type and lubrication method on the binder efficacy for direct compression. *Int J Pharm.* 2021;607:120968. <https://doi.org/10.1016/j.ijpharm.2021.120968>.

19. Iqbal A, Hossain S, Shamim A, Islam M, Siddique AT. Formulation, *in vitro* evaluation and characterization of atorvastatin solid dispersion. *Trop J Pharm Res.* 2020;19(6):1131-8. 10.4314/tjpr.v19i6.2.

20. Liu C, Desai KG, Liu C. Enhancement of dissolution rate of valdecoxib using solid dispersions with polyethylene glycol 4000. *Drug Dev Ind Pharm.* 2005;31(1):1-0. <https://doi.org/10.1081/DDC-43918>.

21. Vasoya JM, Desai HH, Gumaste SG, Tillotson J, Kelemen D, Dalrymple DM. Development of solid dispersion by hot melt extrusion using mixtures of polyoxyglycerides with polymers as carriers for increasing dissolution rate of a poorly soluble drug model. *J Pharm Sci.* 2019;108(2):888-96. <https://doi.org/10.1016/j.xphs.2018.09.019>.

22. Ahmed IS, El-Hosary R, Shalaby S, Abd-Rabo MM, Elkhateeb DG, Nour S. PD-PK evaluation of freeze-dried atorvastatin calcium-loaded poly-ε-caprolactone nanoparticles. *Int J Pharm.* 2016;504(1-2):70-9. <https://doi.org/10.1016/j.ijpharm.2016.03.045>.

23. Kapote DN, Wagner KG. Influence of shellac on the improvement of solubility and supersaturation of loratadine amorphous solid dispersion using a new grade of HPMC. *J Drug Deliv Sci Technol.* 2021;61:102116. <https://doi.org/10.1016/j.jddst.2020.102116>.

24. Shete G, Puri V, Kumar L, Bansal AK. Solid state characterization of commercial crystalline and amorphous atorvastatin calcium samples. *AAPS Pharm Sci Tech.* 2010;11(2):598-609. <https://doi.org/10.1208/s12249-010-9419-7>.

25. Onoue S, Sato H, Ogawa K, Kawabata Y, Mizumoto T, Yuminoki K, et al. Improved dissolution and pharmacokinetic behavior of cyclosporine A using high-energy amorphous solid dispersion approach. *Int J Pharm.* 2010;399(1-2):94-101. <https://doi.org/10.1016/j.ijpharm.2010.08.007>.

26. Biswal S, Sahoo J, Murthy PN. Physicochemical properties of solid dispersions of glimepiride in polyvinylpyrrolidone K90. *AAPS Pharm Sci Tech.* 2009;10(2):329-34. <https://doi.org/10.1208/s12249-009-9212-7>.

27. Choudhary A, Rana AC, Aggarwal G, Kumar V, Zakir F. Development and characterization of an atorvastatin solid dispersion formulation using skimmed milk for improved oral bioavailability. *Acta Pharm Sin B.* 2012;2(4):421-8. <https://doi.org/10.1016/j.apsb.2012.05.002>.

28. Ambike AA, Mahadik KR, Paradkar A. Spray-dried amorphous solid dispersions of simvastatin, a low T<sub>g</sub> drug: *in vitro* and *in vivo* evaluations. *Pharm Res.* 2005;22:990-8. <https://doi.org/10.1007/s11095-005-4594-z>.

29. Khan A, Iqbal Z, Shah Y, Ahmad L, Ullah Z, Ullah A. Enhancement of dissolution rate of class II drugs (Hydrochlorothiazide); a comparative study of the two novel approaches;

solid dispersion and liqui-solid techniques. *Saudi Pharm J.* 2015;23(6):650-7. <https://doi.org/10.1016/j.jsps.2015.01.025>.

30. Shoormeij Z, Taheri A, Homayouni A. Preparation and physicochemical characterization of meloxicam orally fast disintegration tablet using its solid dispersion. *Braz J Pharm S.* 2018;53.

31. Pusapati RT, Kumar MK, Rapeti SS, Murthy TE. Development of co-processed excipients in the design and evaluation of atorvastatin calcium tablets by direct compression method. *Int J Pharm Investig.* 2014;4(2):102. <https://doi.org/10.1590/s2175-97902017000400176>.

32. Singh S, Sharma N, Kaur G. Central composite designed solid dispersion for dissolution enhancement of fluvastatin sodium by kneading technique. *Ther Deliv.* 2020;11(5):313-28. <https://doi.org/10.4155/tde-2020-0025>.

33. Ruan L-P, Yu B-Y, Fu G-M, Zhu D-n. Improving the solubility of ampelopsin by solid dispersions and inclusion complexes. *J Pharm Biomed.* 2005;38(3):457-64. <https://doi.org/10.1016/j.jpba.2005.01.030>.

34. Frizon F, de Oliveira Eloy J, Donaduzzi CM, Mitsui ML, Marchetti JM. Dissolution rate enhancement of loratadine in polyvinylpyrrolidone K-30 solid dispersions by solvent methods. *Powder Technol.* 2013;235:532-9. <https://doi.org/10.1016/j.powtec.2012.10.019>.

35. Sethia S, Squillante E. Solid dispersion of carbamazepine in PVP K30 by conventional solvent evaporation and supercritical methods. *Int J Pharm.* 2004;272(1-2):1-10. <https://doi.org/10.1016/j.ijpharm.2003.11.025>.

36. Kyaw Oo M, Mandal UK, Chatterjee B. Polymeric behavior evaluation of PVP K30-poloxamer binary carrier for solid dispersed nisoldipine by experimental design. *Pharm Dev Technol.* 2017;22(1):2-12. <https://doi.org/10.3109/10837450.2015.1116568>.

37. Tantishaiyakul V, Kaewnopparat N, Ingkawatornwong S. Properties of solid dispersions of piroxicam in polyvinylpyrrolidone. *Int J Pharm.* 1999;181(2):143-51. [https://doi.org/10.1016/S0378-5173\(99\)00070-8](https://doi.org/10.1016/S0378-5173(99)00070-8).

38. Abedinoghli D, Charkhpour M, Osouli-Bostanabad K, Selsehjonban S, Emami S, Barzegar-Jalali M, et al. Electrospayed nanosystems of carbamazepine-PVP K30 for enhancing its pharmacologic effects. *Iran J Pharm Res.* 2018;17(4):1431.

39. Karalia D, Siamidi A, Karalis V, Vlachou M. 3D-Printed Oral Dosage Forms: Mechanical Properties, Computational Approaches and Applications. *Pharmaceutics.* 2021 Sep;13(9):1401. <https://doi.org/10.3390/pharmaceutics13091401>.

40. Gosai AR, Patil SB, Sawant KK. Formulation and evaluation of orodispersible tablets of ondansetron hydrochloride by direct compression using superdisintegrants. *Int J Pharm Sci Nanotechnol.* 2008;26(1):106-11.

41. Khan LG, Razvi N, Anjum F, Siddiqui SA, Ghayas S. Effects of various excipients on tizanidine hydrochloride tablets prepared by direct compression. *Pak J Pharm Sci.* 2014;27(5).

42. Ferrero C, Munoz N, Velasco M, Muñoz-Ruiz A, Jiménez-Castellanos R. Disintegrating efficiency of croscarmellose sodium in a direct compression formulation. *Int J Pharm.* 1997;147(1):11-21. [https://doi.org/10.1016/S0378-5173\(96\)04784-9](https://doi.org/10.1016/S0378-5173(96)04784-9).

43. Setty CM, Prasad D, Gupta V, Sa B. Development of fast dispersible aceclofenac tablets: effect of functionality of superdisintegrants. *Indian J Pharm Sci.* 2008;70(2):180. <https://doi.org/10.4103/0250-474X.41452>

# Determination of riboflavin bioaccessibility in legumes by *in vitro* digestion using different cooking methods

Sultan KESİK<sup>1\*</sup>, Jale ÇATAK<sup>1</sup>, Kübra ADA<sup>1</sup>, Kübra DEMİR<sup>1</sup>, Halime UĞUR<sup>2</sup>,  
Mustafa YAMAN<sup>3</sup>

<sup>1</sup> Department of Nutrition and Dietetics, Faculty of Health Sciences, Istanbul Sabahattin Zaim University, Istanbul, 34303, Türkiye

<sup>2</sup> Department of Nutrition and Dietetics, Faculty of Health Science, Kutahya Health Sciences University, Kütahya, 43020, Türkiye

<sup>3</sup> Department of Molecular Biology and Genetics, Faculty of Engineering and Natural Sciences, Istanbul Sabahattin Zaim University, Istanbul, 34303, Türkiye

---

## ABSTRACT

This research aimed to investigate the riboflavin cooking losses and bioaccessibilities according to the cooking methods in legumes. Considerable nutrient losses occur during the cooking/preparation of foods. Updating old data is important today to support and complement a healthy diet. The riboflavin contents of legumes were measured in raw, pressure-cooked, pan-cooked, and digested cooked legumes. For the bioaccessibility determination, *in vitro* method was used to simulate the human gastrointestinal tract. Average riboflavin cooking losses of pressure- and pan-cooked legumes were 13.5% and 38.6% and the average riboflavin bioaccessibility was 58.1% and 57.6%, respectively. As a result of High Performance Liquid Chromatography analysis, it has been determined that there were fewer cooking losses and higher bioaccessibility in the pressure cooking method. However, there was no statistical difference between the two cooking methods. The pressure cooking method may be recommended due to fewer riboflavin cooking losses.

**Keywords:** Bioaccessibility, cooking loss, legumes, riboflavin

---

\*Corresponding Author: Email: sultankesik@gmail.com

ORCIDs:

Sultan Kesik: 0000-0002-2393-1487

Jale Çatak: 0000-0002-2718-0967

Kübra Ada: 0000-0001-6243-9703

Kübra Demir: 0000-0001-5396-4477

Halime Uğur: 0000-0002-2932-4215

Mustafa Yaman: 0000-0001-9692-0204

(Received 23 Feb 2023, Accepted 24 Mar 2023)

## INTRODUCTION

Legumes are a good source of protein and nutrients for developing countries in the world. They provide fiber, B group vitamins, and other micro-nutrients such as magnesium, zinc, phosphorus, iron, and copper<sup>1</sup>. The consumption of legumes worldwide is 21 grams/person/day but the consumption of meat as a source of protein is more than legumes<sup>2</sup>.

Legumes contain 0.062 mg/100 g of riboflavin as a good source<sup>3</sup>. The main source of riboflavin in the diet comes from eggs, organ meats, lean meats, and milk, but some vegetables are also rich in riboflavin<sup>4</sup>. Riboflavin, also known as lactoflavin composed of ribitol and lumichrome, and its chemical formula is  $C_{17}H_{24}ON_4O_6$ . It is heat-stable and water-soluble like other group B vitamins<sup>5</sup>. Riboflavin can be converted to FMN (flavin mononucleotide) and FAD (flavin adenine dinucleotide) in tissues, and these coenzyme forms release energy from carbohydrates, fats, and protein through the Krebs cycle, mitochondrial electron transport, and other electron transfer mechanisms. These compounds play essential roles in accepting electrons in biochemical reactions. In addition, it plays essential roles in protein stabilization and apo-protein synthesis<sup>6</sup>. Recommended Dietary Allowance (RDA) of riboflavin for women and men respectively: 1.1 mg/day and 1.3 mg/day<sup>7</sup>.

Riboflavin has low stability in alkaline conditions and maximum stability at pH 2.0 –5.0 against heat degradation<sup>8</sup>. In addition, riboflavin, FMN, and FAD can easily degrade by visible light<sup>9</sup>. For these reasons, exposure to light as sun-drying processes causes riboflavin losses. Another factor that causes riboflavin loss is spilling the cooking water. The levels of B vitamins in foods are affected by cooking. During cooking, the losses of B vitamins occur due to their high ability to be dissolved and thermal uncertainty<sup>10,11</sup>. All the listed factors affect the bioaccessibility of riboflavin and the amount of losses that occur during cooking<sup>12</sup>.

The energy circulating in the ecosystem is essential for all possessions. The laws of thermodynamics handle the energy flow in ecological systems<sup>13,14</sup>. However, each energy transfer along the food chain causes the loss of usable metabolic energy<sup>15,16</sup>. Biologicals gain ATP and thermal energy in mitochondria from the energy stored in the food's chemical bonds due to cellular metabolism<sup>17,18</sup>. Mitochondria are named as a "the cell powerhouses" due to its functions that are regulating ATP production and cellular metabolism<sup>19</sup>. Lately, researchers have given their attention to the role of mitochondria in the regulation of cellular energy production<sup>20</sup>. Recent investigations reveal that the deficiency of

some B-group vitamins decreases mitochondrial function and disrupts energy metabolism<sup>21,22</sup>. The B-group vitamins deficiency is vital for energy metabolism. If it occurs, these situations threaten ,cellular growth, function, and survival.

Bioaccessibility is the quantity of digested nutrients that potentially become available for absorption in the gastrointestinal tract<sup>23-25</sup>. Bioavailability studies are important for making nutrition plans and providing the closest requirements. However, bioavailability studies are disadvantageous in terms of both procedures and time and cost<sup>26</sup>. Therefore, this study aimed to update the limited and outdated data and determine the cooking losses and bioaccessibility of riboflavin with an *in vitro* gastrointestinal model.

## **2. METHODOLOGY**

### **2.1. Reagents and Materials**

The riboflavin standard and acid phosphatase from potatoes, taka diastase from *Aspergillus oryzae*, alpha-amylase from *Aspergillus oryzae*, beta-glucosidase from almonds, pepsin from porcine gastric mucosa, pancreatin, lipase, hydrochloric acid (HCl, 37%), NaCl, CaCl<sub>2</sub>.2H<sub>2</sub>O, KCl, NaHCO<sub>3</sub>, mucin, bovine serum albumin, urea, uric acid, bile salts mixture, methanol (MeOH), acetonitrile (ACN), trichloroacetic acid (TCA), 1-heptane sulfonic acid and a sodium salt were supplied from Sigma-Aldrich (St. Louis, Missouri, USA).

### **2.2. Samples and Cooking Methods**

In this study, four different legumes (dry beans, chickpeas, red lentils, and green lentils) were obtained from local markets in Istanbul, Turkey. Legume samples were divided into 3 groups with 3 legumes each. The first group (raw) was uncooked, while the other two groups were cooked by pressure and pan cooking methods.

After 130 grams of chickpeas and beans were weighed, soaked in 500 mL of water for 12 hours. Then, 150 grams of each sample and 600 mL of water were added to the pan and pressure cooker, and the cooking process was carried out. No pre-cooking preparation was made for the red lentil sample, but 300 grams of green lentils were boiled by adding 800 mL of water for 10 minutes, and the boiling water was spilled. For both samples, 150 grams were weighed, and two different cooking methods were applied. While 800 mL of water was used in both methods during cooking for red lentils, 500 mL of water was used for green lentils.

The legumes were put on the pressure cooker and cooked at 125 °C for 1 hour (chickpeas), 45 minutes (beans), 10 minutes (red lentils), and 20 minutes (green lentils). Pan cooking of samples was performed in a pan at 100 °C for 1 hour 50 min for chickpeas, 1 hour 45 min for beans, 20 minutes for red lentils, and 30 minutes for green lentils. Finally, the samples were homogenized with the blender together with the cooking water. Each sample was analyzed 3 times in each cooking method. The cooked legume samples were cooled to room temperature.

### **2.3. Extraction of Riboflavin from Legumes and HPLC Analysis of Riboflavin**

The extraction and HPLC determination method for riboflavin described by Çatal *et al.*

was used with some modifications<sup>27</sup>. First, a 5 g homogenized sample was added to a 100 mL Erlenmeyer flask. Next, 60 mL 0.1 N HCl solution was added and autoclaved at 121 °C for 30 min. An enzymatic procedure was accomplished to release the phosphorylated forms of riboflavin (FAD and FMN). The solution was cooled to room temperature and the pH was adjusted to 4.5 using a sodium acetate (2.5 mM) solution. In the enzymatic extraction stage, 100 mg taka diastase and 10 mg acid phosphatase were added to the sample and incubated at 37 °C for 3 h in a shaking water bath. Then, after cooling to room temperature, the volume was completed to 100 mL with 0.1 HCl solution, filtered, and injected into HPLC for riboflavin analysis.

### **2.4. HPLC Determination of Riboflavin**

A Shimadzu Nexera-i HPLC with a Shimadzu RF-20A fluorescence detector (Shimadzu Corporation, Kyoto, Japan) was used for the separation of riboflavin. The mobile phase consisted of 75% deionized water and 25% methanol. The separation was with an Eclipse X08-C18, 5  $\mu\text{m}$ , 4.6×150mm column (Agilent, USA) with a flow rate of 1 mL/min. The fluorescence detector excitation and emission wavelengths were 290 and 395 nm, respectively. The column oven temperature was 25 °C.

## 2.5. *In-Vitro* Gastrointestinal Model and Riboflavin Bioaccessibility

*In vitro* analysis was achieved via the methodology described by Lee *et al.* with some modifications<sup>28</sup>. The preparation of the *in vitro* digestion condition and the digestion process are shown in Fig. 1. Saliva solution, gastric, duodenal, and bile juices were prepared using organic and inorganic chemicals and enzymes (Fig. 1). In this *in vitro* human digestion model, organic and inorganic constituents were prepared with 500 mL of distilled water for each digestive enzyme. Next, each enzyme was mixed into that solution. Then, using 1M HCl or 0.2M NaOH, the pH was adjusted to the proper value for each solution (given in Fig. 1).

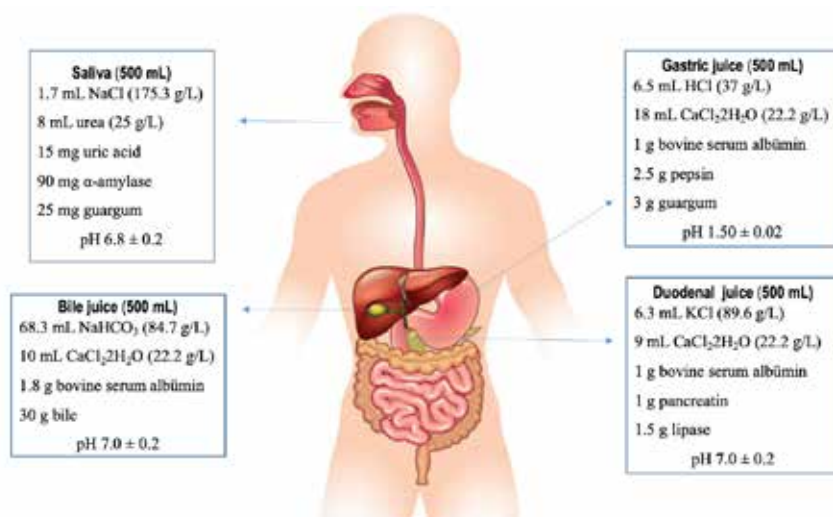


**Fig 1.** *In vitro* digestion model and digestion process

In the mouth step, a 5 g test sample was mixed with 5 mL saliva solution in a 50 mL falcon tube for 20 s with a vortex. This mixture was incubated for 5 min at 37 °C in a shaking water bath. After this stage, in the gastric step, 12 mL of gastric juice was added to the test sample provided from the mouth stage, and this mixture was allowed to incubate once more in a shaking water bath at 37 °C for two hours. Next, 10 mL of duodenal juice and 5 mL of bile juice were added to the test sample provided from the gastric stage. This mixture was incubated for two hours at 37 °C in a shaking water bath. Using trichloroacetic acid, the pH of the solution was adjusted to 4.5 after the digestion procedure was accomplished, finishing volume was diluted to 50 mL by deionized water and centrifuged for 10 minutes at 8000 rpm. The obtained solution was used in riboflavin determination analysis.

## 2.6. Statistical Analysis

Analyses with samples were performed three times and the mean value was used. Significant differences within groups were statistically identified by ANOVA ( $p < 0.05$ , Tukey's test).

## 3. RESULTS AND DISCUSSION

Scope of the study, 4 different legume species were cooked with two different methods (pan, and pressure cooker) and digested by *in vitro* methods. At each step, riboflavin levels were measured, and cooking losses and bioaccessibility values were calculated due to the cooking methods. The HPLC chromatogram of riboflavin in the chickpea sample is given in Fig. 2.

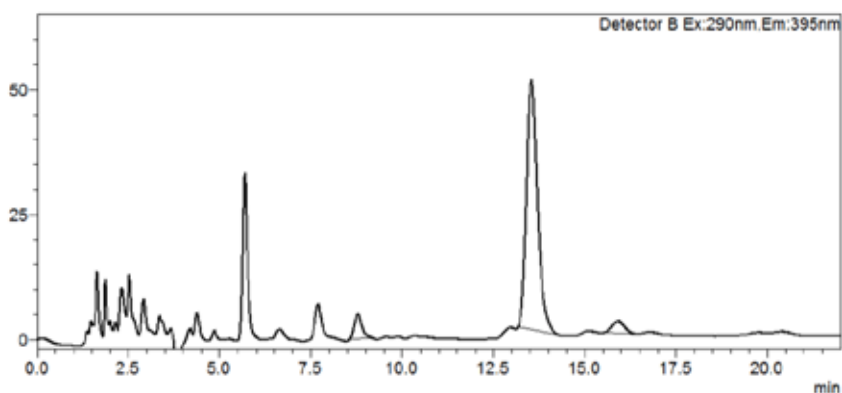


**Fig 2.** HPLC chromatogram of riboflavin in chickpea

### 3.1. Content of Riboflavin in Samples

Pre-cooking, and post-cooking riboflavin levels and cooking loss rates in legumes are given in Table 1. The amount of riboflavin in raw legumes varied between 130.33 and 219.67  $\mu\text{g}/100\text{ g}$ . The chickpea had the highest riboflavin level in two different cooking methods performed on legumes (pressure cooker: 176.33  $\mu\text{g}/100\text{ g}$ ; pan: 115.33  $\mu\text{g}/100\text{ g}$ ). The riboflavin cooking losses were between 4.6% and 21.4% when cooked with a pressure cooker, and between 23% - 47.7% in a pan. The riboflavin contents and riboflavin cooking losses in legumes are listed in Table 1.

**Table 1.** Content of riboflavin in legumes and riboflavin cooking losses.

| Samples      | Raw<br>( $\mu\text{g}/100\text{ g}$ ) | Cooked with<br>a pressure<br>cooker<br>( $\mu\text{g}/100\text{ g}$ ) | Cooking loss<br>in a pressure<br>cooker<br>(%) | Cooked with<br>a pan<br>( $\mu\text{g}/100\text{ g}$ ) | Cooking loss<br>in pan<br>(%) |
|--------------|---------------------------------------|---|--|--|-------------------------------|
| Bean         | 196.33 $\pm$ 7.23 <sup>a</sup>        | 154.0 $\pm$ 5.0 <sup>b</sup>  | 21.4   | 111.0 $\pm$ 5.5 <sup>c</sup>                           | 43.3                          |
| Chickpea     | 219.67 $\pm$ 8.79 <sup>a</sup>        | 176.33 $\pm$ 7.51 <sup>b</sup>  | 20.0   | 115.33 $\pm$ 4.51 <sup>c</sup>                         | 47.7                          |
| Red lentil   | 130.33 $\pm$ 5.34 <sup>a</sup>        | 124.33 $\pm$ 4.79 <sup>a</sup>  | 4.6  | 100.0 $\pm$ 3.87 <sup>b</sup>                          | 23.0                          |
| Green lentil | 154.67 $\pm$ 6.51 <sup>a</sup>        | 142.33 $\pm$ 5.51 <sup>b</sup>  | 8.3  | 92.33 $\pm$ 3.51 <sup>c</sup>                          | 40.6                          |

*Different letters within the same row indicate statistical differences between the applications ( $p < 0.05$ ).*

### 3.2. In-Vitro Digestion Results

The riboflavin amount of digested legume samples and bioaccessibility values are given in Table 2. After digestion, the amount of riboflavin in cooked legumes varied between 57.67 and 128.0  $\mu\text{g}/100\text{ g}$  in a pressure cooker, 40.33 and 95.67  $\mu\text{g}/100\text{ g}$  in a pan. As seen in the table, the riboflavin bioaccessibility in cooked legumes varied between 41.1 – 73.2% in a pressure cooker and 40.4 – 83% in a pan (Table 2).

**Table 2.** Bioaccessibility of riboflavin in legumes.

| Samples         | Cooked<br>with a<br>pressure<br>cooker<br>( $\mu\text{g}/100\text{ g}$ ) | Cooked with<br>pressure<br>cooker+digested<br>( $\mu\text{g}/100\text{ g}$ ) | Bioaccessibility<br>by a pressure<br>cooker<br>(%) | Cooked with<br>a pan<br>( $\mu\text{g}/100\text{ g}$ ) | Cooked with<br>pan+digested<br>( $\mu\text{g}/100\text{ g}$ ) | Bioaccessibility<br>by pan<br>(%) |
|-----------------|--|--|--|--|---|-----------------------------------|
| Bean            | 154.0 $\pm$ 5.0 <sup>b</sup>   | 80.67 $\pm$ 0.31 <sup>a</sup>  | 52.2   | 111.0 $\pm$ 5.5 <sup>c</sup>                           | 56.0 $\pm$ 0.5 <sup>b</sup>                                   | 50.4                              |
| Chickpea        | 176.33 $\pm$ 7.5 <sup>b</sup>  | 128.0 $\pm$ 3.03 <sup>a</sup>  | 73.2   | 115.33 $\pm$ 4.51 <sup>c</sup>                         | 95.67 $\pm$ 4.51 <sup>b</sup>                                 | 83.1                              |
| Red lentil      | 124.33 $\pm$ 4.7 <sup>a</sup>  | 80.33 $\pm$ 0.31 <sup>a</sup>  | 65.7   | 100.0 $\pm$ 3.87 <sup>b</sup>                          | 40.33 $\pm$ 0.51 <sup>b</sup>                                 | 40.4                              |
| Green<br>lentil | 142.33 $\pm$ 5.5 <sup>b</sup>  | 57.67 $\pm$ 0.35 <sup>a</sup>  | 41.1   | 92.33 $\pm$ 3.51 <sup>c</sup>                          | 52.33 $\pm$ 0.55 <sup>a</sup>                                 | 56.5                              |

*Different letters within the same row indicate statistical differences between the applications ( $p < 0.05$ ).*

Considering the results of the analysis, the riboflavin losses in legumes were higher by pan cooking than by pressure cooking. Since riboflavin undergoes photochemical degradation (like sunlight exposure, and cooking in an open pan), all processes, such as cooking should be done in the dark or under subdued red light. Studies suggested that exposing milk to sunlight in glass bottles can destroy more than half of the riboflavin in one day<sup>29</sup>. On the contrary, riboflavin is stable in the heat process. So, the riboflavin content of foods is not affected by sterilization, canning, or cooking<sup>30</sup>. In line with this information, since the lid is never opened in pressure cookers, the product is not exposed to light. However, since the pans we used in the study had glass lids, and the lids were frequently opened to check whether they were cooked, there was constant exposure to light.

Riboflavin in cereal grains is mainly found in seeds and bran, and grinding or hulling, which removes these tissues, causes significant losses in vitamin content. About half of the riboflavin in whole-grain rice and more than one-third of the riboflavin in whole wheat is lost when these grains are milled<sup>23,31-33</sup>. During the processes carried out within the scope of the study, husking was not applied to red and green lentils. Therefore, the loss of riboflavin in red and green lentils was considerably lower than in chickpeas and beans.

The environment's pH is another factor that affects riboflavin stability and absorption. The maximum stability for riboflavin is between pH 2 and 4<sup>31</sup>. Since the pH of the small intestine environment *in vitro* is 7, it is thought that vitamins are affected by this pH, and their bioaccessibility decreases. In a study, it was shown that 70% of the riboflavin content of chickpeas was lost by soaking in a sodium bicarbonate solution and cooking. It was seen that the soaking of chickpeas/beans in carbonated water, which is common among people, also causes high vitamin losses<sup>32</sup>. In our study, soaking processes were carried out in plain drinking water for all samples.

Dietary fiber content affects riboflavin bioaccessibility. In the study on how dietary fiber addition in breads affects riboflavin bioaccessibility, it was found to be 40.9 – 91.2% for riboflavin<sup>33</sup>. Similarly, bioaccessibility was found to be low in our study. In addition, forms of riboflavin can be found bound to proteins by non-covalent bonds, and denaturation of proteins may be less in an alkaline environment in the gastrointestinal tract *in vitro*<sup>31,34,42</sup>. This causes the forms of these vitamins to become less free, which can therefore lead to low bioaccessibility.

Today, the consumption of vegetable protein sources and their effects on health are the subject of more studies<sup>35,36</sup>. For this reason, it is essential to study and update the nutritional and bioaccessibility values of legumes. In the Turkey Nutrition Health Survey 2017, the rate of cooking legumes in a pressure cooker was determined 45%<sup>37</sup>. Processes such as long cooking times in a pan and changing the boiling water increase the loss of vitamins. For this reason, the pressure cooker does not pose any danger when used correctly and is a good cooking method to reduce losses.

A group of population studies available about the vitamin status report on riboflavin deficiency in children, young adults, and especially in young women<sup>38</sup>. These studies achieved on riboflavin status are old. When we look at the situations that are getting riboflavin deficiency worse, the current changes in lifestyle, especially in well-nourished countries, with diets based on a lack of dairy and species of meat combination with more exercise, could potentially increase the risk of riboflavin deficiency. In line with these studies, studies on the daily riboflavin intake of people who adhere to a vegan diet lifestyle have shown that these individuals meet less than 48% of the daily intake level recommendation, which increases the risk for riboflavin deficiency<sup>39-41</sup>.

This research was conducted *in vitro* by simulating the gastrointestinal system and aimed to evaluate bioaccessibility. From this point of view, the interaction of foods consumed together during digestion and whether their bioaccessibility changes as a result of the interaction have not been tested. However, since *in vivo* studies are expensive and require a lot of equipment, an *in vitro* model, which is a more advantageous and faster method, has been developed. In addition, the strongest aspect of this study is that it determines the most realistic vitamin content and bioaccessibility by taking into account the losses due to the cooking method in the vitamin content declaration.

As a result of our study, it has been seen that using the vitamin contents of raw foods in food composition charts can lead to misleading/incomplete guidance and results. At the end of this study, we concluded that bioaccessibility is important in determining how much of the daily nutrient requirement can be met by diet. In line with this knowledge, we think that it is realistic and necessary to include the nutritional content values after cooking and digestion in the food composition tables. When the bioaccessibility data obtained as a result of the study is evaluated, another noteworthy issue is that the evaluation of bioaccessibility only on the baked product may be misleading. When we look at the literature; the term bioaccessibility compares the state of the food when it first enters the digestive system with the state when it comes out. The point that is

overlooked here is that it seems to affect bioaccessibility positively due to the high cooking losses in the food. Vitamin losses are so high that there is no more vitamin to be lost. In conclusion; although the amount of vitamins absorbed and used in the digestive system is much higher in products with low cooking loss; it was found that the bioaccessibility of the products with high cooking loss was high, and the bioaccessibility of the products with low cooking loss was found to be low.

#### **CONFLICT OF INTEREST STATEMENT**

The authors affirm that they have no competing interests in relation to the work reported in this paper.

#### **AUTHOR CONTRIBUTIONS**

All authors contributed equally to this research.

## REFERENCES

1. Polak R, Phillips EM, Campbell A. Legumes: Health Benefits and Culinary Approaches to Increase Intake. *Clin Diabetes*. 2015;33(4):198-205. <https://doi.org/10.2337/diaclin.33.4.198>.
2. Semba RD, Rahman N, Du S, Ramsing R, Sullivan V, Nussbaumer E, et al. Patterns of Legume Purchases and Consumption in the United States. *Front Nutr*. 2021;8:765. <https://doi.org/10.3389/fnut.2021.732237>.
3. Carbas B, Machado N, Pathania S, Brites C, Rosa EAS, Barros AIB. Potential of Legumes: Nutritional Value, Bioactive Properties, Innovative Food Products, and Application of Eco-friendly Tools for Their Assessment. 2021;39(1):160-188 <https://doi.org/10.1080/87559129.2021.1901292>.
4. NIH. Riboflavin - Health Professional Fact Sheet [Internet]. 2022 [cited 2022 Jun 14]. <https://ods.od.nih.gov/factsheets/Riboflavin-HealthProfessional/>.
5. NCBI. Riboflavin | C<sub>17</sub>H<sub>20</sub>N<sub>4</sub>O<sub>6</sub> - PubChem [Internet]. 2022 [cited 2022 Jun 14]. <https://pubchem.ncbi.nlm.nih.gov/compound/Riboflavin>.
6. Medeiros DM, Wildman REC. Metabolism and Roles of Riboflavine. In: *Advanced Human Nutrition*. Fourth Edition. Burlington, MA: Jones & Bartlett Learning; 2018. p. 318–9. [https://books.google.com.tr/books?id=sD1DDwAAQBAJ&printsec=frontcover&hl=tr&source=gbs\\_ge\\_summary\\_r&cad=0#v=onepage&q&f=false](https://books.google.com.tr/books?id=sD1DDwAAQBAJ&printsec=frontcover&hl=tr&source=gbs_ge_summary_r&cad=0#v=onepage&q&f=false).
7. IOM. Dietary Reference Intakes (DRIs): Recommended Dietary Allowances and Adequate Intakes, Vitamins [Internet]. 2011 [cited 2023 Feb 22]. <https://www.ncbi.nlm.nih.gov/books/NBK56068/table/summarytables.t2/?report=objectonly>.
8. Ball GFM. Water-soluble vitamin assays in human nutrition. In: *Water-soluble vitamin assays in human nutrition*. Chapman & Hall. 1994;416. <https://doi.org/10.1093/ajcn/62.5.1031>.
9. Ottaway PB. Stability of vitamins in food. *The Technology of Vitamins in Food*. 1993;90–113. [https://doi.org/10.1007/978-1-4615-2131-0\\_5](https://doi.org/10.1007/978-1-4615-2131-0_5).
10. Çatak J, Çaman R, Ceylan Z. Critical Vitamin Assessment: Pyridoxal, Pyridoxamine, and Pyridoxine Levels for Three Species of Raw and Cooked Fish Samples. 2020 ;29(10):981–9. <https://doi.org/10.1080/10498850.2020.1827113>.
11. Çatak J, Çaman R. Pyridoxal, pyridoxamine, and pyridoxine cooking loss: Characterizing vitamin B6 profiles of chicken meats before and after cooking. *J Food Process Preserv*. 2020 ;44(10):e14798. <https://doi.org/10.1111/jfpp.14798>.
12. Çatak J. Determination of the Cooking Losses of Vitamins B<sub>1</sub>, B<sub>2</sub>, and B<sub>3</sub> in Chicken Meats Using Boiling and Frying Methods. *Journal of the Institute of Science and Technology*. 2022;12(3):1569–76. <https://doi.org/10.21597/jist.1037373>.
13. Çatak J, Semerciöz AS, Yalçinkaya BH, Yılmaz B, Özilgen M. Bioenergy Conversion. In: *Comprehensive Energy Systems*. Oxford, Elsevier Inc.; 2018. p. 1131–58. <https://www.elsevier.com/books/comprehensive-energy-systems/dincer/978-0-12-809597-3>.
14. Çatak J, Develi E, Bayram S. Women, Men, and Thermal Response: An Entropic Account of Gender Differences in Breathing During Exercise. *International Journal of Innovative Research and Reviews*. 2022 ;6(1):17–21. <https://dergipark.org.tr/en/pub/injirr/issue/71377/1147790>.
15. Yıldız C, Semerciöz AS, Yalçinkaya BH, Ipek TD, Öztürk-İsık E, Özilgen M. Entropy generation and accumulation in biological systems. *International Journal of Exergy*. 2020;33(4):444–68. <https://doi.org/10.1504/IJEX.2020.111691>.

16. Dutta A, Chattopadhyay H. Performance analysis of human cardiorespiratory system based on the second law of thermodynamics. *International Journal of Exergy*. 2021;34(1):29. <https://doi.org/10.1504/IJEX.2021.10034154>.
17. Dutta A, Chattopadhyay H, Çatak J. Thermodynamic Performance Analysis of Human Cardiovascular System for Normal and Cardiomegaly Conditions. *J Mech Med Biol*. 2022;23(1):1-17. <https://doi.org/10.1142/S0219519423500021>.
18. Çatak J, Develi E, Bayram S. How does obesity affect bioenergetics in human respiratory muscles? *Human Nutrition & Metabolism*. 2021;26:200136. <https://doi.org/10.1016/j.hnm.2021.200136>.
19. Putti R, Sica R, Migliaccio V, Lionetti L. Diet impact on Mitochondrial Bioenergetics and Dynamics. *Front Physiol*. 2015;6:109. <https://doi.org/10.3389/fphys.2015.00109>.
20. Forbes JM, Thorburn DR. Mitochondrial dysfunction in diabetic kidney disease. *Nat Rev Nephrol*. 2018;14(5):291–312. <https://doi.org/10.1038/nrneph.2018.9>.
21. Udhayabanu T, Manole A, Rajeshwari M, Varalakshmi P, Houlden H, Ashokkumar B. Riboflavin Responsive Mitochondrial Dysfunction in Neurodegenerative Diseases. *J Clin Med*. 2017;6(5):52. <https://doi.org/10.3390/jcm6050052>.
22. Mkrtchyan GV, Üçal M, Müllebnner A, Dumitrescu S, Kames M, Moldzio R, et al. Thiamine preserves mitochondrial function in a rat model of traumatic brain injury, preventing inactivation of the 2-oxoglutarate dehydrogenase complex. *Biochimica et Biophysica Acta (BBA) - Bioenergetics*. 2018;1859(9):925–31. <https://doi.org/10.1016/j.bbabi.2018.05.005>.
23. Onyambu ZM, Nawiri MP, Nyambaka HN, Noah NM. *In Vitro* Bioaccessibility of the Vitamin B Series from Thermally Processed Leafy African Indigenous Vegetables. *J Food Qual*. 2021;2021:1-8. <https://doi.org/10.1155/2021/5540724>.
24. Demir B, Gürbüz M, Çatak J, Uğur H, Duman E, Beceren Y, et al. *In vitro* bioaccessibility of vitamins B1, B2, and B3 from various vegetables. *Food Chem*. 2023;398:133944. <https://doi.org/10.1016/j.foodchem.2022.133944>.
25. Çatak J, Gizlici MN. The effect of *in vitro* simulated gastrointestinal digestive system on the biodegradation of B group vitamins in bread. *Heliyon*. 2022;8(10):e11061. <https://doi.org/10.1016/j.heliyon.2022.e11061>.
26. Hur SJ, Lim BO, Decker EA, McClements DJ. *In vitro* human digestion models for food applications. *Food Chem*. 2011;125(1):1–12. <https://doi.org/10.1016/j.foodchem.2010.08.036>.
27. Çatak J, Çaman R, Yaman M, Ceylan Z. Effect of Baking and Grilling on B Vitamins of Selected Fishes and Chicken Parts. *Journal of Culinary Science and Technology*. 2022;1-16. <https://doi.org/10.1080/15428052.2022.2060161>.
28. Lee SJ, Lee SY, Chung MS, Hur SJ. Development of novel *in vitro* human digestion systems for screening the bioavailability and digestibility of foods. *J Funct Foods*. 2016;22:113–21. <https://doi.org/10.1016/j.jff.2016.01.005>.
29. Arslaner A, Bakırcı İ. Effect of Milk Type, Pasteurization and Packaging Materials on Some Physicochemical Properties and Free Fatty Acid Profiles of Tulum Cheese. *Akademik Gıda*. 2016; 14(2): 98 - 104. <https://dergipark.org.tr/en/pub/akademik-gida/issue/55784/763608>.
30. Combs GF, McClung JP. Riboflavin. In: *The Vitamins*. Fourth Edition. London, UK: Elsevier Inc.; 2012. p. 315–29. <https://doi.org/10.1016/C2009-0-63016-6>.
31. Yaman M, Çatak J, Uğur H, Gürbüz M, Belli İ, Tanyıldız SN, et al. The bioaccessibility of water-soluble vitamins: A review. *Trends Food Sci Technol*. 2021;109:552–63. <https://doi.org/10.1016/j.tifs.2021.01.056>.

32. Prodanov M, Sierra I, Vidal-Valverde C. Influence of soaking and cooking on the thiamin, riboflavin and niacin contents of legumes. *Food Chem.* 2004;84(2):271–7. [https://doi.org/10.1016/S0308-8146\(03\)00211-5](https://doi.org/10.1016/S0308-8146(03)00211-5).
33. Kurek MA, Wyrwiz J, Karp S, Wierzbicka A. Particle size of dietary fiber preparation affects the bioaccessibility of selected vitamin B in fortified wheat bread. *J Cereal Sci.* 2017;77:166–171. <https://doi.org/10.1016/j.jcs.2017.07.016>.
34. Arkbåge K. Vitamin B<sub>12</sub>, folate and folate-binding proteins in dairy products : analysis, process retention and bioavailability. *Acta Universitatis Agriculturae Sueciae.* 2003. <https://res.slu.se/id/publ/9848>.
35. Andac-Ozturk S, Garipoğlu G, Çatak J, Yaman M. Investigation of the vitamins B<sub>1</sub>, B<sub>2</sub>, and B<sub>6</sub> vitamers bioaccessibilities of canned, dried legumes after *in vitro* gastrointestinal digestion system. *Food Res Int.* 2022;160. <https://doi.org/10.1016/j.foodres.2022.111671>.
36. Çatak J. Determination of niacin profiles in some animal and plant-based foods by high performance liquid chromatography: association with healthy nutrition. *J Anim Sci Technol.* 2019;61(3):138. <https://doi.org/10.5187/jast.2019.61.3.138>.
37. Republic Of Turkey Ministry of Health. Turkey Nutrition and Health Survey (TNHS) 2017 [Internet]. Ankara; 2019 [cited 2023 Feb 22]. [https://hsgm.saglik.gov.tr/depo/birimler/saglikli-beslenme-hareketli-hayat-db/TBSA\\_RAPOR\\_KITAP\\_2017\\_ENG\\_.pdf](https://hsgm.saglik.gov.tr/depo/birimler/saglikli-beslenme-hareketli-hayat-db/TBSA_RAPOR_KITAP_2017_ENG_.pdf).
38. Smithers G, Gregory JR, Bates CJ, Prentice A, Jackson LV, Wenlock R. The National Diet and Nutrition Survey: young people aged 4–18 years. *Nutr. Bull.* 2000;25(2):105–111. <https://doi.org/10.1046/j.1467-3010.2000.00027.x>.
39. Waldmann A, Koschizke JW, Leitzmann C, Hahn A. Dietary intakes and lifestyle factors of a vegan population in Germany: results from the German Vegan Study. *Eur. J. Clin. Nutr.* 2003; 57(8):947–955. <https://doi.org/10.1038/sj.ejcn.1601629>.
40. Larsson CL, Johansson GK. Dietary intake and nutritional status of young vegans and omnivores in Sweden. *Am. J. Clin. Nutr.* 2002;76:100–106. <https://doi.org/10.1093/ajcn/76.1.100>.
41. Majchrzak D, Singer I, Manner M, Rust P, Genser D, Wagner KH, Elmadfa I. B-vitamin status and concentrations of homocysteine in Austrian omnivores, vegetarians and vegans. *Ann. Nutr. Metab.* 2006;50:485–491. <https://doi.org/10.1159/000095828>.
42. Kesik S, Çatak J, Ada K, Yaman M. Cooking Losses and Bioaccessibility of Thiamine by *in vitro* Gastrointestinal System in Selected Legumes. *Journal of Culinary Science & Technology.* 2022;1-13. <https://doi.org/10.1080/15428052.2022.2148593>.



# Assessment of compressional, mechanical and release properties of *Terminalia randii* gum in paracetamol tablet formulation

Oluyemisi A. BAMIRO<sup>1\*</sup>, Lateef G. BAKRE<sup>1</sup>, Olutayo A. ADELEYE<sup>2</sup>

<sup>1</sup> Department of Pharmaceutics and Pharmaceutical Technology, Faculty of Pharmacy, Olabisi Onabanjo University, Nigeria

<sup>2</sup> Department of Pharmaceutics and Pharmaceutical Technology, Federal University Oye-Ekiti, Ekiti State, Nigeria

---

## ABSTRACT

Paracetamol tablets were formulated with *Terminalia randii* gum as a binder at varying concentrations (1-10%, w/w) and the compressional characteristics was compared with polyvinyl pyrrolidone (PVP). The compressional properties were evaluated using density measurements, Heckel and Kawakita equations. The mechanical properties were evaluated using friability, crushing strength, and crushing strength-friability ratio (CSFR), while the release properties were studied using disintegration time, dissolution time and Kitazawa equations. Formulations containing *Terminalia* gum showed faster onset of plastic deformation with a lower total amount of plastic deformation. The crushing strength and release properties of the formulations increased, while friability decreased, with increase in binder concentration. Formulations containing PVP had better mechanical properties as seen in the high CSFR values. Formulations produced with *Terminalia* gum produced tablets with slower dissolution. This study shows that the onset of plastic deformation was faster, but the total amount of plastic deformation was lower in formulations containing *Terminalia* gum.

**Keywords:** *Terminalia randii* gum, compressional characteristics, Heckel equation, Kawakita equation

---

## INTRODUCTION

A powdered drug or active pharmaceutical ingredient cannot be made into a tablet without the use of excipients such as binders, diluents, disintegrants, gli-

---

\*Corresponding Author: E-mail: oluyemisi.bamiro@oouagoiwoye.edu.ng

ORCID:

Oluyemisi A. BAMIRO: 0000-0002-6032-6075

Lateef G. BAKRE: 0000-0003-1222-1057

Olutayo A. ADELEYE: 0000-0001-8716-4064

(Received 24 Jun 2022, Accepted 24 Mar 2023)

dants and lubricants. Binders are known to promote bonding between the particles of a powder and other excipients in the powder mixture, hence improving the mechanical properties of the tablet <sup>1,2</sup>. Binders can be classified as natural or synthetic/semisynthetic polymers. Some natural polymers that have been used as binders are *Cedrela odorata* <sup>2</sup>, *Eucalyptus tereticornis* <sup>3</sup>, *Albizia zygia* <sup>4</sup>, while xanthan gum <sup>5</sup>, and hydroxyl methyl cellulose <sup>6</sup> are synthetic/semisynthetic polymers used as binders. Compressibility and compactibility of binders are some of the physicochemical properties which bear direct relationship to the tableting performance of a particulate solid <sup>7</sup>. Decrease in volume of a powder under pressure is known as compressibility, while the compression of a powdered material into a tablet of specified strength is known as compactibility and this influences bioavailability. Various mathematical equations such as Heckel, Kawakita, Leuenberger and Gurnham equations have been used in studying the compression and compaction of powders and tablets <sup>7-10</sup>. In Heckel's equation, the applied pressure is related to the relative density of powder during compression, the Kawakita's equation relates degree of volume reduction of powders to applied pressure during compression and Leuenberger's equation relates deformation hardness of powders during compression to applied pressure.

*Terminalia* gum is exudate obtained by cutting the trunk of *Terminalia randii*. This gum has been characterised and assessed as a binder, disintegrant, and in oral film formulation <sup>11-13</sup>. However, when *Terminalia* was characterised, the compressional characteristics was not evaluated. Hence, in this study, the compressional characteristics and release properties of *Terminalia* gum as a binder in paracetamol tablet formulation in comparison with PVP was evaluated.

## **METHODOLOGY**

### **Materials**

The materials used were paracetamol powder BP, corn starch (S.D Fine chemicals Ltd, Mumbai, India) polyvinylpyrrolidone USP K29/32 (molecular weight: 58,000) (ISP Technologies, Inc Wayne, USA), lactose monohydrate (Ind-Swift Labs Ltd, Parwanoo, India), magnesium stearate (Loba Chemie Pvt Ltd, Mumbai, India), Talc ((Loba Chemie Pvt Ltd, Mumbai, India), *Terminalia* plant was collected from Olabisi Onabanjo University Ago-Iwoye and authenticated at the Forest Research Institute of Nigeria, Ibadan with a Voucher number FHL NO 107917.

### **Collection and extraction of terminalia gum**

*Terminalia* gum was obtained from the incised trunk of *Terminalia randii* (*Family Combretaceae*). The trunk of the tree was incised, and the gum exu-

date was allowed to dry and then hand-picked from the trees. The dried gum was washed and dried in hot air oven at 40 °C and then crushed with a pestle and mortar to break up the gum. The gum was hydrated in double strength chloroform water for 5 days while stirring intermittently. The mucilage obtained was strained through a clean calico cloth and the gum obtained was precipitated with 95%, v/v ethanol. The precipitated gum was filtered, washed with diethyl-ether, and then dried in hot air oven. The dried gum was pulverized and passed through a number 60 mesh sieve (250 µm) <sup>11</sup>.

### **Preparation of granules**

A 250 g quantity of basic formulation containing paracetamol (60%, w/w), lactose (30%, w/w) and corn starch (10%, w/w), was dry mixed for 5 minutes in a planetary mixer (Model A120, Hobart Manufacturing Co, U.K) and moistened with water or appropriate amount of aqueous solution of PVP or mucilage of *Terminalia* gum (1-10%, w/w) to produce granules containing different concentrations of the binders. Massing was continued for 5 minutes, and the wet masses were granulated by passing them manually through a number 12 mesh sieve (1400 µm), dried in a hot air oven for 16 hours at 60 °C and then re-sieved through a number 16 mesh sieve (1000 µm) and then stored in air tight container.

### **Granule size distribution**

The size distribution of the granules was determined by sieve analysis method (British standard 1460). A stack of sieves of the following sizes: 16 mesh (1000 µm), 22 mesh (710 µm), 30 mesh (500 µm), 44 mesh (355 µm), 60 mesh (250 µm), mesh (150 µm) and the receiver were arranged in descending order of aperture size with the receiver at the bottom. 200 g quantity of granules was placed on the uppermost sieve, the cover was firmly placed, and the stack of sieves was shaken for 10 minutes using a mechanical shaker. The quantity of granules retained on each sieve was carefully weighed; the cumulative percentage oversize was calculated and the mean granule size which corresponds to the sieve size (µm) at 50% cumulative weight percentage oversize was calculated. The granules of size 500 - 1000 µm were collected and stored in an air tight container.

### **Determination of particle density**

The particle density of granules was determined by the liquid pycnometer method using xylene as the displacement fluid. An empty 50 mL pycnometer bottle was weighed ( $w$ ), then filled to the brim overflowing with xylene and the excess wiped off. The bottle with the xylene was weighed again ( $w_1$ ). A 2 g

weight of the sample was weighed ( $w_3$ ) and quantitatively transferred into the pycnometer bottle. The excess xylene was wiped off and the bottle weighed again ( $w_4$ ). The particle density was calculated from the equation <sup>5</sup>.

$$P_i = \frac{W_2 W_3}{50(W_3 - W_4 + W_2 + W)} \quad (1)$$

### Determination of bulk (loose) density

The bulk density <sup>3</sup> was determined by weighing 30 g (W) of terminalia gum into a 50 mL measuring cylinder of internal diameter 21 mm. The height, h (cm) of the powder bed and internal radius, r (cm) of the measuring cylinder were used to compute the loose bulk volume,  $V_o$ .

$$V_o = \pi r^2 h \dots \dots (2)$$

The value obtained was used to calculate the loose bulk density

$$P_o = \frac{W}{V_o} \quad (3)$$

### Preparation of Tablets

500 mg of granules was compressed with predetermined load at a dwell time of 30 seconds on a Carver hydraulic press (Model C, Carver Inc. Wisconsin, USA), using a 10.5 mm die and flat faced punches lubricated with a 1% dispersion of magnesium stearate in acetone prior to compression. After ejection, the tablets were stored over silica gel for 24 hours to allow for elastic recovery and hardening. The weights (w) and dimensions of the tablets were measured to within  $\pm 1$  mg and  $\pm 0.01$  mm respectively, and their relative density D was calculated using the equation <sup>2</sup>:

$$D = \frac{W}{V_{tPs}} \quad (4)$$

Where is the volume,  $\text{cm}^3$ , of the tablet and is the particle density,  $\text{gcm}^{-3}$ , of the granules.

### Compression Properties

The Heckel and Kawakita equations were used to determine the compressional characteristics <sup>3,14</sup>. The Heckel equation relates the relative density of a powder bed D to the compressional pressure P. The equation is written as:

$$\ln \frac{1}{1-D} = KP + A \dots \dots (5)$$

A plot of  $\ln(1 - D_A)$  against pressure P was constructed to obtain a linear graph with slope K, which is the reciprocal of the mean yield pressure  $P_y$ , of the material and intercept A, which is used to calculate the relative density  $D_A$  using the equation:

$$D_A = 1 - e^{-A/P} \dots\dots (6)$$

The relative density of powder bed when applied pressure is zero  $D_0$ , is the initial rearrangement phase of densification as a result of the die filling. The relative density of powder at low pressure,  $D_B$ , describes the phase of rearrangement of particles during initial stages of compression and it is the difference between  $D_A$  and  $D_0$ :

$$D_B = D_A - D_0 \dots\dots (7)$$

The Kawakita equation<sup>15</sup> was used to evaluate powder compression using the degree of volume reduction C and applied pressure. The equation is expressed as:

$$C = \frac{V_0 - V_p}{V_0} = \frac{abP}{1 + bp} \dots\dots (8)$$

The equation is simplified to give:

$$\frac{P}{c} = \frac{P}{a} + \frac{1}{ab} \dots\dots (9)$$

$V_0$  is the initial volume of powder bed before compression;  $V_p$  is the volume after compression. The constant a is the minimum porosity before compression, while reciprocal of constant b, gives a pressure term  $P_K$ , which is the pressure required to reduce the powder bed by 50%<sup>16-18</sup>.

### **Determination of mechanical properties**

The friability test was carried out on a friabilitor (MAC, Macro Scientific Works, New Delhi India). Ten tablets were selected at random, weighed together using an electronic balance and then placed in the friabilitor. The machine was operated at 25 revolutions per minute for 4 minutes. The tablets were dusted and reweighed and the percentage loss was calculated. Determinations were done in triplicate.

The crushing strength of the tablets was determined using a Monsanto hardness tester (MAC, Macro Scientific Works, New Delhi, India). Tablet was placed between spindle and anvil of the tester and the calibrated length adjusted to zero. The knob was then screwed to apply a diametric compression force on the

tablet and the position on the calibrated length at which the tablet broke into two halves was recorded. Six tablets were used for each batch and the results are given as the mean and SD.

### **Determination of release properties**

The disintegration test was carried out in 900 mL of distilled water at  $37\text{ }^{\circ}\text{C} \pm 0.5\text{ }^{\circ}\text{C}$  using a Mac disintegration test apparatus (Macro Scientific Works, New Delhi, India) (USP/NF2007). Six tablets from each batch were placed in the cylindrical tubes of the basket. The time taken for the tablets to break up into particles and pass through the mesh was recorded and the mean disintegration time was calculated.

### **Calibration Plot**

Stock solution of pure paracetamol was prepared and scanned on a UV spectrophotometer (Genesys 6, Thermospectronic, USA) at a wavelength range of 200 - 400 nm. The wavelength of 243 nm was obtained for maximum absorbance. Different concentrations of the paracetamol solution were prepared from the stock solution by dilution and their absorbance taken. A plot of absorbance against concentration was plotted to obtain the calibration plot that was used in calculating the concentration of paracetamol released from each formulation.

### **Dissolution test**

The *in vitro* dissolution test was carried out in 900 mL 0.1 M HCL maintained at a constant temperature of  $37\text{ }^{\circ}\text{C} \pm 0.5\text{ }^{\circ}\text{C}$  using a USP Type 2 dissolution apparatus (Labindia Dissolution test apparatus DISSO 2000) rotated at 50 rpm. The pre-weighed tablet was then introduced into the dissolution medium and at different time intervals; 5 mL sample was withdrawn and replaced with 5 mL of fresh medium. The samples were analyzed using a UV spectrophotometer (Genesys 6, Thermospectronic, USA) at a wavelength of 243 nm. All determinations were made in triplicate.

### **Dissolution rate constant**

The plot of Kitazawa *et al.*<sup>19</sup> was used to determine the dissolution rate constant. Employing Noyes and Whitney equation, the values of  $k$  was plotted against time (t)<sup>20</sup>. Two straight lines of slope  $k_1$  and  $k_2$  were obtained from the plot and the time ( $t_1$ ) at which the lines intercept was determined.

### **Statistical analysis**

Statistical analysis was carried out using analysis of variance with computer software GraphPad Prism® 4 (GraphPad Software Inc. San Diego, USA).

## RESULTS AND DISCUSSION

### Compression properties

Increase in binder concentration caused an increase in mean granule size (Table 1). This was in agreement with the work of other researchers<sup>3,21</sup>. This could be due to increase in bond strength between particles as there would be more binder due to increment in concentration<sup>22</sup>. The type of binding agent also affected the granule size. The granule size of formulations comprising *Terminalia* gum were significantly ( $p < 0.001$ ) lower than those comprising PVP. Granule size is important in tableting as it is known to affect flow rate, which may invariably affect tablet weight uniformity. Increase in binder concentration caused a decrease in particle density, while there was increase in relative and loose bulk densities. Granule density has been shown to influence the compression properties of the granules<sup>23</sup>. High compressive loads are required for dense hard granules to produce a strong compact which are less friable. The relative density of the powder bed at the point when the pressure applied is zero ( $D_o$ ) depicts the initial rearrangement phase of densification after die filling. Increasing binder concentration caused a significant ( $p < 0.0001$ ) increase in  $D_o$  values as shown in Table 1. This is an indication that the initial packing due to die filling increased with increment in binder. Formulations containing *Terminalia* gum exhibited significantly lower ( $p < 0.001$ ) extent of packing in the die due to die filling than formulations comprising PVP.

The relative density of the tablets at various applied pressures was used for the Heckel plot by plotting  $\ln(1/1-D)$  against applied pressure. A representative Heckel plot at 5%, w/w binder concentration is shown in figure 1. Each plot shows two compression phases, with the second phase starting at 42.42 MNm<sup>-2</sup> up to 169.68 MNm<sup>-2</sup>, and the formulations having high correlation coefficient for linearity of  $> 0.985$ . The values for mean yield pressure,  $P_y$ , relative densities  $D_A$  and  $D_B$ , and relative density due to die filling,  $D_o$ , for formulations are presented in Table 2. There was decrease in the value of  $P_y$  as the binder concentration increased. Low value of  $P_y$  is an indication of fast onset of plastic deformation<sup>8,24</sup>. Formulations comprising *Terminalia* gum generally exhibited lower  $P_y$  values indicating the beginning plastic deformation at a fast rate when compared with formulations comprising PVP. The relative density  $D_B$ , which depicts the rearrangement phase of particles at the beginning of compression, increased with increasing binder concentration. These values were observed to be greater than the values of  $D_o$  probably due to breaking up of granules at low pressures thereby filling up void spaces between particles<sup>25</sup>. The values of  $D_B$  were generally higher for PVP formulations than for *Terminalia* gum

formulations. This implies that there were more fragmentation and rearrangement of PVP formulation granules than *Terminalia* granules at low pressures. Increasing binder concentration increased the values of  $D_A$ . Lower  $D_A$  values were observed in formulations containing *Terminalia* gum in comparison to those formulations containing PVP. The higher the values of  $D_A$ , the higher the extent of packing at zero and low pressures.

**Table 1.** Values of mean granule size, and densities of the formulation

| Binder type       | Binder Concentration (%w/w) | Mean granule size ( $\mu\text{m}$ ) | Particle density ( $\text{gcm}^{-3}$ ) | Loose bulk density ( $\text{gcm}^{-3}$ ) | Relative density $D_0$ ( $\text{gcm}^{-3}$ ) |
|-------------------|-----------------------------|-------------------------------------|--|--|--|
| <b>PVP</b>        | 0.00                        | 115.00 $\pm$ 5.00                   | 1.532 $\pm$ 0.033                      | 0.405 $\pm$ 0.006                        | 0.264 $\pm$ 0.008                            |
|                   | 1.00                        | 300.00 $\pm$ 2.65                   | 1.450 $\pm$ 0.100                      | 0.454 $\pm$ 0.017                        | 0.313 $\pm$ 0.003                            |
|                   | 2.00                        | 350.00 $\pm$ 3.00                   | 1.441 $\pm$ 0.004                      | 0.462 $\pm$ 0.004                        | 0.321 $\pm$ 0.003                            |
|                   | 3.00                        | 670.00 $\pm$ 1.00                   | 1.428 $\pm$ 0.013                      | 0.469 $\pm$ 0.006                        | 0.328 $\pm$ 0.002                            |
|                   | 5.00                        | 700.33 $\pm$ 2.52                   | 1.419 $\pm$ 0.002                      | 0.475 $\pm$ 0.011                        | 0.335 $\pm$ 0.005                            |
|                   | 10.00                       | 739.67 $\pm$ 1.53                   | 1.396 $\pm$ 0.006                      | 0.477 $\pm$ 0.018                        | 0.342 $\pm$ 0.007                            |
| <b>Terminalia</b> | 1.00                        | 112.00 $\pm$ 2.00                   | 1.498 $\pm$ 0.021                      | 0.411 $\pm$ 0.018                        | 0.274 $\pm$ 0.005                            |
|                   | 2.00                        | 140.00 $\pm$ 1.00                   | 1.444 $\pm$ 0.032                      | 0.417 $\pm$ 0.007                        | 0.289 $\pm$ 0.001                            |
|                   | 3.00                        | 359.67 $\pm$ 3.79                   | 1.432 $\pm$ 0.120                      | 0.424 $\pm$ 0.007                        | 0.296 $\pm$ 0.003                            |
|                   | 5.00                        | 460.00 $\pm$ 2.65                   | 1.430 $\pm$ 0.080                      | 0.425 $\pm$ 0.017                        | 0.297 $\pm$ 0.003                            |
|                   | 10.00                       | 605.33 $\pm$ 2.08                   | 1.397 $\pm$ 0.075                      | 0.434 $\pm$ 0.014                        | 0.311 $\pm$ 0.014                            |

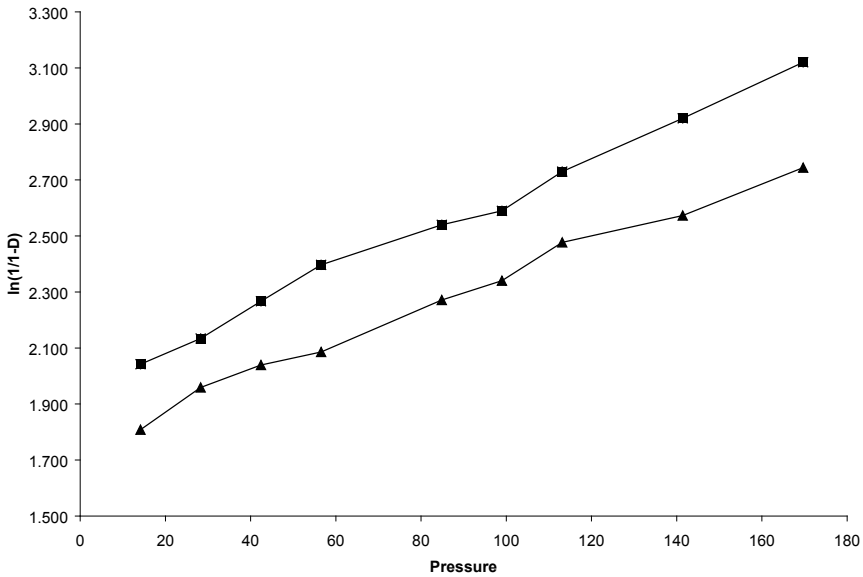


**Figure 1.** Heckel plots for paracetamol tablets containing 5% w/w binders terminalia gum ▲, PVP ■

A representative Kawakita plot of the formulations at 5%, w/w binder concentration is shown in figure 2. A correlation coefficient  $> 0.999$  was obtained for all formulations at all compressional pressures. The slope and intercept gave values of  $a$ , and  $ab$  respectively. The initial relative density  $D_i$ , was obtained as  $1 - a$ , from the values of  $a$ . From the reciprocal of  $b$  values,  $P_K$  values were obtained. The values of  $D_i$  and  $P_K$  are presented in Table 2. The values  $D_i$  reduced generally with increase in binder content for the formulations and it is generally greater than the values of  $D_o$ . The difference in values of  $D_o$  and  $D_i$  could be due largely to the fact that  $D_o$  depicts the loose initial relative density of the formulations due to die filling,  $D_i$  depicts the initial packed relative density of the formulations with the application of small pressure or tapping of the formulations <sup>4</sup>.

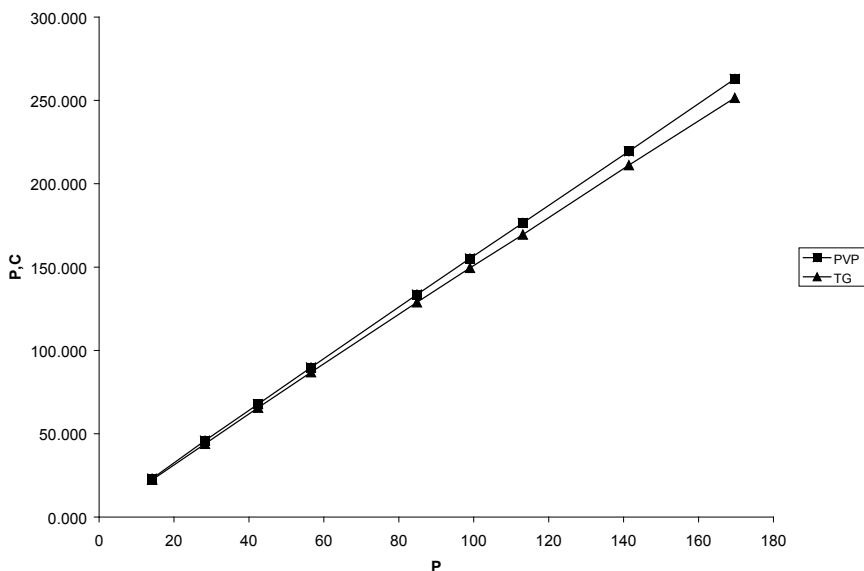


**Figure 2.** Kawakita plots for paracetamol tablets containing 5% w/w binder

**Table 2.** Parameters obtained from Heckel and Kawakita plots

| Binder type       | Binder concentration (%w/w) | $P_Y$  | $D_A$ | $D_B$ | $D_i (1-a)$ | $P_K$ |
|-------------------|-----------------------------|--------|-------|-------|-------------|-------|
| <b>PVP</b>        | 0.00                        | 204.08 | 0.768 | 0.504 | 0.529       | 5.643 |
|                   | 1.00                        | 208.33 | 0.832 | 0.519 | 0.504       | 3.712 |
|                   | 2.00                        | 196.08 | 0.846 | 0.525 | 0.465       | 2.999 |
|                   | 3.00                        | 188.68 | 0.854 | 0.526 | 0.436       | 2.140 |
|                   | 5.00                        | 151.52 | 0.863 | 0.528 | 0.372       | 1.681 |
|                   | 10.00                       | 151.52 | 0.871 | 0.529 | 0.346       | 1.553 |
| <b>Terminalia</b> | 1.00                        | 217.39 | 0.778 | 0.504 | 0.485       | 3.772 |
|                   | 2.00                        | 181.82 | 0.806 | 0.517 | 0.386       | 2.480 |
|                   | 3.00                        | 178.57 | 0.827 | 0.531 | 0.362       | 2.113 |
|                   | 5.00                        | 175.44 | 0.833 | 0.536 | 0.321       | 1.912 |
|                   | 10.00                       | 147.06 | 0.824 | 0.513 | 0.315       | 1.882 |

Low  $P_k$  values are an indication of materials that are soft and easily deform plastically under pressure. The reduction in  $P_k$  values with increase in binder content is an indication that increment in binder concentration leads to softness and capability of formulations to deform plastically under pressure.  $P_k$  values of formulations comprising PVP were generally lesser than those of formulations comprising *Terminalia* gum. This indicates that formulations containing PVP are softer than those containing *Terminalia* gum and they would readily undergo plastic deformation.

### **Mechanical properties of tablets**

The crushing strength and friability of the tablets were evaluated and their values at 0.9 relative densities which represent those of commercial tablets are presented in Table 3. Crushing strength (CS) is an estimate of tablet strength while friability (FR) is an estimate of tablet weakness<sup>26</sup>. The crushing strength increased significantly ( $p < 0.0001$ ) with increment in relative density of the paracetamol formulations and binder concentrations. This may be due to a reduction in porosity resulting in an increment in the number of points in contact thus leading to an increment in the formation of solid interparticle bonds<sup>22, 27</sup> and also during compression, the heat produced caused melting of binding agents which solidifies on cooling to form strong bonds between the particles. The crushing strength of formulations containing *Terminalia* gum was significantly low ( $p < 0.001$ ) at low concentrations (1-3%, w/w), but at higher concentrations (5% - 10%, w/w), there was no significant difference ( $p > 0.05$ ) in the crushing strength. At 5% - 10%, w/w concentrations it was observed that the friability of paracetamol formulations containing *Terminalia* binder was significantly higher ( $p < 0.01$ ) than that of formulations containing PVP. This shows that having a high crushing strength does not necessarily mean that a tablet would be strong enough for transportation and handling by patients. This was also confirmed by the low crushing strength-friability ratio (CSFR) that was obtained for formulations containing *Terminalia* binder. CSFR is a parameter that is also used in measuring the mechanical strength of tablets. High CSFR value is an indication of strong tablets since it harmonizes the tablet weakness and strength<sup>28</sup>.

**Table 3.** Mechanical properties of Paracetamol tablets at relative density 0.9 gcm<sup>-3</sup>

| Binder type | Binder Concentration (%w/w) | Crushing strength (N) | Friability (%) | CSFR   |
|-------------|-----------------------------|-----------------------|----------------|--------|
| PVP         | 0.00                        | 54.88±4.14            | 3.5±0.08       | 15.68  |
|             | 1.00                        | 102.10±2.67           | 0.84±0.00      | 121.55 |
|             | 2.00                        | 109.40±5.42           | 0.80±0.00      | 136.75 |
|             | 3.00                        | 111.50±1.52           | 0.72±0.02      | 154.86 |
|             | 5.00                        | 115.70±1.34           | 0.56±0.00      | 206.61 |
|             | 10.00                       | 119.50±2.62           | 0.51±0.00      | 234.31 |
| Terminalia  | 1.00                        | 74.40±1.61            | 1.55±0.02      | 48.00  |
|             | 2.00                        | 85.20±1.12            | 1.10±0.00      | 77.45  |
|             | 3.00                        | 102.00±3.98           | 0.84±0.01      | 121.43 |
|             | 5.00                        | 117.60±2.44           | 0.73±0.00      | 161.10 |
|             | 10.00                       | 120.50±1.52           | 0.72±0.00      | 167.36 |

### Release properties of tablets

Disintegration time of the tablets increased ( $p < 0.0001$ ) with increment in binder concentration (Table 4). This increase could have been due to formation of solid bonds formed by binders during compression<sup>3</sup>. The relative density of the tablets was directly proportional to the disintegration of the tablets, and this was in agreement with the work of other researchers<sup>3, 29, 30</sup>. It was observed that the disintegration of paracetamol formulations containing *Terminalia* gum binder, which incidentally gave lower CSFR values were higher than that of formulations containing PVP. The disintegration time of the tablet is influenced by the ease of fluid penetration into the tablet. This may be due to the swelling of *Terminalia* gum on contact with water, thus forming a gelatinous viscous barrier between the granules and the water, which reduced the penetration of fluid into the interstitial void spaces thus prolonging the disintegration time of the tablet<sup>12</sup>. All the formulations disintegrated within the 15 minutes specified for uncoated tablets in the Pharmacopeia<sup>31</sup>. All the tablets released more than 70% of their paracetamol content within 30 minutes of dissolution (Figure 3).

**Table 4.** Release properties of Paracetamol tablets at relative density of 0.9

| Binder     | Binder Concentration (%w/w) | Disintegration time (mins) | $t_{50}$ (mins) | $t_{80}$ (mins) | $t_1$ (mins) | $k_1$     | $k_2$     |
|------------|-----------------------------|----------------------------|-----------------|-----------------|--------------|-----------|-----------|
| PVP        | 0.00                        | 0.60±0.00                  | 1.65±0.03       | 3.01±0.02       | 1.50±0.04    | 0.18±0.01 | 0.83±0.01 |
|            | 1.00                        | 0.75±0.01                  | 3.20±0.01       | 6.80±0.03       | 4.00±0.06    | 0.60±0.00 | 1.10±0.01 |
|            | 2.00                        | 1.10±0.00                  | 3.21±0.01       | 8.00±0.21       | 8.50±0.32    | 0.52±0.00 | 1.21±0.00 |
|            | 3.00                        | 1.15±0.03                  | 3.40±0.03       | 8.40±0.05       | 9.28±0.04    | 0.22±0.00 | 1.85±0.00 |
|            | 5.00                        | 1.55±0.02                  | 3.42±0.11       | 8.42±0.02       | 9.40±0.01    | 0.42±0.00 | 1.67±0.02 |
|            | 10.00                       | 4.52±0.01                  | 3.60±0.06       | 9.20±0.42       | 12.00±0.11   | 0.24±0.00 | 2.10±0.00 |
| Terminalia | 1.00                        | 0.88±0.00                  | 5.25±0.02       | 7.40±0.11       | 5.53±0.11    | 0.25±0.00 | 1.17±0.01 |
|            | 2.00                        | 0.95±0.01                  | 5.60±0.12       | 7.62±0.04       | 5.57±0.02    | 0.24±0.00 | 1.24±0.00 |
|            | 3.00                        | 1.18±0.04                  | 8.20±0.04       | 12.00±0.01      | 6.50±0.07    | 0.22±0.00 | 0.86±0.00 |
|            | 5.00                        | 5.25±0.00                  | 10.00±0.13      | 18.20±0.15      | 6.75±0.15    | 0.29±0.00 | 1.05±0.00 |
|            | 10.00                       | 6.48±0.00                  | 11.00±0.23      | 18.50±0.08      | 17.90±0.27   | 0.59±0.01 | 2.88±0.01 |

This shows that all the tablets passed the dissolution test as specified by the British Pharmacopoeia <sup>31</sup>. The parameters  $t_{50}$  and  $t_{80}$  (time at which 50% and 80% of the drug were released respectively),  $k_1$ ,  $k_2$  and  $t_1$  obtained from the Kitazawa plot (Figure 4) are presented in Table 5. The values of  $k_1$ ,  $k_2$  and  $t_1$  were seen to increase with increasing binder concentration.  $k_2$  was observed to be generally higher than  $k_1$ , indicating an initial release rate of the drug from the disintegrating tablet followed by a higher release rate after time  $t_1$ . Thus,  $t_1$  can be taken to coincide with the point at which there was complete tablet disintegration which now leads to increase in surface area and release rate of the drug. The fragmentation of tablets caused a change in surface area, and this could be attributed to change from  $k_1$  to  $k_2$  at time  $t_1$  <sup>25, 32</sup>. The disintegration time values were seen to be lower than the corresponding  $t_1$  values and this could be attributed to the greater agitation employed in the disintegration test than in the dissolution test <sup>25</sup>.

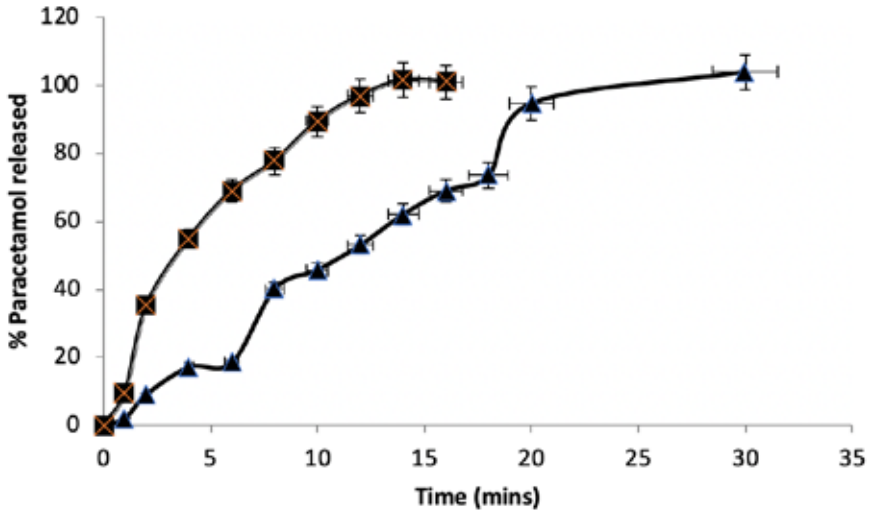


**Figure 3.** Plots of percentage paracetamol released against time for tablets formulated with 5%, w/w of gums as binders *Terminalia*; ▲, PVP ■ (Mean ± SE, n=3)

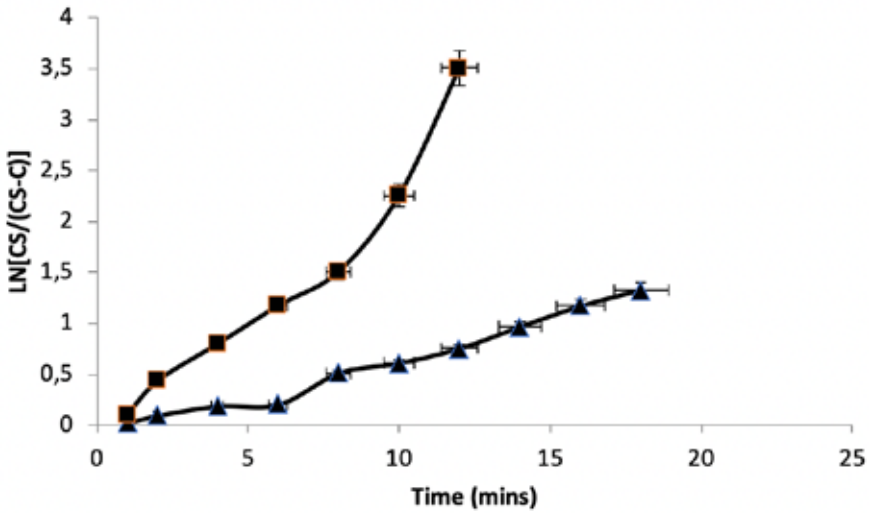


**Figure 4.** In [CS / (CS-C)] versus time for paracetamol tablets containing 5%, w/w binders: *Terminalia*; ▲, PVP ■ (Mean ± SE, n=3)

### CONFLICT OF INTEREST

The authors declare that they don't have any conflict of interest.

### FUNDING SOURCE

Research was funded by the authors.

## **AUTHORS' CONTRIBUTIONS**

Design: Oluyemisi Bamiro

Collection of data: Oluyemisi Bamiro, Olutayo Adeleye, Lateef Bakre

Analysis of data: Oluyemisi Bamiro, Olutayo Adeleye, Lateef Bakre

Drafting of manuscript: Oluyemisi Bamiro

Critical Revision of manuscript: Oluyemisi Bamiro, Olutayo Adeleye, Lateef Bakre

Statistical analysis: Oluyemisi Bamiro, Olutayo Adeleye, Lateef Bakre

Technical or financial support: Oluyemisi Bamiro, Olutayo Adeleye, Lateef Bakre

## REFERENCES

1. Joneja SK, Harkum WW, Skimmer PE, Guo JH. Investigating the fundamental effects of binders on pharmaceutical tablet performance. *Drug Dev Ind Pharm.* 1999;25:29-35. <https://doi.org/10.1081/DDC-100102279>
2. Odeniyi MA, Babalola AO, Ayorinde JO. Evaluation of Cedrela gum as a binder and bio-adhesive component in ibuprofen tablet formulations. *Braz J Pharm Sci.* 2013;49:95-105. <https://doi.org/10.1590/S1984-82502013000100011>
3. Adedokun MO, Ayorinde JO, Odeniyi MA. Compressional, mechanical and release properties of a novel gum in paracetamol tablet formulations, *Curr. Issues Pharm. Med. Sci.* 2014;27:187-194. <https://doi.org/10.1515/cipms-2015-0013>
4. Odeku OA. Assessment of *Albizia zygia* gum as a binding agent in tablet formulations. *Acta Pharm.* 2005;55:263-276.
5. Adeleye OA, Femi-Oyewo MN, Odeniyi MA, Babalola CO. Compaction and mechanical properties of *cissus populnea* gum. *Trop J Nat Pro Res.* 2018;2:447-451.
6. Tank D, Karan K, Gajera BY, Dave RH. Investigate the effect of solvents on wet granulation of microcrystalline cellulose using hydroxypropyl methylcellulose as a binder and evaluation of rheological and thermal characteristics of granules. *Saudi Pharm J.* 2018;26:593-602. <https://doi.org/10.1016/j.j.sps.2018.02.007>
7. Leuenberger H, Dohera BD. Fundamentals of powder compression. I. Compactibility and compressibility of pharmaceutical powders. *Pharm Res.* 1986;3:12-22. <https://doi.org/10.1023/A:1016364613722>
8. Heckel RW. Density-pressure relationships in powder compaction. *Trans Metal Soc AIME.* 1961;221:671-675.
9. Kawakita K, Ludde KH. Some considerations on powder compression equations. *Powder Technol.* 1970;4:61-68.
10. Zhao J, Burt HM, Miller RA. The Gurnham equation in characterizing the compressibility of pharmaceutical materials. *Int J Pharm.* 2006;317:109-113. <https://doi.org/10.1016/j.ijpharm.2006.02.054>
11. Bamiro OA, Sinha VR, Kumar R, Odeku OA. Characterization and evaluation of *Terminalia randii* gum as a binder in carvedilol tablet formulation. *Acta Pharm Sci.* 2010;52:254-262.
12. Bamiro OA, Owoduni AS, Bakre LG, Uwaezuoke OJ. Evaluation of *Terminalia randii* Baker F. gum as a disintegrant in paracetamol tablet formulation. *J Chem Pharm Res.* 2014;6:155-159.
13. Bamiro OA, Bakre LG, Adeleye OA, Babalola CO, Femi-Oyewo MN. Formulation and evaluation of oral dissolving films of naproxen sodium from *Terminalia randii* gum. *West Afri J Pharm.* 2020;31:97 – 110.
14. Okunlola A, Odeku OA. Compressional characteristics and tableting properties of starches obtained from four *Dioscorea* species. *Farmacia.* 2009;57:756-770.
15. Adedokun MO, Itiola OA. Material properties and compaction characteristics of natural and pregelatinized forms of four starches. *Carbohydr Polym.* 2010;79:818-824. <https://doi.org/10.1016/j.carbpol.2009.10.009>
16. Shivanand P, Sprockel OI. Compaction behaviour of cellulose polymers, *Powder Technol.* 1992;67:177-184.
17. Lin C, Cham T. Compression behaviour and tensile strength of heat treated polyethylene-

glycols, *Int J Pharm.* 1995;118:169-179.

18. Bakre LG, Ayodele D. Compressional characteristics of *piper guineense* fruit. *Indonesian J Pharm.* 2013;24:186 – 192.

19. Kitazawa S, Johno I, Ito Y, Teramura S, Okada J. Effects of hardness on the disintegration and dissolution rate of uncoated caffeine tablets. *J Pharm Pharmacol.* 1975;27(10):765-770. <https://doi.org/10.1111/j.2042-7158.1975.tb09397.x>

20. Noyes AA, Whitney WR. The rate of solution of solid substances in their own solutions. *J Am Chem Soc.* 1897;19:930-934. <https://doi.org/10.1021/ja02086a003>

21. Bamiro OA, Adebo O, Bakre LG. Compressional properties of metronidazole tablet formulations containing aloe vera as binding agent. *Int J Pharm Pharm Sci.* 2014;6:261-264.

22. Luangtanan-Anan M, Fell JT. Bonding mechanisms in tableting. *Int J Pharm,* 1990;60:197-202.

23. Alderborn G. Granule Properties of importance to tableting. *Acta Pharm Suec.* 1998;25:229 – 238.

24. Odeku OA, Itiola OA. Evaluation of the effects of khaya gum on the Mechanical and release properties of paracetamol tablet formulation. *Drug Dev Ind Pharm.* 2003;29:311-320. <https://doi.org/10.1081/DDC-120018205>

25. Itiola OA, Pilpel N. Tableting Characteristics of Metronidazole Formulations. *Int J Pharm.* 1986;31:99- 105. [https://doi.org/10.1016/0378-5173\(86\)90218-8](https://doi.org/10.1016/0378-5173(86)90218-8)

26. Ofori-Kwakye K, Mfoafo KA, Kipo SL, Kuntworbe N, El Boakye-Gyasi M. Development and evaluation of natural gum-based extended release matrix tablets of two model drugs of different water solubilities by direct compression. *Saudi Pharm J.* 2016;24:82-91 <https://doi.org/10.1016/j.jsps.2015.03.005>

27. Biu Y, Yonezawa Y, Sunada H. Rapidly Disintegrating Prepared by the Wet Compression Method: Mechanism and Optimization. *J Pharm Sci.* 1999;88:1004-1010 <https://doi.org/10.1021/js990061z>

28. Ajala TO, Bamiro OA, Osahon EM, Lawal T. Characterization of *Cucumis sativus* (Linnaeus) Mucilage and its Excipient Potentials in Metronidazole Tablet Formulation. *Acta Pharm Sci.* 2017;55:67-84 doi: 10.23893/1307-2080.APS.05527

29. Marais AF, Song F, de Villiers MM. Effect of compression force, humidity and disintegrant concentration on the disintegration and dissolution of directly compressed furosemide tablets using croscarmellose sodium as disintegrant. *Trop J Pharm Res.* 2003;2:125-135 DOI: 10.4314/tjpr.v2i1.14577

30. Alebiowu G, Adeagbo AA. Disintegrant properties of a paracetamol tablet formulation lubricated with co - processed lubricants, *Farmacia.* 2009;57:500-510

31. *British Pharmacopeia* Vol. 4. Her Majesty Stationery Office, London. 2003, 2051.

32. Adedokun M, Itiola O. Mechanical and Release Properties of Paracetamol Tablets Formulated With Some Natural and Modified Starch Mucilages. *Nig J Pharm Appl Sci Res.* 2012;1:46-66





